

The curse of random quantum data

Kaining Zhang,^{1,*} Junyu Liu,^{2,3,4,5,†} Liu Liu,^{1,‡} Liang Jiang,^{2,§} Min-Hsiu Hsieh,^{6,¶} and Dacheng Tao^{1,**}

¹*School of Computer Science, Faculty of Engineering, University of Sydney, Australia*

²*Pritzker School of Molecular Engineering, The University of Chicago, Chicago, IL 60637, USA*

³*Department of Computer Science, The University of Chicago, Chicago, IL 60637, USA*

⁴*Kadanoff Center for Theoretical Physics, The University of Chicago, Chicago, IL 60637, USA*

⁵*Department of Computer Science, The University of Pittsburgh, Pittsburgh, PA 15260, USA*

⁶*Hon Hai Quantum Computing Research Center, Taipei, Taiwan*

(Dated: August 20, 2024)

Quantum machine learning, which involves running machine learning algorithms on quantum devices, may be one of the most significant flagship applications for these devices. Unlike its classical counterparts, the role of data in quantum machine learning has not been fully understood. In this work, we quantify the performances of quantum machine learning in the landscape of quantum data. Provided that the encoding of quantum data is sufficiently random, the performance, we find that the training efficiency and generalization capabilities in quantum machine learning will be exponentially suppressed with the increase in the number of qubits, which we call “the curse of random quantum data”. Our findings apply to both the quantum kernel method and the large-width limit of quantum neural networks. Conversely, we highlight that through meticulous design of quantum datasets, it is possible to avoid these curses, thereby achieving efficient convergence and robust generalization. Our conclusions are corroborated by extensive numerical simulations.

I. INTRODUCTION

The attainment of quantum advantage [1, 2] using noisy intermediate-scale quantum (NISQ) devices [3] has significantly advanced research in various fields where quantum computing shows promise. Among these, the variational quantum algorithm (VQA) [4] emerges as a prominent framework for harnessing NISQ devices, owing to its relatively modest requirements on gate noise and circuit connectivity. VQAs have been applied in diverse areas, including machine learning (so-called quantum machine learning) [5–12], numerical analysis [13–17], quantum simulation [18–27], and quantum chemistry [28–36]. The concepts of variational quantum circuits have also been utilized for practical demonstrations of quantum control and quantum error correction, thereby bridging current developments in noisy quantum computing towards future fault-tolerant quantum computing [37, 38].

On the other hand, despite the existence of practical demonstrations of variational quantum algorithms, their theoretical foundation has not been completely established. People still lack confidence regarding when and how variational quantum circuits could be utilized, how to design them from first principles, and where theoretical quantum advantage could potentially exist in a generic setup [39–44]. An existing theoretical proposal, known as the quantum neural tangent kernel (QNTK),

has proven helpful in understanding the dynamics of gradient descent in quantum machine learning, particularly in the realm of wide quantum neural networks where the number of training parameters and the dimension of the Hilbert space are considered large [40]. However, in scenarios where the number of training parameters is not comparable to the dimension of Hilbert spaces, the QNTK might become small, and training efficiency may be unsatisfactory, leading to what is termed the barren plateau problem [45]. Conversely, a large number of training parameters will linearize the quantum neural network towards the frozen kernel limit, where an emergent fixed kernel could be used akin to linear regression. This limit linearizes the dynamics and obscures information about the quantum data. The effects of data, which appear to be significant in practical training performances, become less clear in the limit of a frozen kernel. Hence, an important question naturally arises: how are quantum data and its encoding related to the training efficiency and practical performance of quantum machine learning?

In this paper, we uncover a novel phenomenon related to the interplay between quantum machine learning performance and the distribution of quantum data, which we term *the curse of random quantum data*. We discover that, similar to the barren plateau phenomenon in the gradient efficiency for training dynamics, across a typical class of quantum machine learning algorithms, when quantum data is encoded randomly, the algorithm’s learning performance markedly declines. Specifically, the spectrum of the quantum neural tangent kernel diminishes in line with the dimension of the Hilbert space, and similarly, the reduction in the generalization error during training is also constrained by the Hilbert space’s dimension. This phenomenon may not be restricted to any particular training strategy; it is observable in both

* kzha3670@uni.sydney.edu.au

† junyuliucaltech@gmail.com

‡ liuliubh@gmail.com

§ liang.jiang@uchicago.edu

¶ min-hsiu.hsieh@foxconn.com

** dacheng.tao@sydney.edu.au

the quantum kernel method and the variational quantum algorithm at or beyond the frozen kernel limit. Hence, we identify this as a new type of the curse of large dimensions of Hilbert spaces occurring within the realm of quantum data rather than conventional barren plateau statements in the conventional parameter space associated with the loss function landscape [45–51]. Importantly, this curse can emerge irrespective of the training method employed, indicating that it is a fundamental aspect of quantum data space, affecting both kernel methods and gradient descent approaches alike. Furthermore, we discover that a carefully curated data distribution, as opposed to one that is uniformly random across the Hilbert space, can significantly mitigate the curse. This is demonstrated through direct examples where certain input state datasets and encoding schemes markedly enhance the performance of quantum machine learning algorithms, particularly affecting the spectra of the QNTK. Our theoretical examples are substantiated by numerical simulations of quantum machine learning on tasks including the quantum dynamics learning and the binary classification.

II. THEORETICAL RESULTS

A. Background of quantum machine learning

We begin by setting up notations and methods for quantum machine learning. The training set is denoted by $\mathcal{A} = \{a\} = \{(\rho_a, y_a)\}$, where each sample a consists of the input state in the density matrix form ρ_a and the label y_a . The test set is denoted by $\mathcal{B} = \{\hat{b}\}$. In the task of QML, we aim to approximate the label y with the parameterized prediction function $z(\boldsymbol{\theta})$. Here a common approach is to minimize the mean squared error on the training set as the loss function:

$$\mathcal{L}_{\mathcal{A}}(\boldsymbol{\theta}) = \frac{1}{2|\mathcal{A}|} \sum_{a \in \mathcal{A}} (z_a(\boldsymbol{\theta}) - y_a)^2 = \frac{1}{2|\mathcal{A}|} \|\mathbf{r}_{\mathcal{A}}(\boldsymbol{\theta})\|_2^2, \quad (1)$$

where

$$\mathbf{r}_{\mathcal{A}}(\boldsymbol{\theta}) := \{r_a(\boldsymbol{\theta})\}_{a \in \mathcal{A}} := \{z_a(\boldsymbol{\theta}) - y_a\}_{a \in \mathcal{A}} \quad (2)$$

is the training residual vector. The prediction function is given by

$$z_a(\boldsymbol{\theta}) = \text{Tr}[O(\boldsymbol{\theta})\rho_a]. \quad (3)$$

In this paper, we focus on two approaches for generating the prediction function. The first is the quantum kernel method:

$$O_{\text{qkm}}(\boldsymbol{\theta}) = \sum_{a \in \mathcal{A}} \theta_a \rho_a. \quad (4)$$

The second approach is the quantum neural network using the observable O and the variational quantum circuit $V(\boldsymbol{\theta})$:

$$O_{\text{qnn}}(\boldsymbol{\theta}) = V(\boldsymbol{\theta})^\dagger O V(\boldsymbol{\theta}). \quad (5)$$

For the QNN case, we train the parameter using gradient descent with some learning rate η , i.e.

$$\boldsymbol{\theta}(t+1) = \boldsymbol{\theta}(t) - \eta \nabla \mathcal{L}_{\mathcal{A}}(\boldsymbol{\theta}(t)). \quad (6)$$

Suppose the parameter $\boldsymbol{\theta} \in \mathbb{R}^D$. Let $\eta \rightarrow 0$, the gradient descent dynamics approximates to the continuous regime known as the gradient flow:

$$\dot{\boldsymbol{\theta}} = -\nabla \mathcal{L}_{\mathcal{A}}(\boldsymbol{\theta}) = -\frac{1}{|\mathcal{A}|} J(\boldsymbol{\theta}) \mathbf{r}_{\mathcal{A}}(\boldsymbol{\theta}), \quad (7)$$

where $J(\boldsymbol{\theta}) \in \mathbb{R}^{D \times |\mathcal{A}|}$ is the Jacobian matrix with entries $J_{da}(\boldsymbol{\theta}) = \frac{\partial z_a}{\partial \theta_d}(\boldsymbol{\theta})$. We are interested in the convergence rate of the loss function, i.e.

$$\begin{aligned} \dot{\mathcal{L}}_{\mathcal{A}}(\boldsymbol{\theta}) &= \nabla \mathcal{L}_{\mathcal{A}}(\boldsymbol{\theta})^T \dot{\boldsymbol{\theta}} \\ &= -\frac{D}{|\mathcal{A}|^2} \mathbf{r}_{\mathcal{A}}(\boldsymbol{\theta})^T K(\boldsymbol{\theta}) \mathbf{r}_{\mathcal{A}}(\boldsymbol{\theta}) \\ &\leq -\frac{2D}{|\mathcal{A}|} \lambda_{\min}[K(\boldsymbol{\theta})] \mathcal{L}_{\mathcal{A}}(\boldsymbol{\theta}), \end{aligned} \quad (8)$$

where

$$K(\boldsymbol{\theta}) = \frac{1}{D} J(\boldsymbol{\theta})^T J(\boldsymbol{\theta}) \quad (9)$$

is the QNTK at the point $\boldsymbol{\theta}$. Eq. (8) shows that the loss decays linearly when the least eigenvalue of QNTK is lower bounded by some positive constant. In the rest of this paper, we will prove rigorous convergence guarantees based on further analyses to the least eigenvalue of QNTK.

B. Generalization error with quantum data

Since input states are engaged in the training of QML via quantum kernel or QNTK, their distributions could naturally affect training and generalization performances. Here, we provide some negative examples for datasets sampled from state 2-designs. Specifically, we consider the quantum kernel method and the quantum neural network approach separately in Theorems 1 and 2. Related proofs can be found in Appendix C. The generalization error has up to exponentially small improvement from the extremely overfitting situation, when the size of datasets is relatively small compared with the Hilbert dimension.

Theorem 1. *Suppose all N -qubit quantum states in the training and test datasets \mathcal{A} and \mathcal{B} are independently sampled from state 2-designs and the size of datasets is smaller than $2^{N/2}$. Let $\mathcal{L}_{\mathcal{A}}(t)$ and $\mathcal{L}_{\mathcal{B}}(t)$ be the training and the test loss function of the quantum kernel method (Eqs. (3) and (4)), respectively. Then, with high probability,*

$$\mathbb{E} \mathcal{L}_{\mathcal{B}}(\infty) \gtrsim \mathbb{E} \mathcal{L}_{\mathcal{B}}(0) - \frac{|\mathcal{A}|}{2^{N-1}} \mathbb{E} \sqrt{\mathcal{L}_{\mathcal{A}}(0) \mathcal{L}_{\mathcal{B}}(0)}, \quad (10)$$

where the expectation is taken under state 2-designs for states in \mathcal{A} and \mathcal{B} .

Theorem 2. Suppose all N -qubit quantum states in the training and test datasets \mathcal{A} and \mathcal{B} are independently sampled from state 2-designs. Let $\mathcal{L}_{\mathcal{A}}(t)$ and $\mathcal{L}_{\mathcal{B}}(t)$ be the training and the test loss function of the quantum neural network (Eqs. (3) and (5)), where the label is given as $y := \text{Tr}[OU\rho U^\dagger]$ for a target unitary U with the zero trace observable O . Then, under the frozen QNTK regime,

$$\mathbb{E} \mathcal{L}_{\mathcal{B}}(\infty) \geq \left(1 - \frac{|\mathcal{A}|}{2^{2N} - 1}\right) \mathbb{E} \mathcal{L}_{\mathcal{B}}(0), \quad (11)$$

where the expectation is taken under 2-designs distributions for states in \mathcal{A} and \mathcal{B} and the target unitary U .

We remark that Theorem 2 provides a novel result about learning quantum dynamics from the no-free-lunch framework perspective. Compared with existing results [52] that mainly focus on the lower bound with an absolute formulation, we provide a bound with a relative formulation for the test loss with trained parameters. As shown in Eq. (11), the bound is in terms of the initial test loss times a constant, which is exponentially close to 1 with polynomially scaled training datasets. Therefore, the loss on the test set with 2-design states only has exponentially small improvements from its initial value, unless the size of the training set exceeds an exponentially large threshold. However, training QNN with exponentially large datasets requires tremendous computational resources. Such kind of datasets are also unavailable in practice for large-scale problems.

Theorems 1 and 2 reveal one critical issue of quantum machine learning from the data perspective, which we name as *the curse of random quantum data*. For input states distributed uniformly in the Hilbert space, the corresponding QML task exhibits poor generalization performance. This phenomenon is universal and is independent of certain QML method employed. One intuitive explanation of the curse of random quantum data is that uniformly distributed quantum states have inherently bad learnability, unless the dataset has exponentially large size. Specifically, quantum representation learning is hard for datasets composed of nearly orthogonal states without prior knowledge. However, practical QML datasets do not grow exponentially with increasing qubits in general. Therefore the distribution of input states given as quantum data or quantum encoding would play an essential role, which may rule out the potential of benign generalization.

C. Spectrum of QNTK with quantum data

We have shown the *learnability* issue from uniformly random quantum data, i.e., datasets with 2-design states have bad generalization performances. Here we present another *trainability* issue induced by uniformly random quantum data from the optimization perspective in QNN.

Theorem 3. Let $\mathcal{A}\{(\rho_a, y_a)\}$ be the training datasets with independent N -qubit 2-design states ρ_a . Denote by $z_a = \text{Tr}[OV(\boldsymbol{\theta})\rho_a V(\boldsymbol{\theta})^\dagger]$ the QNN with the observable O and the variational circuit $V(\boldsymbol{\theta}) = \prod_{d=D}^1 \exp[-iH_d\theta_d/2]W_d$, where the hamiltonian H_d is Hermitian unitary and W_d is the fixed unitary. Then there exists a constant $C > 0$ such that

$$\lambda_{\max}[K(\boldsymbol{\theta})] \leq \frac{\|O\|_F^2}{4^N} \left(1 + \frac{C|\mathcal{A}|}{2^{N\delta}} \sqrt{\ln|\mathcal{A}|}\right) \quad (12)$$

with probability at least $1 - \delta$.

As shown in Theorem 3, the QNTK has exponentially small spectrum with increased qubits N . Since the convergence rate is controlled by the spectrum of QNTK, we should avoid using uniformly distributed input states in the training of QNN. One appropriate substitute is a biased state distribution. For convenience, we first show the state 2-design distribution in the form of Pauli decomposition. Let $A \in \mathbb{R}^{4^N \times |\mathcal{A}|}$ be the matrix that stores the Pauli decomposition coefficients of states in \mathcal{A} , i.e.

$$\rho_a = \sum_{\mathbf{i} \in \{0,1,2,3\}^{\otimes N}} \frac{1}{2^N} A_{\mathbf{i}a} \sigma_{\mathbf{i}}, \quad (13)$$

where the basis $\sigma_{\mathbf{i}} := \sigma_{i_0} \otimes \cdots \otimes \sigma_{i_N}$ is the tensor product of Pauli matrices. When each ρ_a is sampled independently from a 2-design distribution,

$$\mathbb{E}_{2\text{-design}} A_{\mathbf{i}a} = 0, \quad (14)$$

$$\mathbb{E}_{2\text{-design}} A_{\mathbf{i}a} A_{\mathbf{j}b} = \frac{1}{2^N + 1} \delta_{\mathbf{i}\mathbf{j}} \delta_{ab}. \quad (15)$$

for all $\mathbf{i}, \mathbf{j} \neq \mathbf{0}$. We recap that the Pauli coefficient coefficients of 2-designs states has the following two properties: 1) zero mean and covariance; 2) unbiased variance with the value $(2^N + 1)^{-1}$. Therefore, each element of A except $A_{\mathbf{0}a}$ has a small size around $\mathcal{O}(2^{-N/2})$, which technically contributes to exponentially small generalization improvement and QNTK. To overcome this issue, we introduce the state distribution in Proposition 1. The proposed distribution is generalized from Eqs. (14) and (15), such that coefficients have biased variances on different Pauli bases.

Proposition 1. States ρ_a in the dataset \mathcal{A} are generated independently from the same distribution, such that for all $\mathbf{i}, \mathbf{j} \neq \mathbf{0}$,

$$\begin{aligned} \mathbb{E} A_{\mathbf{i}a} &= 0, \\ \mathbb{E} A_{\mathbf{i}a} A_{\mathbf{j}b} &= \alpha_{\mathbf{i}} \delta_{\mathbf{i}\mathbf{j}} \delta_{ab}. \end{aligned}$$

Here we present an example that lead to the coefficient distribution in Proposition 1. We consider states from finite local-depth circuits (FLDC) [53], where the parameter in circuits are independently sampled from the uniform distribution on $[0, 2\pi]$. Numerical evidence is provided in Figure 1. Denote by $\mu_{\mathbf{i}}$ the expectation of each

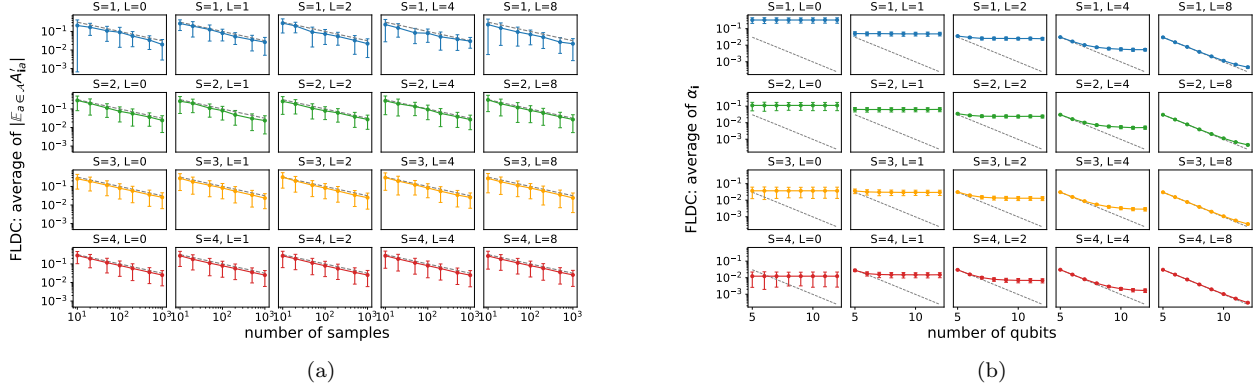


FIG. 1: Scaling of Pauli decomposition coefficients of finite local-depth circuit states over $S \in \{1, 2, 3, 4\}$ and circuit layer $L \in \{0, 1, 2, 4, 8\}$. Figure 1a shows the average of $|\mathbb{E}_{a \in \mathcal{A}} A'_{ia}|$ in Eq. (16) w.r.t. all $\|\mathbf{i}\|_1 = S$ with 1D connectivity, where $|\mathcal{A}| \in \{10, 20, 50, 100, 200, 500, 1000\}$. The grey dashed line plots $|\mathcal{A}|^{-0.5}$. Figure 1b shows the average of α_i in Proposition 1 w.r.t. all $\|\mathbf{i}\|_1 = S$ with 1D connectivity, where $N \in \{5, 6, 7, 8, 9, 10, 11, 12\}$, and each α_i is calculated by taking the average over $|\mathcal{A}| = 1000$ samples. The grey dashed line plots the Haar limit. The error bar in all figures shows the standard deviation over variables with different i .

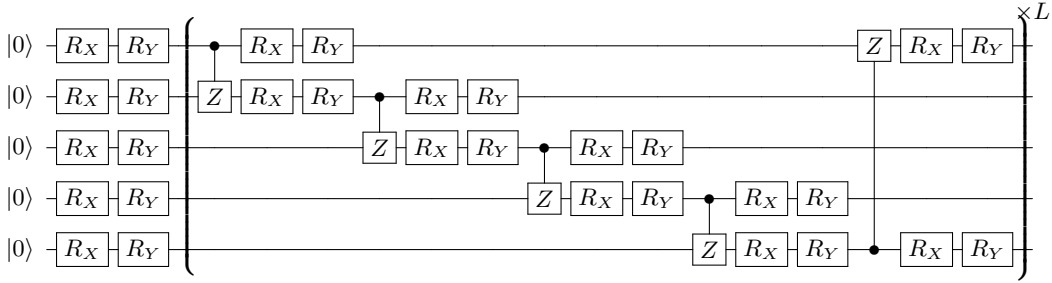


FIG. 2: Finite local-depth circuits with L blocks for $N = 5$.

Pauli decomposition coefficient A_{ia} over the distribution of a . Firstly, we demonstrate that the expectation μ_i is zero. Due to the central limit theorem, the statistical term

$$\left| \mathbb{E}_{a \in \mathcal{A}} A'_{ia} \right| := \left| \frac{\mathbb{E}_{a \in \mathcal{A}} A_{ia}}{\text{SD}_{a \in \mathcal{A}} A_{ia}} \right| \lesssim |\mu_i| + \frac{1}{\sqrt{|\mathcal{A}|}} |g|, \quad (16)$$

where g is a standard normal distributed variable. As illustrated in Figure 1a, the average of the statistical term in Eq. (16) decays inversely with the square root of $|\mathcal{A}|$ when it grows. Therefore each $\mu_i = 0$ for $S \in \{1, 2, 3, 4\}$. Next, we reveal the scaling of the variance α_i in terms of the qubit number and the block layer. As shown in Figure 1b, when the qubit number increases, the variance remains large when the number of circuit layer is small. With growing circuit layers, the variance converges to the Haar limit $1/(2^N + 1)$ for $S \in \{1, 2, 3, 4\}$. In summary, input states prepared from FLDC with finite circuit layers are expected to have large Pauli decomposition coefficients on local bases with small S .

Datasets with the property in Proposition 1 have the potential to induce large QNTK. Here we provide one example in Lemma 1. The least eigenvalue of the QNTK at

$\theta = \mathbf{0}$ has a lower bound that is proportional to the least variance of coefficients corresponding to quantum gates qubits. Therefore, we expect that an appropriate state distribution should have variances at least $\mathcal{O}(1/\text{poly}(N))$ for local Pauli bases.

Lemma 1. Let the observable be $O = \sum_{k=1}^N o_k Z_k$, where each Z_k is the product of Pauli matrices that is Z on the k -th qubit and I on other qubits. Denote by H_d the Hamiltonian of the d -th quantum gate in the circuit $V(\theta) = \prod_{d=D}^1 \exp[-iH_d \theta_d / 2]$ that acts on qubits $\mathcal{S}_d \subseteq \{1, 2, \dots, N\}$. We assume that H_d is randomly sampled from the set $\mathcal{H} := \{X, Y, Z\}^{\otimes \mathcal{S}_d}$. Let $\mathcal{Q} := \{\mathcal{S}_d\}$. Let $\rho_a = \sum_{\mathbf{p} \in \{0,1,2,3\}^{\otimes N}} \frac{1}{2^N} A_{\mathbf{p}a} \sigma_{\mathbf{p}}$ be the Pauli decomposition of state ρ_a , where A follows Proposition 1. Denote by $A_{\mathcal{Q}}$ the matrix with dimension $((3^S - 1)|\mathcal{Q}|, |\mathcal{A}|)$ formed by vertically concatenating matrices $A_{\mathcal{Q},w}$ for $w \in \{0, 1, \dots, S-1\}$. Denote by $\text{Var}_{\mathcal{Q}} := \text{diag}(\alpha_i)$, $\alpha_{\max} := \max_i \alpha_i$, and $\alpha_{\min} := \min_i \alpha_i$, where i corresponds to the index of rows of $A_{\mathcal{Q}}$. Denote by $A'_{\mathcal{Q}} := \text{Var}_{\mathcal{Q}}^{-1/2} A_{\mathcal{Q}}$, $A'_{\mathcal{Q},\max} := \frac{1}{\sqrt{(3^S - 1)|\mathcal{Q}|}} \max_{a \in \mathcal{A}} \| [A'_{\mathcal{Q}}]_{\cdot, a} \|_2$ and $A'_{\mathcal{Q},\min} := \frac{1}{\sqrt{(3^S - 1)|\mathcal{Q}|}} \min_{a \in \mathcal{A}} \| [A'_{\mathcal{Q}}]_{\cdot, a} \|_2$. Then when $|\mathcal{A}|$ is suffi-

ciently large, there exists two constants $C_1, C_2 > 0$ such that for any $\delta, k \in (0, 1)$, the following holds with probability at least $1 - \delta$

$$(1 - k)\Delta_S \alpha_{\min} A_{\mathcal{Q}, \min}^{\prime 2} \leq \lambda[K(\mathbf{0})] \leq (1 + k)\|O\|_2^2 \alpha_{\max} A_{\mathcal{Q}, \max}^{\prime 2}, \quad (17)$$

for $D \geq D_0 \ln \frac{D_0}{\delta}$ with $D_0 = C_2 \frac{\|O\|_2^4 \alpha_{\max}^2 A_{\mathcal{Q}, \max}^{\prime 2}}{k^2 \Delta_S^2 \alpha_{\min}^2 A_{\mathcal{Q}, \min}^{\prime 4}} |\mathcal{A}| \ln \frac{|\mathcal{A}|}{\delta}$ and $S \geq \log_3 \left[1 + \frac{C_1^2 |\mathcal{A}|^2 \ln |\mathcal{A}|}{k^2 A_{\mathcal{Q}, \min}^{\prime 4} |\mathcal{Q}| \delta^2} \right]$, where $\Delta_S := \min_{\mathbf{g} \in \{0, \pm 1\}^{\otimes N}, 1 \leq \|\mathbf{g}\|_1 \leq S} (\mathbf{g}^T \mathbf{o})^2$.

We remark that Proposition 1 could be applied for designing quantum encoding strategies. One example that Proposition 1 holds is the qubit embedding [54] for random vectors. Here, we encode the vector $\mathbf{x} \in \mathbb{R}^N$ into the state

$$|\psi(\mathbf{x})\rangle = \bigotimes_{n=1}^N e^{-iZ\pi x_n/2} \frac{|0\rangle + |1\rangle}{\sqrt{2}} \quad (18)$$

and each entry of \mathbf{x} is normalized in $[-1, 1]$. An example of QNNs with qubit embedding is presented in Lemma 2, where the least eigenvalue of the QNTK at $\boldsymbol{\theta} = \mathbf{0}$ has the lower bound around $\mathcal{O}(2^{-S})$.

Lemma 2. *We follow conditions and notations in Lemma 1 except the Hamiltonian set $\mathcal{H} := \{X, Y\}^{\otimes S}$. Let ρ_a be the density matrix of the qubit embedding of the vector \mathbf{x}_a via Eq. (18), where each entry of \mathbf{x}_a is an independent random variable distributed uniformly in $[-1, 1]$. Then when $|\mathcal{A}|$ is sufficiently large, there exists two constants $C_1, C_2 > 0$ such that for any $\delta, k \in (0, 1)$, the following holds with probability at least $1 - \delta$*

$$(1 - k) \frac{\Delta_S}{2^S} \leq \lambda[K(\mathbf{0})] \leq (1 + k) \frac{\|O\|_2^2}{2^S}, \quad (19)$$

for $D \geq D_0 \ln \frac{D_0}{\delta}$ with $D_0 = C_2 \frac{|\mathcal{A}| \|O\|_2^4}{k^2 \Delta_S^2} \ln \frac{|\mathcal{A}|}{\delta}$ and $S \geq 2 + \log_2 \frac{C_1^2 |\mathcal{A}|^2 \ln |\mathcal{A}|}{k^2 |\mathcal{Q}| \delta^2}$, where $\Delta_S := \min_{\mathbf{g} \in \{0, \pm 1\}^{\otimes N}, 1 \leq \|\mathbf{g}\|_1 \leq S} (\mathbf{g}^T \mathbf{o})^2$.

Both bounds in Lemma 1 and Lemma 2 holds with mild conditions on the number of gates in the circuit and the number of qubits involved for each gate, i.e. $D = \tilde{\mathcal{O}}(|\mathcal{A}| \ln^2 |\mathcal{A}|)$ and $S = \tilde{\mathcal{O}}(\ln |\mathcal{A}|)$. Derivations of Theorem 3 and Theorems 1 and 2 are provided in Appendix D.

D. Convergence analysis of training QNNs

Here we provide two examples of QNNs with rigorous convergence analysis, where the input state in the training dataset satisfies Proposition 1. The optimization of the loss function in Eq. (1) exhibits proven linear convergence during gradient descent training with high probability, when the locally smooth assumption of the Jacobian matrix in Assumption 1 holds. Technically, we employ Lemmas 1 and 2 to bound the largest and the least

eigenvalue of the initial QNTK. Thus we obtain necessary conditions given as the lower bound of the number of parameters D and the number of local qubits S , such that D gate Hamiltonians are sampled independently from $\{X, Y, Z\}^{\otimes S}$ or $\{X, Y\}^{\otimes S}$. These Lemmas are employed with Assumption 1 for deriving the convergence results in Theorems 4 and 5 with proof in Appendix E. For the general case with Proposition 1, the linear convergence rate requires $S \geq \tilde{\mathcal{O}}(\ln |\mathcal{A}|)$ and $D \geq \tilde{\mathcal{O}}(|\mathcal{A}| \ln^2 |\mathcal{A}|)$. For the qubit embedding case in Eq. (18), the linear convergence rate requires $S \geq \tilde{\mathcal{O}}(\ln |\mathcal{A}|)$ and $D \geq \tilde{\mathcal{O}}(|\mathcal{A}|^5 \ln |\mathcal{A}|)$. We remark that the condition on D is smaller than previous results that scale $\mathcal{O}(2^N)$ [55] when the size of dataset is polynomial to the qubit number. Apart from the linear convergence regime, we also obtain some by-products including the lazy training property shown as the small parameter changes and the stability of the QNTK during the training.

Assumption 1 (Locally smooth condition). *Let $J(\boldsymbol{\theta}) \in \mathbb{R}^{D \times |\mathcal{A}|}$ be the Jacobian matrix of a QNN. Then for any constant $C_0 > 0$, we call $\mathcal{Z}(C_0, R_0, \boldsymbol{\theta})$ a locally smooth region if for any $\boldsymbol{\theta}'$ with $\|\boldsymbol{\theta}' - \boldsymbol{\theta}\|_2 \leq R_0/\sqrt{D}$, the following holds:*

$$\|J(\boldsymbol{\theta}') - J(\boldsymbol{\theta})\|_2 \leq \sqrt{C_0 D} \|\boldsymbol{\theta}' - \boldsymbol{\theta}\|_2. \quad (20)$$

Theorem 4 (Linear convergence of QNN training w.r.t. Proposition 1). *We follow conditions and notations in Lemma 1. Denote $\lambda'_{\min} := \frac{2}{3} \Delta_S \alpha_{\min} A_{\mathcal{Q}, \min}^{\prime 2}$ and $\lambda'_{\max} := \frac{4}{3} \|O\|_2^2 \alpha_{\max} A_{\mathcal{Q}, \max}^{\prime 2}$. Let $\mathcal{L}_{\mathcal{A}}(t)$ be the loss function at the t -th step. Suppose that there exists four constants $c_0, c_1, c_2, c_3 > 0$ and $\delta \in (0, 1)$, such that Assumption 1 holds for the parameter $\boldsymbol{\theta}(0) = \mathbf{0}$ with the constant c_0 and $R_0 := \frac{5}{2} \lambda'_{\min}{}^{-1} \sqrt{2} |\mathcal{A}| \lambda'_{\max} \mathcal{L}_{\mathcal{A}}(0)$ for every $S \geq \log_3 \left[1 + c_3 \frac{|\mathcal{A}|^2 \ln |\mathcal{A}|}{A_{\mathcal{Q}, \min}^{\prime 4} |\mathcal{Q}| \delta^2} \right]$ some $D \geq \max(D_1 \ln \frac{D_1}{\delta}, D_2)$, where*

$$D_1 = \left(\frac{\lambda'_{\max}}{\lambda'_{\min} A_{\mathcal{Q}, \max}^{\prime 2}} \right)^2 c_1 |\mathcal{A}| \ln \frac{|\mathcal{A}|}{\delta},$$

$$D_2 = \frac{\lambda'_{\max}{}^2}{\lambda'_{\min}{}^4} c_2 |\mathcal{A}| \mathcal{L}_{\mathcal{A}}(0).$$

Then the following holds with probability at least $1 - \delta$ when applying gradient descent with learning rate $\eta = \eta_0 |\mathcal{A}|/D$ with $\eta_0 \in (0, \lambda'_{\min}{}^{-1})$,

$$\mathcal{L}_{\mathcal{A}}(T) \leq \left(1 - \frac{1}{2} \eta_0 \lambda'_{\min} \right)^{2T} \mathcal{L}_{\mathcal{A}}(0), \quad (21)$$

$$\|\boldsymbol{\theta}(T) - \boldsymbol{\theta}(0)\|_2 \leq \frac{R_0}{\sqrt{D}}. \quad (22)$$

Theorem 5 (Linear convergence of QNN training w.r.t. qubit embedding). *We follow conditions and notations in Lemma 2. Let $\mathcal{L}_{\mathcal{A}}(t)$ be the loss function at the t -th step. Suppose that there exists four constants $c_0, c_1, c_2, c_3 > 0$ and $\delta \in (0, 1)$, such that Assumption 1*

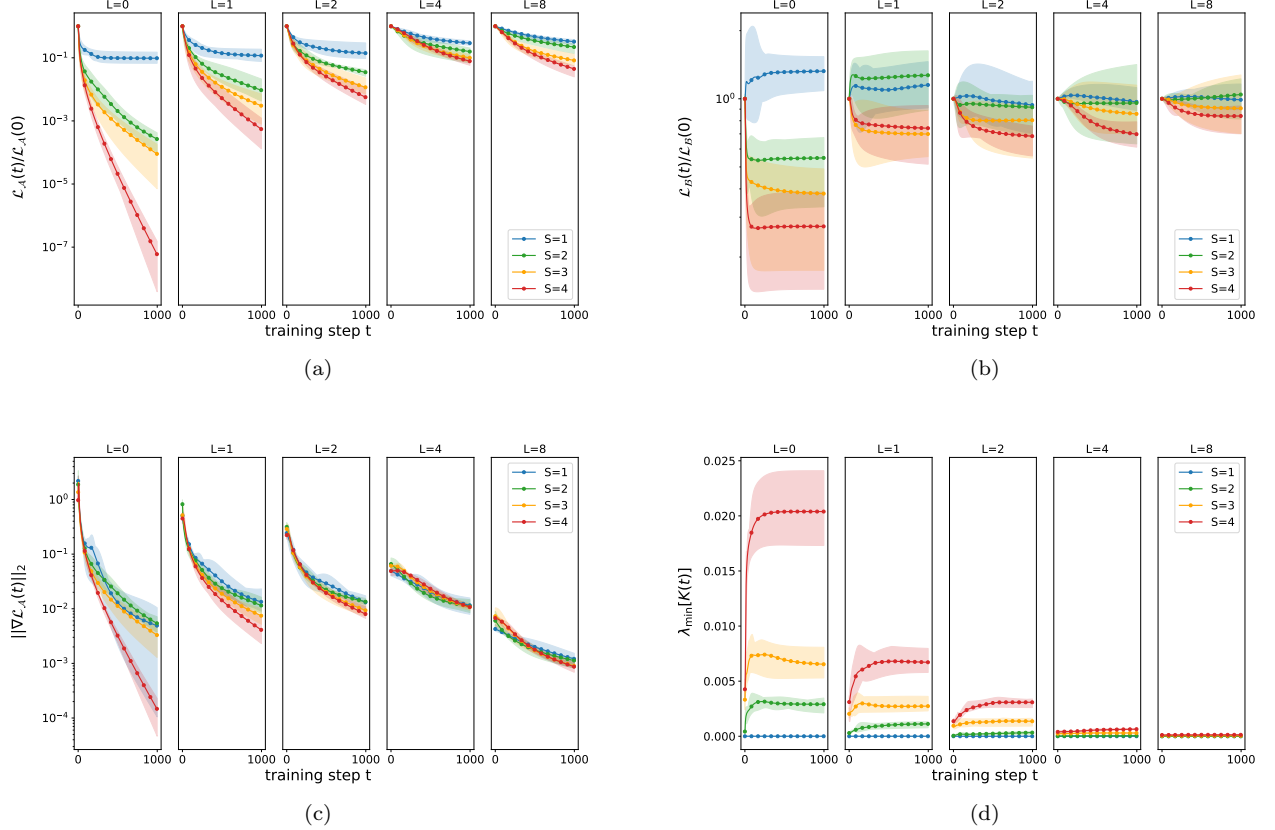


FIG. 3: Numerical results of QDL with FLDC input states, where $(N, D) = (12, 240)$ and $L \in \{0, 1, 2, 4, 8\}$. Figures 3a and 3b show the relative loss of the training and the test dataset during the training, respectively. Figure 3c shows the ℓ_2 -norm of the gradient for the loss function. Figure 3d shows the least eigenvalue of the QNTK. Each solid line denotes the average of 5 rounds of simulations with independent circuits and parameters.

holds for the parameter $\boldsymbol{\theta}(0) = \mathbf{0}$ with the constant c_0 and $R_0 := \frac{5}{2} \|O\|_2 \Delta_S^{-1} \sqrt{6 \times 2^S |\mathcal{A}| \mathcal{L}_{\mathcal{A}}(0)}$ for some $S \geq 2 + \log_2 \frac{c_3 |\mathcal{A}|^2 \ln |\mathcal{A}|}{|\mathcal{Q}| \delta^2}$ and $D \geq \max(D_1 \ln \frac{D_1}{\delta}, D_2)$, where

$$D_1 = c_1 \frac{\|O\|_2^4}{\Delta_S^2} |\mathcal{A}| \ln \frac{|\mathcal{A}|}{\delta},$$

$$D_2 = c_2 \frac{\|O\|_2^4}{\Delta_S^4} 2^{2S} |\mathcal{A}| \mathcal{L}_{\mathcal{A}}(0).$$

Then the following holds with probability at least $1 - \delta$ when applying gradient descent with learning rate $\eta = \eta_0 |\mathcal{A}| / D$ with $\eta_0 \in (0, 3 \times 2^{S-1} \Delta_S^{-1})$,

$$\mathcal{L}_{\mathcal{A}}(T) \leq \left(1 - \eta_0 \frac{\Delta_S}{3 \times 2^S}\right)^{2T} \mathcal{L}_{\mathcal{A}}(0), \quad (23)$$

$$\|\boldsymbol{\theta}(T) - \boldsymbol{\theta}(0)\|_2 \leq \frac{R_0}{\sqrt{D}}. \quad (24)$$

III. NUMERICAL RESULTS

Here we provide some numerical evidence that suggests the separated performances of training QNNs with different input states, regarding the convergence rate and the generalization behavior.

A. Quantum dynamics learning

The first task is to learn quantum dynamics, where the aim is to approximate the measurement performance of the target unitary using variational quantum circuits. Given the target unitary U , the observable O , and an ensemble of input states $\{(\rho_a, y_a)\}_{a \in \mathcal{A}}$, we consider the optimization of the loss defined in Ref. [52], i.e.

$$\mathcal{L}_{\text{QDL}} := \frac{1}{2|\mathcal{A}|} \sum_{a \in \mathcal{A}} (\text{Tr}[OV(\boldsymbol{\theta})\rho_a V(\boldsymbol{\theta})^\dagger] - y_a)^2, \quad (25)$$

with the label $y_a := \text{Tr}[OU\rho_a U^\dagger]$. In the experiment, we set the qubit number $N = 12$. The observable is set to

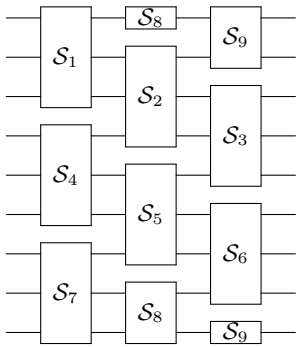


FIG. 4: An assignment of $\mathcal{Q} = \{\mathcal{S}_1, \dots, \mathcal{S}_N\}$ in the hardware-efficient manner for $(N, S) = (9, 3)$.

be

$$O = \sum_{n=1}^N c_n Z_n \quad (26)$$

with independent normal variables $c_n \sim \mathcal{N}(0, 1)$. The target unitary is set to be the time evolution of the Heisenberg model [56] with open boundary conditions

$$U = \exp \left[-it \sum_{n=1}^N X_n X_{n+1} + Y_n Y_{n+1} + Z_n Z_{n+1} \right],$$

where we use $t = 1$. Input states are generated from the state $|0\rangle$ after finite local-depth circuits (Fig 2) with L blocks. The size of both training and test sets are 40. Hamiltonians of variational quantum gates are sampled from the set $\{X, Y, Z\}^{\otimes S}$, and the deployment of quantum gates assumes the 1D connectivity with $|\mathcal{Q}| = N$. The variational circuit part consists of $\{5, 7, 10, 14, 20\}$ layers of gates in Figure 4. We initialize parameters as $\boldsymbol{\theta}(0) = \mathbf{0}$, which is consistent with the analysis in Theorem 4. During the training stage, we use gradient descent with learning rate $\eta = N/D$ for $L \in \{0, 1, 2, 4\}$. For the case $L = 8$, the initial gradient is at least an order of magnitude smaller than that with other L values, as shown in Figure 3c. Therefore, we adopt a larger learning rate $\eta = 10N/D$ when $L = 8$ to guarantee the convergence of the training set loss.

We exhibit numerical results in Figures 3 and 5. Figures 3a and 3b plot the training and the test loss over their initial values during the training. The convergence rate decreases towards the Haar limit as the input layer L increases, while the test loss in Figure 3b illustrates the separation of the generalization capability using different input states. In general, the test loss has worse performance with larger L . Meanwhile, the convergence performance is also influenced by the choice of parameterized gates, which is marked by different S values. For the case $S = 1$, the loss converges to non-zero values, implying the insufficient hypothesis space of the single-qubit unitary product. With larger S , the training loss exhibits increasingly pronounced and rapid linear convergence, which

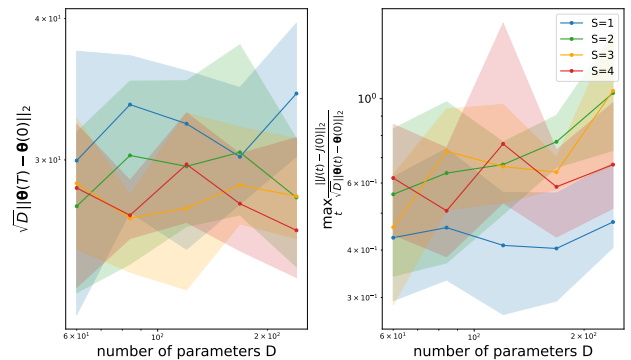


FIG. 5: Numerical results of QDL with FLDC input states, where $(N, L) = (12, 1)$ and $D \in \{60, 84, 120, 168, 240\}$. The left figure illustrates the ℓ_2 -norm distance in the parameter space from the initial to the final step. The right figure illustrates the largest coefficient in Eq. (20) during the training. Each solid line denotes the average of 5 rounds of simulations with independent circuits and parameters.

is further corroborated by the larger $\lambda_{\min}[K]$ shown in Figure 3d. Finally, we evaluate $D^{-1/2}$ and $D^{1/2}$ dependences in the frozen parameter result in Eq. (22) and the locally smooth assumption in Eq. (20). The results are shown in Figure 5 where we employ VQCs with different depths, such that the number of parameters has values $D \in \{60, 84, 120, 168, 240\}$. Both dependences are more evident as S increases to 4. In summary, we have verified theoretical results in Theorem 4.

B. Binary classification

In the second task, we evaluate the performance of binary classification using variational quantum circuits on the wine dataset [57]. This dataset comprises 138 instances from three different cultivars, with each instance featuring 13 measurements of various chemical components. For our experiment, we choose two wine types and divide the dataset into a training and a test set, each containing 30 samples, where samples from different classes $y = \pm 1$ are balanced in both sets. We use qubit embedding in Eq. (18) to encode the dataset information into $N = 13$ qubits quantum states. Variational quantum circuits are generated randomly in accordance with all-to-all connectivity, where Hamiltonians are sampled from $\{X, Y\}^{\otimes S}$ with $S \in \{1, 2, 3, 4\}$. We use the loss function (1) with the observable in Eq. (26). Coefficients are sampled from $c_n \sim \mathcal{N}(0, 2^S/N)$ to mitigate the local minima issue raised in recent studies [58, 59]. We training each optimization task with gradient descent with the learning rate $\eta = N/D$ for $T = 200$ steps.

We present numerical results in Figures 6 and 7. Figures 6a, 6b, 6c, and 6d plot the training loss, the test error, the gradient norm, and the least eigenvalue of the

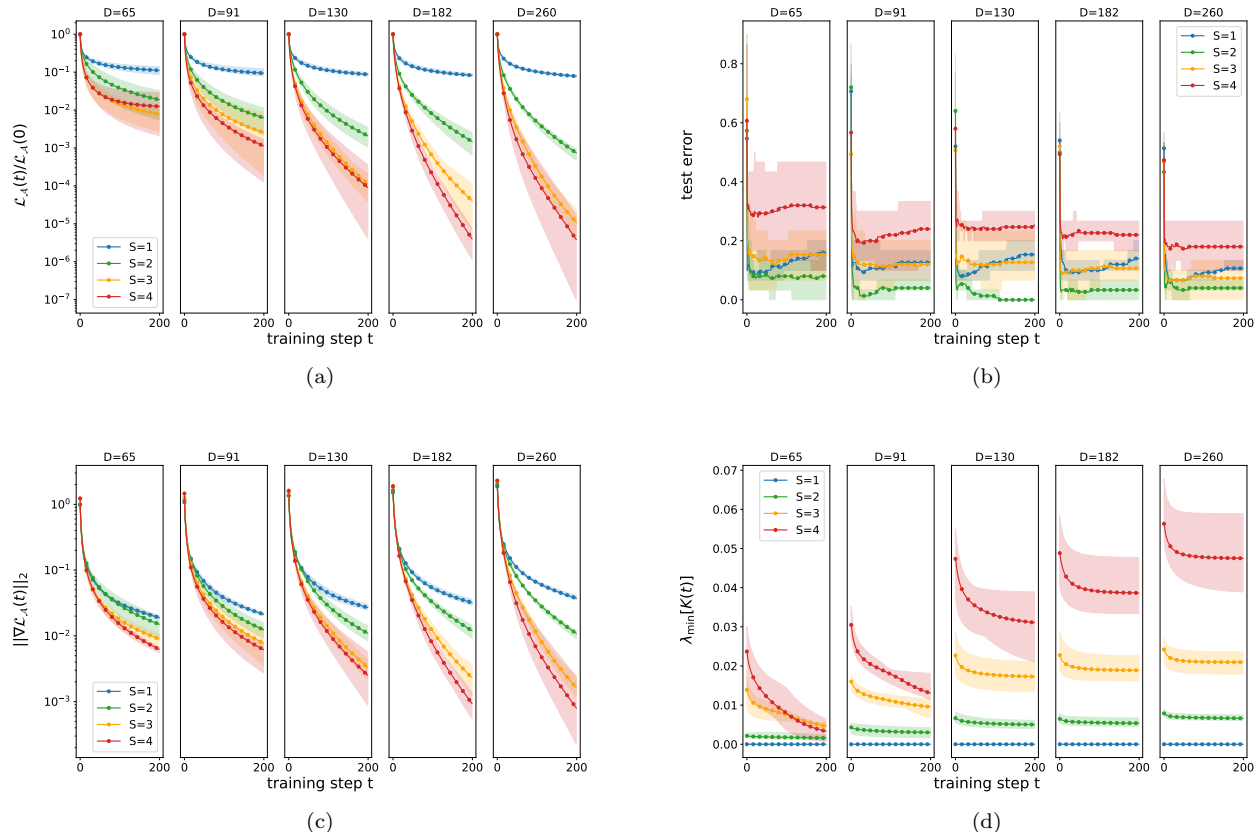


FIG. 6: Numerical results of the binary classification with the wine dataset, where $N = 13$ and $D \in \{65, 91, 130, 182, 260\}$. Figures 6a and 6b show the training loss the test error during the training, respectively. Figure 6c shows the $\ell - 2$ -norm of the gradient of the training loss. Figure 6d shows the least eigenvalue of the QNTK during the training. Each solid line denotes the average of 5 rounds of simulations with independent circuits and parameters.

QNTK during the training. Similar to Section III A, the training loss with qubit embedding exhibits increasingly pronounced and rapid linear convergence with increased S , which is further corroborated by the $\lambda_{\min}[K]$ performance in Figure 6d. However, the advantage on the training loss convergence does not always induce smaller error on the test set. As shown in Figure 6b, the test error increases slightly in later training stages, which is known as the overtraining issue. For the case $S = 1$, the error increases the most. Another phenomenon is the relatively worse performance of the case $S = 4$ compared with that of other S values, i.e. the overfitting. One potential reason of this phenomenon is that VQCs with large S could extract excessive features from input states. Thus the training of parameters could capture each training sample easily before learning enough knowledge to classify test samples. Therefore, an appropriate selection of S in a QNN should strike a balance between training convergence and generalization performance. We note that a detailed generalization analysis of QNNs with input states generated from qubit embed-

ding or other ensembles that deviate from 2-design states is beyond the scope of this work and could be an interesting direction for future research. Finally, we evaluate $D^{-1/2}$ and $D^{1/2}$ dependences in the frozen parameter result in Eq. (24) and the locally smooth assumption in Eq. (20). The results are shown in Figure 7. Similar to Section III A, both dependences are more evident as S increases to 4. In summary, we have verified theoretical results in Theorem 5.

IV. DISCUSSION

In this manuscript, we uncover the training and generalization issues of quantum machine learning with uniformly random quantum data. We demonstrate the separation performances of quantum datasets with different distributions in terms of the convergence rate and the generalization capability. Specifically, we prove fast linear convergence when optimizing the ℓ_2 -norm loss function under certain input state conditions. By studying

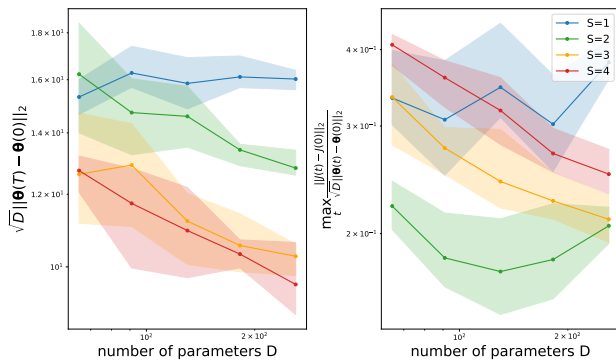


FIG. 7: Numerical results of the binary classification with the wine dataset, where $N = 13$ and $D \in \{65, 91, 130, 182, 260\}$. The left figure illustrates the ℓ_2 -norm distance in the parameter space from the initial to the final step. The right figure illustrates the largest coefficient in Eq. (20) during the training. Each solid line denotes the average of 5 rounds of simulations with independent circuits and parameters.

the lower bound of QNTK, we derive reasonable convergence rate when the number of parameters and the number of qubits in local Hamiltonians exceed some moderate thresholds. All proposed theorems are verified by numerical experiments.

Despite these advancements, further research is imperative for a more profound understanding of QNN training. Notably, our analysis relies on the random matrix theory and assumes certain stochastic properties of datasets. Although numerical experiments indicate favorable convergence with real-world datasets, elucidating training dynamics on datasets with explicit real-world or

quantum characteristics remains an area for future exploration. Furthermore, this research primarily analyzes QNNs from the perspective of dataset properties, and VQCs are initialized with zero parameters. We expect that theories with zero initialization could be engaged as technical tools in the study with other initializations by merging the initial VQC into input states. Another intriguing direction for future work is to refine the parameter threshold that guarantees the linear convergence, as experiments indicate rapid convergence for circuits with the number of parameters $D \sim 10^2$, which is significantly lower than our theoretical thresholds outlined in Section IID. Additionally, we hope that this manuscript could inspire further research into the convergence behavior of variational models with analogous structures, such as the training of tensor networks [60].

Acknowledgements.—We thank Jens Eisert for useful discussions. JL is supported in part by International Business Machines (IBM) Quantum through the Chicago Quantum Exchange, and the Pritzker School of Molecular Engineering at the University of Chicago through AFOSR MURI (FA9550-21-1-0209). LJ acknowledges support from ARO (W911NF-18-1-0020, W911NF-18-1-0212), ARO MURI (W911NF-16-1-0349, W911NF-21-1-0325), AFOSR MURI (FA9550-19-1-0399, FA9550-21-1-0209), AFRL (FA8649-21-P-0781), DoE Q-NEXT, NSF (OMA-1936118, EEC-1941583, OMA-2137642), NTT Research, and the Packard Foundation (2020-71479). This research used resources of the Oak Ridge Leadership Computing Facility, which is a DOE Office of Science User Facility supported under Contract DE-AC05-00OR22725.

-
- [1] Frank Arute, Kunal Arya, Ryan Babbush, Dave Bacon, Joseph C Bardin, Rami Barends, Rupak Biswas, Sergio Boixo, Fernando GSL Brandao, David A Buell, et al. Quantum supremacy using a programmable superconducting processor. *Nature*, 574(7779):505–510, 2019.
 - [2] Han-Sen Zhong, Hui Wang, Yu-Hao Deng, Ming-Cheng Chen, Li-Chao Peng, Yi-Han Luo, Jian Qin, Dian Wu, Xing Ding, Yi Hu, Peng Hu, Xiao-Yan Yang, Wei-Jun Zhang, Hao Li, Yuxuan Li, Xiao Jiang, Lin Gan, Guangwen Yang, Lixing You, Zhen Wang, Li Li, Nai-Le Liu, Chao-Yang Lu, and Jian-Wei Pan. Quantum computational advantage using photons. *Science*, 370(6523):1460–1463, 2020.
 - [3] John Preskill. Quantum computing in the nisq era and beyond. *Quantum*, 2:79, August 2018.
 - [4] Marco Cerezo, Andrew Arrasmith, Ryan Babbush, Simon C Benjamin, Suguru Endo, Keisuke Fujii, Jarrod R McClean, Kosuke Mitarai, Xiao Yuan, Lukasz Cincio, and Patrick J. Coles. Variational quantum algorithms. *Nature Reviews Physics*, pages 1–20, 2021.
 - [5] Maria Schuld, Alex Bocharov, Krysta M. Svore, and Nathan Wiebe. Circuit-centric quantum classifiers. *Phys. Rev. A*, 101:032308, Mar 2020.
 - [6] Vojtěch Havlíček, Antonio D Córcoles, Kristan Temme, Aram W Harrow, Abhinav Kandala, Jerry M Chow, and Jay M Gambetta. Supervised learning with quantum-enhanced feature spaces. *Nature*, 567(7747):209–212, 2019.
 - [7] Maria Schuld and Nathan Killoran. Quantum machine learning in feature hilbert spaces. *Phys. Rev. Lett.*, 122:040504, Feb 2019.
 - [8] Yuxuan Du, Min-Hsiu Hsieh, Tongliang Liu, and Dacheng Tao. Expressive power of parametrized quantum circuits. *Phys. Rev. Research*, 2:033125, Jul 2020.
 - [9] Samuel Yen-Chi Chen, Chao-Han Huck Yang, Jun Qi, Pin-Yu Chen, Xiaoli Ma, and Hsi-Sheng Goan. Variational quantum circuits for deep reinforcement learning. *IEEE Access*, 8:141007–141024, 2020.
 - [10] Valeria Saggio, Beate E Asenbeck, Arne Hamann, Teodor Strömberg, Peter Schiansky, Vedran Dunjko, Nicolai Friis, Nicholas C Harris, Michael Hochberg, Dirk Englund, et al. Experimental quantum speed-up in rein-

- forcement learning agents. *Nature*, 591(7849):229–233, 2021.
- [11] He-Liang Huang, Yuxuan Du, Ming Gong, Youwei Zhao, Yulin Wu, Chaoyue Wang, Shaowei Li, Futian Liang, Jin Lin, Yu Xu, Rui Yang, Tongliang Liu, Min-Hsiu Hsieh, Hui Deng, Hao Rong, Cheng-Zhi Peng, Chao-Yang Lu, Yu-Ao Chen, Dacheng Tao, Xiaobo Zhu, and Jian-Wei Pan. Experimental quantum generative adversarial networks for image generation. *Phys. Rev. Applied*, 16:024051, Aug 2021.
- [12] Yuxuan Du, Min-Hsiu Hsieh, Tongliang Liu, Shan You, and Dacheng Tao. Learnability of quantum neural networks. *PRX Quantum*, 2:040337, Nov 2021.
- [13] Michael Lubasch, Jaewoo Joo, Pierre Moinier, Martin Kiffner, and Dieter Jaksch. Variational quantum algorithms for nonlinear problems. *Phys. Rev. A*, 101:010301, Jan 2020.
- [14] Kenji Kubo, Yuya O. Nakagawa, Suguru Endo, and Shota Nagayama. Variational quantum simulations of stochastic differential equations. *Phys. Rev. A*, 103:052425, May 2021.
- [15] Yong-Xin Yao, Niladri Gomes, Feng Zhang, Cai-Zhuang Wang, Kai-Ming Ho, Thomas Iadecola, and Peter P. Orth. Adaptive variational quantum dynamics simulations. *PRX Quantum*, 2:030307, Jul 2021.
- [16] Hai-Ling Liu, Yu-Sen Wu, Lin-Chun Wan, Shi-Jie Pan, Su-Juan Qin, Fei Gao, and Qiao-Yan Wen. Variational quantum algorithm for the poisson equation. *Phys. Rev. A*, 104:022418, Aug 2021.
- [17] Oleksandr Kyriienko, Annie E. Paine, and Vincent E. Elfving. Solving nonlinear differential equations with differentiable quantum circuits. *Phys. Rev. A*, 103:052416, May 2021.
- [18] I. M. Georgescu, S. Ashhab, and Franco Nori. Quantum simulation. *Rev. Mod. Phys.*, 86:153–185, Mar 2014.
- [19] Xiao Yuan, Suguru Endo, Qi Zhao, Ying Li, and Simon C. Benjamin. Theory of variational quantum simulation. *Quantum*, 3:191, October 2019.
- [20] Sam McArdle, Tyson Jones, Suguru Endo, Ying Li, Simon C Benjamin, and Xiao Yuan. Variational ansatz-based quantum simulation of imaginary time evolution. *Npj Quantum Inf.*, 5(1):1–6, 2019.
- [21] Suguru Endo, Jinzhao Sun, Ying Li, Simon C. Benjamin, and Xiao Yuan. Variational quantum simulation of general processes. *Phys. Rev. Lett.*, 125:010501, Jun 2020.
- [22] C Neill, T McCourt, X Mi, Z Jiang, MY Niu, W Mruczkiewicz, I Aleiner, F Arute, K Arya, J Atalaya, et al. Accurately computing the electronic properties of a quantum ring. *Nature*, 594(7864):508–512, 2021.
- [23] Xiao Mi, Matteo Ippoliti, Chris Quintana, Ami Greene, Zijun Chen, Jonathan Gross, Frank Arute, Kunal Arya, Juan Atalaya, Ryan Babbush, et al. Time-crystalline eigenstate order on a quantum processor. *Nature*, pages 1–1, 2021.
- [24] J. Randall, C. E. Bradley, F. V. van der Grienden, A. Galicia, M. H. Abobeih, M. Markham, D. J. Twitchen, F. Machado, N. Y. Yao, and T. H. Taminiau. Many-body localized discrete time crystal with a programmable spin-based quantum simulator. *Science*, 374(6574):1474–1478, 2021.
- [25] Amita B. Deb and Niels Kjærgaard. Observation of pauli blocking in light scattering from quantum degenerate fermions. *Science*, 374(6570):972–975, 2021.
- [26] G. Semeghini, H. Levine, A. Keesling, S. Ebadi, T. T. Wang, D. Bluvstein, R. Verresen, H. Pichler, M. Kalinowski, R. Samajdar, A. Omran, S. Sachdev, A. Vishwanath, M. Greiner, V. Vuletić, and M. D. Lukin. Probing topological spin liquids on a programmable quantum simulator. *Science*, 374(6572):1242–1247, 2021.
- [27] K. J. Satzinger, Y.-J. Liu, A. Smith, C. Knapp, M. Newman, C. Jones, Z. Chen, C. Quintana, X. Mi, A. Dunsworth, et al. Realizing topologically ordered states on a quantum processor. *Science*, 374(6572):1237–1241, 2021.
- [28] Sam McArdle, Suguru Endo, Alán Aspuru-Guzik, Simon C. Benjamin, and Xiao Yuan. Quantum computational chemistry. *Rev. Mod. Phys.*, 92:015003, Mar 2020.
- [29] Alberto Peruzzo, Jarrod McClean, Peter Shadbolt, Man-Hong Yung, Xiao-Qi Zhou, Peter J Love, Alán Aspuru-Guzik, and Jeremy L O’Brien. A variational eigenvalue solver on a photonic quantum processor. *Nat. Commun.*, 5(1):1–7, 2014.
- [30] Abhinav Kandala, Antonio Mezzacapo, Kristan Temme, Maika Takita, Markus Brink, Jerry M Chow, and Jay M Gambetta. Hardware-efficient variational quantum eigensolver for small molecules and quantum magnets. *Nature*, 549(7671):242–246, 2017.
- [31] Cornelius Hempel, Christine Maier, Jonathan Romero, Jarrod McClean, Thomas Monz, Heng Shen, Petar Jurcevic, Ben P. Lanyon, Peter Love, Ryan Babbush, Alán Aspuru-Guzik, Rainer Blatt, and Christian F. Roos. Quantum chemistry calculations on a trapped-ion quantum simulator. *Phys. Rev. X*, 8:031022, Jul 2018.
- [32] Oscar Higgott, Daochen Wang, and Stephen Brierley. Variational quantum computation of excited states. *Quantum*, 3:156, July 2019.
- [33] Harper R Grimsley, Sophia E Economou, Edwin Barnes, and Nicholas J Mayhall. An adaptive variational algorithm for exact molecular simulations on a quantum computer. *Nat. Commun.*, 10(1):1–9, 2019.
- [34] Frank Arute, Kunal Arya, Ryan Babbush, Dave Bacon, Joseph C. Bardin, Rami Barends, Sergio Boixo, Michael Broughton, Bob B. Buckley, David A. Buell, et al. Hartree-fock on a superconducting qubit quantum computer. *Science*, 369(6507):1084–1089, 2020.
- [35] Ho Lun Tang, V.O. Shkolnikov, George S. Barron, Harper R. Grimsley, Nicholas J. Mayhall, Edwin Barnes, and Sophia E. Economou. Qubit-adapt-vqe: An adaptive algorithm for constructing hardware-efficient ansätze on a quantum processor. *PRX Quantum*, 2:020310, Apr 2021.
- [36] Alain Delgado, Juan Miguel Arrazola, Soran Jahangiri, Zeyue Niu, Josh Izaac, Chase Roberts, and Nathan Killoran. Variational quantum algorithm for molecular geometry optimization. *Phys. Rev. A*, 104:052402, Nov 2021.
- [37] Zhongchu Ni, Sai Li, Xiaowei Deng, Yanyan Cai, Libo Zhang, Weiting Wang, Zhen-Biao Yang, Haifeng Yu, Fei Yan, Song Liu, et al. Beating the break-even point with a discrete-variable-encoded logical qubit. *Nature*, 616(7955):56–60, 2023.
- [38] VV Sivak, Alec Eickbusch, Baptiste Royer, Shraddha Singh, Ioannis Tsioutsios, Suhas Ganjam, Alessandro Miano, BL Brock, AZ Ding, Luigi Frunzio, et al. Real-time quantum error correction beyond break-even. *Nature*, 616(7955):50–55, 2023.
- [39] Junyu Liu, Francesco Tacchino, Jennifer R. Glick, Liang Jiang, and Antonio Mezzacapo. Representation learning via quantum neural tangent kernels. *PRX Quantum*,

- 3:030323, Aug 2022.
- [40] Junyu Liu, Khadijeh Najafi, Kunal Sharma, Francesco Tacchino, Liang Jiang, and Antonio Mezzacapo. Analytic theory for the dynamics of wide quantum neural networks. *Phys. Rev. Lett.*, 130:150601, Apr 2023.
- [41] Junyu Liu, Zexi Lin, and Liang Jiang. Laziness, barren plateau, and noise in machine learning. *arXiv preprint arXiv:2206.09313*, 2022.
- [42] Bingzhi Zhang, Junyu Liu, Xiao-Chuan Wu, Liang Jiang, and Quntao Zhuang. Dynamical phase transition in quantum neural networks with large depth, 2023.
- [43] Xinbiao Wang, Junyu Liu, Tongliang Liu, Yong Luo, Yuxuan Du, and Dacheng Tao. Symmetric pruning in quantum neural networks. In *The Eleventh International Conference on Learning Representations*, 2023.
- [44] Zimu Li, Han Zheng, Yunfei Wang, Liang Jiang, Zi-Wen Liu, and Junyu Liu. Su (d)-symmetric random unitaries: Quantum scrambling, error correction, and machine learning. *arXiv preprint arXiv:2309.16556*, 2023.
- [45] Jarrod R McClean, Sergio Boixo, Vadim N Smelyanskiy, Ryan Babbush, and Hartmut Neven. Barren plateaus in quantum neural network training landscapes. *Nat. Commun.*, 9(1):1–6, 2018.
- [46] Marco Cerezo, Akira Sone, Tyler Volkoff, Lukasz Cincio, and Patrick J Coles. Cost function dependent barren plateaus in shallow parametrized quantum circuits. *Nat. Commun.*, 12(1):1–12, 2021.
- [47] A V Uvarov and J D Biamonte. On barren plateaus and cost function locality in variational quantum algorithms. 54(24):245301, may 2021.
- [48] Arthur Pesah, M. Cerezo, Samson Wang, Tyler Volkoff, Andrew T. Sornborger, and Patrick J. Coles. Absence of barren plateaus in quantum convolutional neural networks. *Phys. Rev. X*, 11:041011, 2021.
- [49] Andrea Skolik, Jarrod R McClean, Masoud Mohseni, Patrick van der Smagt, and Martin Leib. Layerwise learning for quantum neural networks. *Quantum Mach. Intell.*, 3(1):1–11, 2021.
- [50] Kaining Zhang, Min-Hsiu Hsieh, Liu Liu, and Dacheng Tao. Toward trainability of deep quantum neural networks. *arXiv:2112.15002*, 2021.
- [51] Kaining Zhang, Liu Liu, Min-Hsiu Hsieh, and Dacheng Tao. Escaping from the barren plateau via gaussian initializations in deep variational quantum circuits. 35:18612–18627, 2022.
- [52] Xinbiao Wang, Yuxuan Du, Zhuozhuo Tu, Yong Luo, Xiao Yuan, and Dacheng Tao. Transition role of entangled data in quantum machine learning. *Nature Communications*, 15(1):3716, May 2024.
- [53] Hao-Kai Zhang, Shuo Liu, and Shi-Xin Zhang. Absence of barren plateaus in finite local-depth circuits with long-range entanglement. *Phys. Rev. Lett.*, 132:150603, Apr 2024.
- [54] Seth Lloyd, Maria Schuld, Aroosa Ijaz, Josh Izaac, and Nathan Killoran. Quantum embeddings for machine learning. *arXiv:2001.03622*, 2020.
- [55] Martín Larocca, Nathan Ju, Diego García-Martín, Patrick J. Coles, and Marco Cerezo. Theory of overparametrization in quantum neural networks. *Nat. Comput. Sci.*, 3(6):542–551, Jun 2023.
- [56] F Bonechi, E Celeghini, R Giachetti, E Sorace, and M Tarlini. Heisenberg xxz model and quantum galilei group. *Journal of Physics A: Mathematical and General*, 25(15):L939–L943, aug 1992.
- [57] Dheeru Dua and Casey Graff. UCI machine learning repository, 2017.
- [58] Xuchen You and Xiaodi Wu. Exponentially many local minima in quantum neural networks. In *Proceedings of the 38th International Conference on Machine Learning*, volume 139 of *Proceedings of Machine Learning Research*, pages 12144–12155. PMLR, 18–24 Jul 2021.
- [59] Eric R Anschuetz and Bobak T Kiani. Quantum variational algorithms are swamped with traps. *Nat. Commun.*, 13(1):7760, 2022.
- [60] Edwin Stoudenmire and David J Schwab. Supervised learning with tensor networks. In D. Lee, M. Sugiyama, U. Luxburg, I. Guyon, and R. Garnett, editors, *Advances in Neural Information Processing Systems*, volume 29. Curran Associates, Inc., 2016.
- [61] Roman Vershynin. Introduction to the non-asymptotic analysis of random matrices. *arXiv:1011.3027*, 2010.
- [62] Pauline J Ollitrault, Alberto Baiardi, Markus Reiher, and Ivano Tavernelli. Hardware efficient quantum algorithms for vibrational structure calculations. *Chemical science*, 11(26):6842–6855, 2020.
- [63] Jaehoon Lee, Lechao Xiao, Samuel Schoenholz, Yasaman Bahri, Roman Novak, Jascha Sohl-Dickstein, and Jeffrey Pennington. Wide neural networks of any depth evolve as linear models under gradient descent. In *Advances in Neural Information Processing Systems*, volume 32. Curran Associates, Inc., 2019.

Supplemental Material

CONTENTS

I. Introduction	1
II. Theoretical results	2
A. Background of quantum machine learning	2
B. Generalization error with quantum data	2
C. Spectrum of QNTK with quantum data	3
D. Convergence analysis of training QNNs	5
III. Numerical Results	6
A. Quantum dynamics learning	6
B. Binary classification	7
IV. Discussion	8
References	9
A. Additional Numerical Results	S2
B. Technical Lemmas	S2
1. Lemmas about unitary t -designs	S3
2. Lemmas about variational quantum algorithms	S3
3. Lemmas about random matrix theory	S4
C. Generalization error of quantum machine learning with random quantum data	S5
1. Generalization error of quantum kernel method	S5
2. Generalization error of quantum neural network	S10
D. Spectral analysis of the quantum neural tangent kernel	S13
1. Bounds of $K_\infty(\mathbf{0})$	S15
2. Bounds of $\lambda_{\min}[K_\infty(\mathbf{0})]$ and $\lambda_{\max}[K_\infty(\mathbf{0})]$	S19
3. Proof of Lemma 1	S23
4. Proof of Lemma 2	S24
E. Linear convergence of QNN training	S26
1. QNN training in the locally smooth region	S26
2. Proof of Theorem 4	S28
3. Proof of Theorem 5	S29

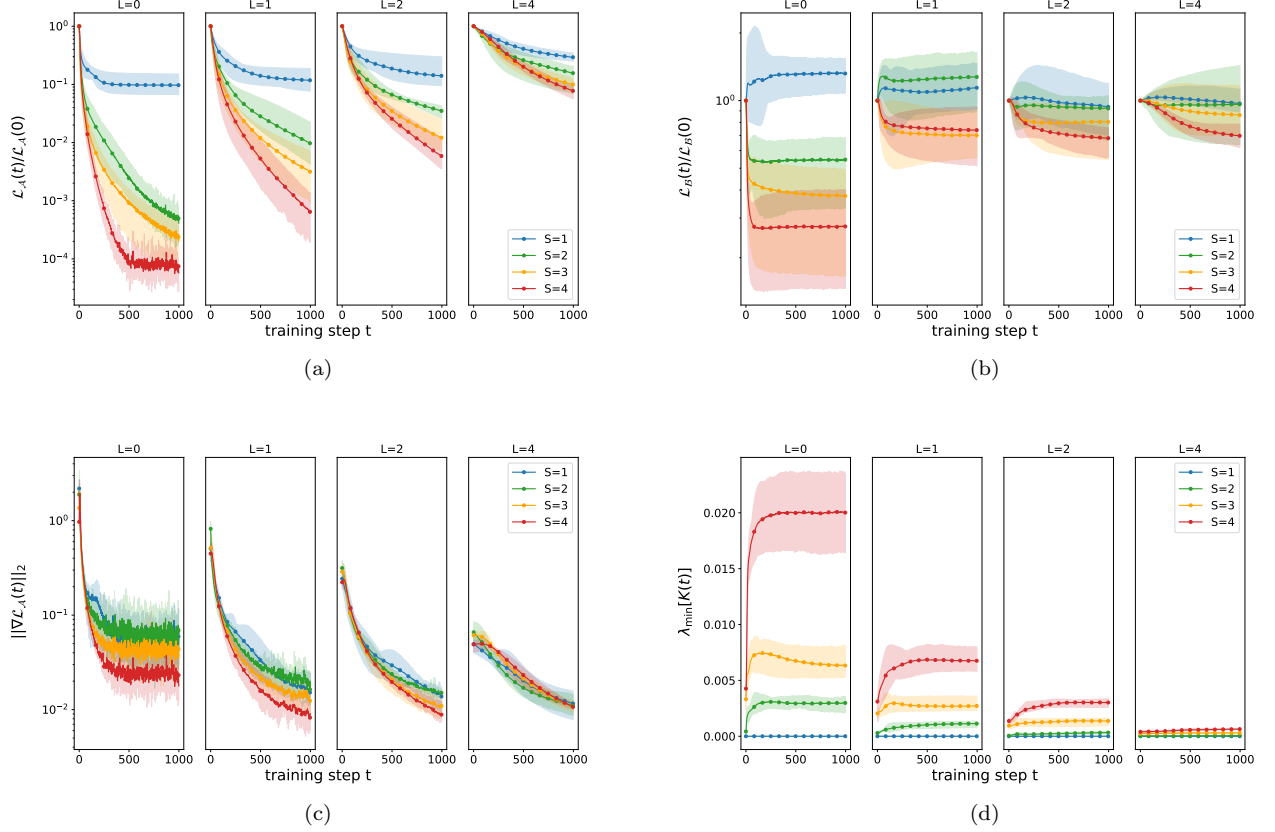


FIG. 8: Numerical results of QDL with FLDC input states and stochastic gradient descent, where $(N, D) = (12, 240)$ and $L \in \{0, 1, 2, 4\}$. Figures 8a and 8b show the relative loss of the training and the test dataset during the training, respectively. Figure 8c shows the ℓ_2 -norm of the gradient for the loss function. Figure 8d shows the least eigenvalue of the QNTK. Each solid line denotes the average of 5 rounds of simulations with independent circuits and parameters.

Appendix A: Additional Numerical Results

Here we present some additional numerical results. Figure 8 shows the training and generalization performance of the quantum dynamics learning with FLDC states using stochastic gradient descent (SGD) optimizer. We add Gaussian noise into gradients to simulate the finite shots noise (1000 shots) when estimating measurement outcomes via the parameter-shift rule. Compared with the exact case, the training loss decays linearly towards the noise level in the SGD case. In terms of the test loss and the least eigenvalue of the QNTK, the exact and noisy cases exhibit comparable performance.

Appendix B: Technical Lemmas

In this section, we introduce some helpful lemmas that are related to unitary t -design distributions, variational quantum algorithms, and random matrix theory.

1. Lemmas about unitary t -designs

Lemma S1 (from Ref. [46]). *Let $\{W_y\}_{y \in Y} \subset \mathcal{U}(d)$ form a unitary t -design with $t \geq 1$, and let $A, B : \mathcal{H}_w \rightarrow \mathcal{H}_w$ be arbitrary linear operators. Then*

$$\frac{1}{|Y|} \sum_{y \in Y} \text{Tr}[W_y A W_y^\dagger B] = \int d\mu(W) \text{Tr}[W A W^\dagger B] = \frac{\text{Tr}[A] \text{Tr}[B]}{d}. \quad (\text{B1})$$

Lemma S2 (from Ref. [46]). *Let $\{W_y\}_{y \in Y} \subset \mathcal{U}(d)$ form a unitary t -design with $t \geq 2$, and let $A, B, C, D : \mathcal{H}_w \rightarrow \mathcal{H}_w$ be arbitrary linear operators. Then*

$$\begin{aligned} \frac{1}{|Y|} \sum_{y \in Y} \text{Tr}[W_y A W_y^\dagger B] \text{Tr}[W_y C W_y^\dagger D] &= \int d\mu(W) \text{Tr}[W A W^\dagger B] \text{Tr}[W C W^\dagger D] \\ &= \frac{1}{d^2 - 1} (\text{Tr}[AC] \text{Tr}[BD] + \text{Tr}[A] \text{Tr}[B] \text{Tr}[C] \text{Tr}[D]) \\ &\quad - \frac{1}{d(d^2 - 1)} (\text{Tr}[A] \text{Tr}[C] \text{Tr}[BD] + \text{Tr}[AC] \text{Tr}[B] \text{Tr}[D]). \end{aligned} \quad (\text{B2})$$

2. Lemmas about variational quantum algorithms

Lemma S3. *Let $J_{da}(\boldsymbol{\theta}) = \frac{\partial z_a}{\partial \theta_d}(\boldsymbol{\theta})$ be the partial derivative of $z_a(\boldsymbol{\theta})$ in Eq. (2), where Hamiltonians $\{H_d\}_{d=1}^D$ in the ansatz $V(\boldsymbol{\theta}) = \prod_{d=D}^1 \exp(-iH_d \theta_d / 2) W_d$ are Hermitian unitary matrices. Let $V_{d:d'}$ be $\exp(-iH_d \theta_d / 2) W_d \exp(-iH_{d-1} \theta_{d-1} / 2) W_{d-1} \cdots \exp(-iH_{d'} \theta_{d'} / 2) W_{d'}$, then we have*

$$J_{da}(\boldsymbol{\theta}) = \frac{\partial z_a}{\partial \theta_d}(\boldsymbol{\theta}) = -\frac{i}{2} \text{Tr} \left[[V_{D:d+1}^\dagger O V_{D:d+1}, H_d] V_{d:1} \rho_a V_{d:1}^\dagger \right]. \quad (\text{B3})$$

Proof. We have

$$J_{da}(\boldsymbol{\theta}) = \frac{\partial}{\partial \theta_d} \text{Tr} \left[O V_{D:d+1} \exp(-iH_d \theta_d / 2) W_d V_{d-1:1} \rho_a V_{d-1:1}^\dagger W_d^\dagger \exp(iH_d \theta_d / 2) V_{D:d+1}^\dagger \right] \quad (\text{B4})$$

$$= \frac{\partial}{\partial \theta_d} \text{Tr} \left[V_{D:d+1}^\dagger O V_{D:d+1} \exp(-iH_d \theta_d / 2) W_d V_{d-1:1} \rho_a V_{d-1:1}^\dagger W_d^\dagger \exp(iH_d \theta_d / 2) \right] \quad (\text{B5})$$

$$\begin{aligned} &= \text{Tr} \left[V_{D:d+1}^\dagger O V_{D:d+1} \left(-\frac{i}{2} H_d \exp(-iH_d \theta_d / 2) W_d V_{d-1:1} \rho_a V_{d-1:1}^\dagger W_d^\dagger \exp(iH_d \theta_d / 2) \right) \right] \\ &\quad + \text{Tr} \left[V_{D:d+1}^\dagger O V_{D:d+1} \left(\exp(-iH_d \theta_d / 2) W_d V_{d-1:1} \rho_a V_{d-1:1}^\dagger W_d^\dagger \exp(iH_d \theta_d / 2) \frac{i}{2} H_d \right) \right] \end{aligned} \quad (\text{B6})$$

$$\begin{aligned} &= -\frac{i}{2} \text{Tr} \left[V_{D:d+1}^\dagger O V_{D:d+1} H_d V_{d:1} \rho_a V_{d:1}^\dagger \right] + \frac{i}{2} \text{Tr} \left[V_{D:d+1}^\dagger O V_{D:d+1} V_{d:1} \rho_m V_{d:1}^\dagger H_d \right] \\ &= -\frac{i}{2} \text{Tr} \left[V_{D:d+1}^\dagger O V_{D:d+1} [H_d, V_{d:1} \rho_a V_{d:1}^\dagger] \right] \\ &= -\frac{i}{2} \text{Tr} \left[[V_{D:d+1}^\dagger O V_{D:d+1}, H_d] V_{d:1} \rho_a V_{d:1}^\dagger \right]. \end{aligned} \quad (\text{B7})$$

Eq. (B4) follows from Eq. (2) and notations $V_{D:d+1}$, $V_{d:1}$. Eq. (B5) is derived by using $\text{Tr}[AB] = \text{Tr}[BA]$. Eq. (B6) follows from the matrix derivative. Eq. (B7) is derived by using the trace property

$$\text{Tr}[A[B, C]] = \text{Tr}[ABC] - \text{Tr}[ACB] = \text{Tr}[ABC] - \text{Tr}[BAC] = \text{Tr}[[A, B]C].$$

Thus, we have proved Eq. (B3). □

Lemma S4. *Let $X = \sum_{i \in \{0,1,2,3\}} \frac{1}{2} c_{X,i} \sigma_i$ and $Y = \sum_{j \in \{0,1,2,3\}} \frac{1}{2} c_{Y,j} \sigma_j$ be the Pauli decomposition of matrices X and Y with dimension $(2, 2)$. Denote by \mathbf{c}_{XY} the Pauli decomposition coefficient of XY , then*

$$\mathbf{c}_{XY} = \frac{1}{2} B(\mathbf{c}_X \otimes \mathbf{c}_Y), \quad (\text{B8})$$

Appendix C: Generalization error of quantum machine learning with random quantum data

This section is composed of two parts, i.e., the generalization error analysis of quantum machine learning using quantum kernel method and quantum neural network, respectively. Specifically, we consider the generalization performance when using 2-design quantum states as input datasets.

1. Generalization error of quantum kernel method

First, we study the generalization error of quantum kernel method. To begin with, we introduce some notations for convenience. The training and the test set are denoted by $\mathcal{A} = \{a\} = \{(\rho_a, y_a)\}$ and $\mathcal{B} = \{\hat{b}\} = \{(\rho_{\hat{b}}, y_{\hat{b}})\}$, respectively. We consider the linear model that gives the prediction

$$z_{\hat{b}}(\boldsymbol{\theta}) = \sum_{a \in \mathcal{A}} k(\rho_a, \rho_{\hat{b}}) \theta_a, \quad (\text{C1})$$

where $\boldsymbol{\theta} \in \mathbb{R}^{|\mathcal{A}|}$ is the parameter and $k(\rho_a, \rho_{\hat{b}}) = \text{Tr}[\rho_a \rho_{\hat{b}}]$ is the quantum kernel. For convenience, we denote $k_{a\hat{b}} = k(\rho_a, \rho_{\hat{b}})$. We use k as the $|\mathcal{A}| \times |\mathcal{A}|$ quantum kernel on the training set \mathcal{A} .

Suppose the loss is defined by the ℓ_2 -norm distance between the prediction vector \mathbf{z} and the label vector \mathbf{y} . Let $\boldsymbol{\theta}(t)$ and $\mathbf{z}(t)$ be the parameter and the prediction vector on training or test datasets at the optimization step t , respectively. Obviously we have

$$\boldsymbol{\theta}(0) = k^{-1} \mathbf{z}_{\mathcal{A}}(0) \quad (\text{C2})$$

from Eq. (C1). After the training, the linear model in Eq. (C1) can be optimized to achieve zero training loss with the parameter

$$\boldsymbol{\theta}(\infty) = k^{-1} \mathbf{y}_{\mathcal{A}}. \quad (\text{C3})$$

At the optimal parameter point, the prediction of a sample $\hat{b} = (\rho_{\hat{b}}, y_{\hat{b}})$ from the test dataset is given by

$$\begin{aligned} z_{\hat{b}}(\infty) &= \sum_{a' \in \mathcal{A}} k_{\hat{b}a'} \theta_{a'}(\infty) && (\text{from Eq. (C1)}) \\ &= \sum_{a, a' \in \mathcal{A}} k_{\hat{b}a'} [k^{-1}]_{a'a} y_a && (\text{from Eq. (C3)}) \\ &= \sum_{a, a' \in \mathcal{A}} k_{\hat{b}a'} [k^{-1}]_{a'a} (z_a(0) - r_a(0)) && (\text{from } r = z - y) \\ &= \sum_{a, a' \in \mathcal{A}} k_{\hat{b}a'} \theta_{a'}(0) - \sum_{a, a' \in \mathcal{A}} k_{\hat{b}a'} [k^{-1}]_{a'a} r_a(0) && (\text{from Eq. (C2)}) \\ &= z_{\hat{b}}(0) - \sum_{a, a' \in \mathcal{A}} k_{\hat{b}a'} [k^{-1}]_{a'a} r_a(0), && (\text{C4}) \end{aligned}$$

where $\mathbf{r}_{\mathcal{A}}(t) := \mathbf{z}_{\mathcal{A}}(t) - \mathbf{y}_{\mathcal{A}}$ is the training residual vector at the optimization step t . So, the residual of the sample \hat{b} after training is given by,

$$r_{\hat{b}}(\infty) = z_{\hat{b}}(\infty) - y_{\hat{b}} = r_{\hat{b}}(0) - \sum_{a, a' \in \mathcal{A}} k_{\hat{b}a'} [k^{-1}]_{a'a} r_a(0). \quad (\text{C5})$$

We denote $\mathcal{L}(t) := \mathcal{L}(\boldsymbol{\theta}(t))$ for convenience. Therefore, we obtain the generalization error,

$$\begin{aligned} \mathcal{E}_{\mathcal{B}|\mathcal{A}} &= \mathcal{L}_{\mathcal{B}}(\infty) - \mathcal{L}_{\mathcal{A}}(\infty) = \mathcal{L}_{\mathcal{B}}(\infty) = \frac{1}{2|\mathcal{B}|} \sum_{\hat{b} \in \mathcal{B}} r_{\hat{b}}^2(\infty) \\ &= \frac{1}{2|\mathcal{B}|} \sum_{\hat{b} \in \mathcal{B}} \left(r_{\hat{b}}(0) - \sum_{a, a' \in \mathcal{A}} k_{\hat{b}a'} [k^{-1}]_{a'a} r_a(0) \right)^2 \end{aligned} \quad (\text{C6})$$

$$= \frac{1}{2|\mathcal{B}|} \sum_{\hat{b} \in \mathcal{B}} r_{\hat{b}}^2(0) + \frac{1}{2|\mathcal{B}|} \sum_{\hat{b} \in \mathcal{B}} \left(\sum_{a, a' \in \mathcal{A}} k_{\hat{b}a'} [k^{-1}]_{a'a} r_a(0) \right)^2 \quad (\text{C7})$$

$$- \frac{1}{|\mathcal{B}|} \sum_{\hat{b} \in \mathcal{B}} \sum_{a, a' \in \mathcal{A}} k_{\hat{b}a'} [k^{-1}]_{a'a} r_{\hat{b}}(0) r_a(0). \quad (\text{C8})$$

We remark that the first term is the loss on the set \mathcal{B} before the training. To show the improvement of the prediction on the test dataset, we define the following quantity as the relative generalization error,

$$\mathcal{R}_{\mathcal{B}|\mathcal{A}} := \mathcal{E}_{\mathcal{B}|\mathcal{A}} - \mathcal{L}_{\mathcal{B}}(0) \quad (\text{C9})$$

$$= \frac{1}{2|\mathcal{B}|} \sum_{\hat{b} \in \mathcal{B}} \left(\sum_{a, a' \in \mathcal{A}} k_{\hat{b}a'} [k^{-1}]_{a'a} r_a(0) \right)^2 - \frac{1}{|\mathcal{B}|} \sum_{\hat{b} \in \mathcal{B}} \sum_{a, a' \in \mathcal{A}} k_{\hat{b}a'} [k^{-1}]_{a'a} r_{\hat{b}}(0) r_a(0) \quad (\text{C10})$$

$$= \frac{1}{2|\mathcal{B}|} \sum_{\hat{b} \in \mathcal{B}, a_1, a_2 \in \mathcal{A}} g_{\hat{b}a_1} g_{\hat{b}a_2} r_{a_1}(0) r_{a_2}(0) - \frac{1}{|\mathcal{B}|} \sum_{\hat{b} \in \mathcal{B}, a \in \mathcal{A}} g_{\hat{b}a} r_{\hat{b}}(0) r_a(0), \quad (\text{C11})$$

where we use the metric

$$g_{\hat{b}a} = \sum_{a' \in \mathcal{A}} k_{\hat{b}a'} [k^{-1}]_{a'a}. \quad (\text{C12})$$

When $\mathcal{R}_{\mathcal{B}|\mathcal{A}} \geq 0$, the element in set \mathcal{B} has equal or worse prediction averagely after the training, i.e., we face the overfitting issue. Therefore we hope $\mathcal{R}_{\mathcal{B}|\mathcal{A}} \leq -C$, where the constant $C > 0$ could be as large as possible.

Next, we analyze the scaling of generalization error when input datasets are sampled from state 2-designs. Specifically, suppose states $\rho_a = |\psi_a\rangle\langle\psi_a|$ in training and test datasets are independent 2-design states, i.e., $|\psi_a\rangle = U_a|0\rangle$ and U_{as} are randomly chosen from $\mathcal{U}(2^N)$ according to the unitary 2-design. The quantum kernel method gives

$$k_{ab} = \text{Tr}[\rho_a \rho_b] = |\langle\psi_a|\psi_b\rangle|^2.$$

Since input states are engaged in the quantum kernel, different state distributions could naturally induce different training and generalization performances. Here, we repeat the generalization error result in the main text in Theorem S1 for convenience, where the notation $\mathcal{L}(t) := \mathcal{L}(\boldsymbol{\theta}(t))$ is employed. The generalization error only has exponentially small improvement from the extremely overfitting situation.

Theorem S1. *Suppose all N -qubit quantum states in the training and test datasets \mathcal{A} and \mathcal{B} are independently sampled from state 2-designs and the size of datasets is smaller than $2^{N/2}$. Let $\mathcal{L}_{\mathcal{A}}(t)$ and $\mathcal{L}_{\mathcal{B}}(t)$ be the training and the test loss function at step t of the quantum kernel method, respectively. Then, with high probability,*

$$\mathbb{E} \mathcal{L}_{\mathcal{B}}(\infty) \gtrsim \mathbb{E} \mathcal{L}_{\mathcal{B}}(0) - \frac{|\mathcal{A}|}{2^{N-1}} \mathbb{E} \sqrt{\mathcal{L}_{\mathcal{A}}(0) \mathcal{L}_{\mathcal{B}}(0)}, \quad (\text{C13})$$

where the expectation is taken under state 2-designs for states in \mathcal{A} and \mathcal{B} .

Proof. The main idea is to find that the metric $g_{\hat{b}a}$ in Eq. (C12) is exponentially small on average. To achieve this, we first prove that for Haar-randomly distributed input states, the quantum kernel is close to the identity matrix with an additional exponentially small term. We refer to the Pauli decomposition form of quantum states with random matrix theory. Specifically, let $A \in \mathbb{R}^{(4^N - 1) \times |\mathcal{A}|}$ be the coefficient matrix that stores coefficients for input states $\{|\psi_a\rangle\}_{a \in \mathcal{A}}$,

$$A_{\mathbf{i}, a} = \frac{1}{2^N} \text{Tr} [|\psi_a\rangle\langle\psi_a| \sigma_{\mathbf{i}}], \quad (\text{C14})$$

where $\mathbf{i} \in \{0, 1, 2, 3\}^{\otimes N} \setminus \mathbf{0}$ denotes the index of Pauli matrices except the identity matrix: $\mathbf{i} = (i_1, i_2, \dots, i_N)$. We remark that the coefficient for the identity matrix is always $1/2^N$ since $\text{Tr}[|\psi_a\rangle\langle\psi_a|] = 1$, and the density matrix could be recovered as

$$|\psi_a\rangle\langle\psi_a| = \frac{1}{2^N} \sigma_{\mathbf{0}} + \sum_{\mathbf{i} \neq \mathbf{0}} A_{\mathbf{i},a} \sigma_{\mathbf{i}}. \quad (\text{C15})$$

Thus, the quantum kernel can be written as

$$\begin{aligned} k_{a'a} &= \text{Tr}[|\psi_{a'}\rangle\langle\psi_{a'}|\psi_a\rangle\langle\psi_a|] \\ &= \frac{1}{2^N} + \sum_{\mathbf{i}, \mathbf{j}} A_{\mathbf{i},a'} A_{\mathbf{j},a} \text{Tr}[\sigma_{\mathbf{i}} \sigma_{\mathbf{j}}] \quad (\text{using Eq. (C15)}) \\ &= \frac{1}{2^N} + 2^N [A^T A]_{a'a}. \end{aligned} \quad (\text{C16})$$

The matrix formulation of Eq. (C16) is

$$k = 2^N A^T A + \frac{1}{2^N} \mathbf{e} \mathbf{e}^T, \quad (\text{C17})$$

where $\mathbf{e} = (1, 1, \dots, 1)^T \in \mathbb{R}^{|\mathcal{A}|}$.

For random input states sampled independently from state 2-designs, the matrix A is a random matrix with independent columns, so we could apply Lemma S7 for analyzing the kernel property. To match the isotropic column condition in Lemma S7, we introduce the matrix

$$B = 2^N \sqrt{2^N + 1} A. \quad (\text{C18})$$

Matrix B has independent isotropic columns since

$$\begin{aligned} \mathbb{E}_{2\text{-design}} [B_{a'} B_a^T]_{ij} &= \mathbb{E}_{2\text{-design}} 2^{2N} (2^N + 1) A_{\mathbf{i},a'} A_{\mathbf{j},a} \quad (\text{using Eq. (C18)}) \\ &= \mathbb{E}_{2\text{-design}} (2^N + 1) \text{Tr}[|\psi_{a'}\rangle\langle\psi_{a'}|\sigma_{\mathbf{i}}] \text{Tr}[|\psi_a\rangle\langle\psi_a|\sigma_{\mathbf{j}}] \quad (\text{using Eq. (C14)}) \\ &= \delta_{a'a} \delta_{ij}. \quad (\text{using Lemmas S1 and S2}) \end{aligned}$$

The ℓ_2 -norm of B_a is $\sqrt{4^N - 1}$ since

$$\begin{aligned} \|B_a\|_2^2 &= 4^N (2^N + 1) \sum_{\mathbf{i}} A_{\mathbf{i},a}^2 \quad (\text{using Eq. (C18)}) \\ &= 4^N (2^N + 1) \frac{1}{2^N} \left(\text{Tr}[|\psi_a\rangle\langle\psi_a|^2] - \frac{1}{2^N} \right) \quad (\text{using Eq. (C15)}) \\ &= 4^N - 1. \end{aligned}$$

Moreover, we have

$$\begin{aligned} &\frac{1}{4^N - 1} \mathbb{E}_{2\text{-design}} \max_a \sum_{a' \neq a} (B_a^T B_{a'})^2 \\ &\leq \frac{1}{4^N - 1} \mathbb{E}_{2\text{-design}} \sum_{a \in \mathcal{A}} \sum_{a' \neq a} (B_a^T B_{a'})^2 \quad (\text{C19}) \\ &= \frac{16^N (2^N + 1)}{2^N - 1} \mathbb{E}_{2\text{-design}} \sum_{a \in \mathcal{A}} \sum_{a' \neq a} \left(\sum_{\mathbf{i}} A_{\mathbf{i},a} A_{\mathbf{i},a'} \right)^2 \quad (\text{using Eq. (C18)}) \\ &= \frac{16^N (2^N + 1)}{2^N - 1} \mathbb{E}_{2\text{-design}} \sum_{a \in \mathcal{A}} \sum_{a' \neq a} \frac{1}{4^N} \left(\text{Tr}[|\psi_a\rangle\langle\psi_a|\psi_{a'}\rangle\langle\psi_{a'}|] - \frac{1}{2^N} \right)^2 \quad (\text{using Eq. (C15)}) \\ &= \frac{4^N (2^N + 1)}{2^N - 1} \sum_{a \in \mathcal{A}} \sum_{a' \neq a} \left[\frac{2}{2^N (2^N + 1)} - \frac{2}{2^{2N}} + \frac{1}{2^{2N}} \right] \quad (\text{using Lemmas S1 and S2}) \\ &= |\mathcal{A}|^2 - |\mathcal{A}| \quad (\text{C20}) \end{aligned}$$

By using Lemma S7 with Eq. (C20), the following holds,

$$\mathbb{E}_{2\text{-design}} \left\| \frac{1}{4^N - 1} B^T B - I \right\|_F \leq C_0 \sqrt{\frac{(|\mathcal{A}|^2 - |\mathcal{A}|) \ln |\mathcal{A}|}{4^N - 1}}, \quad (\text{C21})$$

where C_0 is an absolute constant. Let the matrix $X = \frac{1}{4^N - 1} B^T B - I$. Using Eq. (C21) in the quantum kernel formulation, we have

$$k = I + \frac{1}{2^N} (\mathbf{e}\mathbf{e}^T - I) + \left(1 - \frac{1}{2^N}\right) X, \quad (\text{C22})$$

where $\mathbb{E}\|X\|_F \leq C_0 \sqrt{\frac{(|\mathcal{A}|^2 - |\mathcal{A}|) \ln |\mathcal{A}|}{4^N - 1}}$ by using Eqs. (C17) and (C18). Since $|\mathcal{A}|^2 \leq 2^N$, we use the norm bound of X as $\|X\|_F \leq \mathcal{O}(2^{-N})$ with high probability. Therefore the inverse

$$[k^{-1}]_{a'a} = \delta_{a'a} - \frac{1}{2^N} (1 - \delta_{a'a}) - X_{a'a} + \mathcal{O}\left(\frac{1}{4^N}\right) = 2\delta_{a'a} - k_{a'a} + \mathcal{O}\left(\frac{1}{4^N}\right) \quad (\text{C23})$$

with high probability. By employing Eq. (C23) in the metric g , we have

$$\begin{aligned} g_{\hat{b}a} &= \sum_{a' \in \mathcal{A}} k_{\hat{b}a'} \left(2\delta_{a'a} - k_{a'a} + \mathcal{O}\left(\frac{1}{4^N}\right) \right) \\ &= \mathcal{O}\left(\frac{|\mathcal{A}|}{4^N}\right) + \sum_{a' \in \mathcal{A}} k_{\hat{b}a'} (2\delta_{a'a} - k_{a'a}) \end{aligned} \quad (\text{C24})$$

which holds with high probability for all \hat{b} and a .

Then, we proceed to analyze the relative generalization error. By using Eq. (C11), we have

$$\mathbb{E} [\mathcal{E}_{\mathcal{B}|\mathcal{A}} - \mathcal{L}_{\mathcal{B}}(0)] = \frac{1}{2|\mathcal{B}|} \sum_{\hat{b} \in \mathcal{B}, a_1, a_2 \in \mathcal{A}} \mathbb{E}_{\hat{b}} \mathbb{E}_{a_1} \mathbb{E}_{a_2} \left[g_{\hat{b}a_1} g_{\hat{b}a_2} r_{a_1}(0) r_{a_2}(0) \right] - \frac{1}{|\mathcal{B}|} \sum_{\hat{b} \in \mathcal{B}, a \in \mathcal{A}} \mathbb{E}_{\hat{b}} \mathbb{E}_a \left[g_{\hat{b}a} r_{\hat{b}}(0) r_a(0) \right], \quad (\text{C25})$$

where \mathbb{E}_a or $\mathbb{E}_{\hat{b}}$ denotes the expectation of unitary 2-design distribution with respect to the unitary U that generates $U|0\rangle = |\psi_a\rangle$ or $U|0\rangle = |\psi_{\hat{b}}\rangle$.

Next, we analyze two terms in Eq. (C25) separately. First, we integrate the distribution with respect to \hat{b} in Eq. (C25). With high probability, we have

$$\begin{aligned} \mathbb{E}_{\hat{b}} \left[g_{\hat{b}a_1} g_{\hat{b}a_2} \right] &= \mathcal{O}\left(\frac{|\mathcal{A}|^2}{16^N}\right) + \mathcal{O}\left(\frac{|\mathcal{A}|}{4^N}\right) \sum_{a \in \{a_1, a_2\}} \sum_{a' \in \mathcal{A}} \mathbb{E}_{\hat{b}} [k_{\hat{b}a'}] (2\delta_{a'a} - k_{a'a}) \\ &\quad + \sum_{a'_1, a'_2 \in \mathcal{A}} \mathbb{E}_{\hat{b}} \left[k_{\hat{b}a'_1} k_{\hat{b}a'_2} \right] (2\delta_{a'_1 a_1} - k_{a'_1 a_1}) (2\delta_{a'_2 a_2} - k_{a'_2 a_2}) \end{aligned} \quad (\text{C26})$$

$$\begin{aligned} &= \mathcal{O}\left(\frac{|\mathcal{A}|^2}{16^N}\right) + \mathcal{O}\left(\frac{|\mathcal{A}|}{8^N}\right) \sum_{a \in \{a_1, a_2\}} \sum_{a' \in \mathcal{A}} (2\delta_{a'a} - k_{a'a}) + \frac{1}{2^N(2^N + 1)} [(2I - k)k(2I - k)]_{a_1 a_2} \\ &\quad + \frac{1}{2^N(2^N + 1)} \sum_{a'_1, a'_2 \in \mathcal{A}} (2\delta_{a'_1 a_1} - k_{a'_1 a_1}) (2\delta_{a'_2 a_2} - k_{a'_2 a_2}) \end{aligned} \quad (\text{C27})$$

$$\simeq \frac{1}{4^N} (2\delta_{a_1 a_2} - k_{a_1 a_2}) + \frac{1}{4^N} \sum_{a'_1, a'_2 \in \mathcal{A}} (2\delta_{a'_1 a_1} - k_{a'_1 a_1}) (2\delta_{a'_2 a_2} - k_{a'_2 a_2}). \quad (\text{C28})$$

Eq. (C26) follows from Eq. (C24). Eq. (C27) follows from Lemmas S1 and S2, which give $\mathbb{E}_{\hat{b}} [k_{\hat{b}a'}] = 2^{-N}$ and $\mathbb{E}_{\hat{b}} [k_{\hat{b}a'_1} k_{\hat{b}a'_2}] = \frac{1}{2^N(2^N + 1)} [k_{a'_1 a'_2} + 1]$, respectively. Eq. (C28) follows from $k^{-1} \approx 2I - k$ and the condition $|\mathcal{A}|^2 \leq 2^N$.

Thus, by writing the summation as the matrix-vector production form, we have

$$\begin{aligned}
& \sum_{a_1, a_2 \in \mathcal{A}} \mathbb{E}_{\hat{b}} \mathbb{E}_{a_1} \mathbb{E}_{a_2} \left[g_{\hat{b}a_1} g_{\hat{b}a_2} r_{a_1}(0) r_{a_2}(0) \right] \\
& \simeq \frac{1}{4^N} \mathbb{E}_{\mathcal{A}} \mathbf{r}_{\mathcal{A}}(0)^T (2I - k) \mathbf{r}_{\mathcal{A}}(0) + \frac{1}{4^N} \left[\mathbb{E}_{\mathcal{A}} \mathbf{e}^T (2I - k) \mathbf{r}_{\mathcal{A}}(0) \right]^2 \quad (\text{using Eq. (C28)}) \\
& = \frac{1}{4^N} \mathbb{E}_{\mathcal{A}} (\boldsymbol{\theta}(0)^T k - \mathbf{y}_{\mathcal{A}}^T) (2I - k) (k\boldsymbol{\theta}(0) - \mathbf{y}_{\mathcal{A}}) + \frac{1}{4^N} \left[\mathbb{E}_{\mathcal{A}} \mathbf{e}^T (2I - k) (k\boldsymbol{\theta}(0) - \mathbf{y}_{\mathcal{A}}) \right]^2 \quad (\text{using } \mathbf{r} = \mathbf{z} - \mathbf{y} \text{ and Eq. (C2)}) \\
& \simeq \frac{1}{4^N} \mathbb{E}_{\mathcal{A}} [\boldsymbol{\theta}(0)^T k \boldsymbol{\theta}(0) - \mathbf{y}_{\mathcal{A}}^T k \mathbf{y}_{\mathcal{A}} + 2\mathbf{y}_{\mathcal{A}}^T \mathbf{y}_{\mathcal{A}} - 2\boldsymbol{\theta}(0)^T \mathbf{y}_{\mathcal{A}}] \\
& + \frac{1}{4^N} \left\{ \mathbf{e}^T \boldsymbol{\theta}(0) - 2\mathbf{e}^T \mathbf{y}_{\mathcal{A}} + \mathbb{E}_{\mathcal{A}} \mathbf{e}^T k \mathbf{y}_{\mathcal{A}} \right\}^2 \quad (\text{using } k^{-1} \approx 2I - k) \\
& \simeq \frac{1}{4^N} \left\{ \boldsymbol{\theta}(0)^T \left[\left(1 - \frac{1}{2^N}\right) I + \frac{1}{2^N} \mathbf{e} \mathbf{e}^T \right] \boldsymbol{\theta}(0) - \mathbf{y}_{\mathcal{A}}^T \left[\left(1 - \frac{1}{2^N}\right) I + \frac{1}{2^N} \mathbf{e} \mathbf{e}^T \right] \mathbf{y}_{\mathcal{A}} + 2\mathbf{y}_{\mathcal{A}}^T \mathbf{y}_{\mathcal{A}} - 2\boldsymbol{\theta}(0)^T \mathbf{y}_{\mathcal{A}} \right\} \\
& + \frac{1}{4^N} \left\{ \mathbf{e}^T \boldsymbol{\theta}(0) - 2\mathbf{e}^T \mathbf{y}_{\mathcal{A}} + \mathbb{E}_{\mathcal{A}} \mathbf{e}^T \left[\left(1 - \frac{1}{2^N}\right) I + \frac{1}{2^N} \mathbf{e} \mathbf{e}^T \right] \mathbf{y}_{\mathcal{A}} \right\}^2 \quad (\text{using Eq. (C22) and } |\mathcal{A}|^2 \leq 2^N) \\
& \simeq \frac{1}{4^N} \left\{ \|\boldsymbol{\theta}(0) - \mathbf{y}_{\mathcal{A}}\|_2^2 + [\mathbf{e}^T (\boldsymbol{\theta}(0) - \mathbf{y}_{\mathcal{A}})]^2 \right\}. \quad (\text{C29})
\end{aligned}$$

Finally we proceed to the second term in Eq. (C25). With high probability, we have

$$\begin{aligned}
\mathbb{E}_{\hat{b}} [g_{\hat{b}a} r_{\hat{b}}(0)] & = \mathbb{E}_{\hat{b}} \left[g_{\hat{b}a} \left(-y_{\hat{b}} + \sum_{a' \in \mathcal{A}} k_{\hat{b}a'} \theta_{a'}(0) \right) \right] \quad (\text{using } r_{\hat{b}}(0) = z_{\hat{b}}(0) - y_{\hat{b}} = \sum_{a' \in \mathcal{A}} k_{\hat{b}a'} \theta_{a'}(0) - y_{\hat{b}}) \\
& = \mathbb{E}_{\hat{b}} \left[\left(\mathcal{O} \left(\frac{|\mathcal{A}|}{4^N} \right) + \sum_{a'' \in \mathcal{A}} k_{\hat{b}a''} (2\delta_{a''a} - k_{a''a}) \right) \left(-y_{\hat{b}} + \sum_{a' \in \mathcal{A}} k_{\hat{b}a'} \theta_{a'}(0) \right) \right] \quad (\text{C30})
\end{aligned}$$

$$\begin{aligned}
& = -\mathcal{O} \left(\frac{|\mathcal{A}|}{4^N} \right) y_{\hat{b}} + \mathcal{O} \left(\frac{|\mathcal{A}|}{4^N} \right) \sum_{a' \in \mathcal{A}} \theta_{a'}(0) \mathbb{E}_{\hat{b}} [k_{\hat{b}a'}] - y_{\hat{b}} \sum_{a'' \in \mathcal{A}} \mathbb{E}_{\hat{b}} [k_{\hat{b}a''}] (2\delta_{a''a} - k_{a''a}) \\
& + \sum_{a'' \in \mathcal{A}} \mathbb{E}_{\hat{b}} [k_{\hat{b}a''} k_{\hat{b}a''}] (2\delta_{a''a} - k_{a''a}) \theta_{a'}(0) \\
& = -\mathcal{O} \left(\frac{|\mathcal{A}|}{4^N} \right) y_{\hat{b}} + \mathcal{O} \left(\frac{|\mathcal{A}|}{8^N} \right) \sum_{a' \in \mathcal{A}} \theta_{a'}(0) - y_{\hat{b}} \sum_{a'' \in \mathcal{A}} \frac{1}{2^N} (2\delta_{a''a} - k_{a''a}) \\
& + \sum_{a'' \in \mathcal{A}} \frac{1}{2^N (2^N + 1)} [1 + k_{a''a''}] (2\delta_{a''a} - k_{a''a}) \theta_{a'}(0) \quad (\text{C31})
\end{aligned}$$

$$\begin{aligned}
& \simeq -y_{\hat{b}} \sum_{a'' \in \mathcal{A}} \frac{1}{2^N} (2\delta_{a''a} - k_{a''a}) + \sum_{a'' \in \mathcal{A}} \frac{1}{4^N} [1 + k_{a''a''}] (2\delta_{a''a} - k_{a''a}) \theta_{a'}(0). \quad (\text{C32})
\end{aligned}$$

Eq. (C30) follows from Eq. (C24). Eq. (C31) is derived by using Lemmas S1 and S2. By writing the summation as

the matrix-vector production form, we have

$$\begin{aligned} & \frac{1}{|\mathcal{B}|} \sum_{\hat{b} \in \mathcal{B}, a \in \mathcal{A}} \mathbb{E}_{\hat{b}} \mathbb{E}_a [g_{\hat{b}a} r_{\hat{b}}(0) r_a(0)] \\ & \simeq -\frac{1}{2^N |\mathcal{B}|} (\mathbf{e}^T \mathbf{y}_{\mathcal{B}}) \mathbb{E}_{\mathcal{A}} [\mathbf{e}^T (2I - k) \mathbf{r}_{\mathcal{A}}(0)] + \frac{1}{4^N |\mathcal{B}|} \mathbb{E}_{\mathcal{A}} [\boldsymbol{\theta}(0)^T (\mathbf{e} \mathbf{e}^T + k) (2I - k) \mathbf{r}_{\mathcal{A}}(0)] \quad (\text{using Eq. (C32)}) \end{aligned}$$

$$\begin{aligned} & = -\frac{1}{2^N |\mathcal{B}|} (\mathbf{e}^T \mathbf{y}_{\mathcal{B}}) \mathbb{E}_{\mathcal{A}} [\mathbf{e}^T (2I - k) (k\boldsymbol{\theta}(0) - \mathbf{y}_{\mathcal{A}})] + \frac{1}{4^N |\mathcal{B}|} \mathbb{E}_{\mathcal{A}} [\boldsymbol{\theta}(0)^T (\mathbf{e} \mathbf{e}^T + k) (2I - k) (k\boldsymbol{\theta}(0) - \mathbf{y}_{\mathcal{A}})] \quad (\text{C33}) \\ & \simeq -\frac{1}{2^N |\mathcal{B}|} (\mathbf{e}^T \mathbf{y}_{\mathcal{B}}) \left[\mathbf{e}^T \boldsymbol{\theta}(0) - \left(1 - \frac{|\mathcal{A}| - 1}{2^N}\right) \mathbf{e}^T \mathbf{y}_{\mathcal{A}} \right] \end{aligned}$$

$$+ \frac{1}{4^N |\mathcal{B}|} \left[\left(1 + \frac{1}{2^N}\right) (\mathbf{e}^T \boldsymbol{\theta}(0))^2 - \left(1 - \frac{|\mathcal{A}| - 1}{2^N}\right) \mathbf{e}^T \boldsymbol{\theta}(0) \mathbf{e}^T \mathbf{y}_{\mathcal{A}} + \left(1 - \frac{1}{2^N}\right) \boldsymbol{\theta}(0)^T \boldsymbol{\theta}(0) - \boldsymbol{\theta}(0)^T \mathbf{y}_{\mathcal{A}} \right] \quad (\text{C34})$$

$$\simeq -\frac{1}{2^N |\mathcal{B}|} (\mathbf{e}^T \mathbf{y}_{\mathcal{B}}) [\mathbf{e}^T \boldsymbol{\theta}(0) - \mathbf{e}^T \mathbf{y}_{\mathcal{A}}]. \quad (\text{C35})$$

Eq. (C33) is derived by using $\mathbf{r} = \mathbf{z} - \mathbf{y}$ and Eq. (C2). Eq. (C34) is derived by using $k^{-1} \approx 2I - k$ and

$$\mathbb{E} k_{aa'} = \frac{1}{2^N} + \left(1 - \frac{1}{2^N}\right) \delta_{aa'}, \quad (\text{C36})$$

where Eq. (C36) follows from Lemma S1. We remark that

$$\begin{aligned} \mathbb{E}_{\mathcal{A}} \mathbf{e}^T \mathbf{r}_{\mathcal{A}}(0) & = \mathbb{E}_{\mathcal{A}} \mathbf{e}^T k \boldsymbol{\theta}(0) - \mathbf{e}^T \mathbf{y}_{\mathcal{A}} \simeq \mathbf{e}^T \boldsymbol{\theta}(0) - \mathbf{e}^T \mathbf{y}_{\mathcal{A}}, \\ \mathbb{E}_{\mathcal{B}} \mathbf{e}^T \mathbf{r}_{\mathcal{B}}(0) & = \mathbb{E}_{\mathcal{B}} \sum_{\hat{b} \in \mathcal{B}} \sum_{a \in \mathcal{A}} k_{\hat{b}a} \theta_a(0) - y_{\hat{b}} \simeq -\mathbf{e}^T \mathbf{y}_{\mathcal{B}}. \end{aligned} \quad (\text{C37})$$

Using Eqs. (C29) and (C35) in Eq. (C25), we have

$$\mathbb{E} [\mathcal{E}_{\mathcal{B}|\mathcal{A}} - \mathcal{L}_{\mathcal{B}}(0)] \simeq \frac{1}{2^N |\mathcal{B}|} (\mathbf{e}^T \mathbf{y}_{\mathcal{B}}) [\mathbf{e}^T \boldsymbol{\theta}(0) - \mathbf{e}^T \mathbf{y}_{\mathcal{A}}] \quad (\text{C38})$$

$$\simeq -\frac{1}{2^N |\mathcal{B}|} \mathbb{E}_{\mathcal{A}} \mathbf{e}^T \mathbf{r}_{\mathcal{A}}(0) \mathbb{E}_{\mathcal{B}} \mathbf{e}^T \mathbf{r}_{\mathcal{B}}(0) \quad (\text{C39})$$

$$\geq -\frac{\sqrt{|\mathcal{A}||\mathcal{B}|}}{2^N |\mathcal{B}|} \mathbb{E}_{\mathcal{A}} \|\mathbf{r}_{\mathcal{A}}(0)\|_2 \mathbb{E}_{\mathcal{B}} \|\mathbf{r}_{\mathcal{B}}(0)\|_2 \quad (\text{C40})$$

$$= -\frac{|\mathcal{A}|}{2^{N-1}} \mathbb{E} \sqrt{\mathcal{L}_{\mathcal{A}}(0) \mathcal{L}_{\mathcal{B}}(0)}. \quad (\text{C41})$$

□

2. Generalization error of quantum neural network

Next, we consider the quantum machine learning model utilizing variational quantum circuit to generate predications for input samples. Specifically, we denote by

$$V(\boldsymbol{\theta}) = \prod_{d=D}^1 G_d(\theta_d) W_d = \prod_{d=D}^1 \exp(-iH_d \theta_d / 2) W_d \quad (\text{C42})$$

the variational quantum circuit parameterized by $\boldsymbol{\theta} \in \mathbb{R}^D$, where W_d and H_d denote the fixed unitary gate and the Hamiltonian, respectively. We assume that all Hamiltonians $\{H_d\}$ are unitary Hermitians. Let the observable be O . For the sample $\rho_a \in \mathcal{A}$, the predication at training step t is given by

$$z_a(t) = \text{Tr} [OV(\boldsymbol{\theta}(t))\rho_a V(\boldsymbol{\theta}(t))^\dagger]. \quad (\text{C43})$$

The QNTK is

$$K(t) := K(\boldsymbol{\theta}(t)) = \frac{1}{D} J(\boldsymbol{\theta}(t))^T J(\boldsymbol{\theta}(t)), \quad (\text{C44})$$

where the Jacobian matrix $J(\boldsymbol{\theta}) \in \mathbb{R}^{D \times |\mathcal{A}|}$ with elements $J_{da}(\boldsymbol{\theta}) = \frac{\partial z_a}{\partial \theta_d}(\boldsymbol{\theta})$. For convenience, we assume the value of initial parameter $\theta_d(0)$ is absorbed into the fixed unitary W_d , i.e., $\theta_d(0) \equiv 0$. By using Lemma S3, we denote

$$J_{da} := J_{da}(\mathbf{0}) = -\frac{i}{2} \text{Tr} \left[[W_{D:d+1}^\dagger O W_{D:d+1}, H_d] W_{d:1} \rho_a W_{d:1}^\dagger \right], \quad (\text{C45})$$

where $W_{d:d'} = W_d W_{d-1} \cdots W_{d'}$. We assume the frozen QNTK during training, i.e.

$$K(t) = K(0) = K = \frac{1}{D} J^T J. \quad (\text{C46})$$

Similar to the quantum kernel method, property of input states could affect QNTK and the corresponding generalization behavior. Here we provide a negative example under the frozen QNTK regime for datasets from state 2-designs. The generalization error result in the main text is repeated in Theorem S2 for convenience.

Theorem S2. *Suppose all N -qubit quantum states in the training and test datasets \mathcal{A} and \mathcal{B} are independently sampled from state 2-designs. Let $\mathcal{L}_{\mathcal{A}}(t)$ and $\mathcal{L}_{\mathcal{B}}(t)$ be the training and the test loss function of the quantum neural network (Eqs. (3) and (5)) at the t -th step, where the label is given as $y := \text{Tr}[OU\rho U^\dagger]$ for a target unitary U with the zero trace observable O . Then, under the frozen QNTK regime,*

$$\mathbb{E} \mathcal{L}_{\mathcal{B}}(\infty) \geq \left(1 - \frac{|\mathcal{A}|}{2^{2N} - 1}\right) \mathbb{E} \mathcal{L}_{\mathcal{B}}(0), \quad (\text{C47})$$

where the expectation is taken under 2-designs distributions for states in \mathcal{A} and \mathcal{B} and the target unitary U .

Proof. After the training, the loss on the training set \mathcal{A} should be zero. By using Eq. (34) in Ref. [39], we have

$$z_{\hat{b}}(\infty) = z_{\hat{b}}(0) - \sum_{a, a' \in \mathcal{A}} \tilde{K}_{\hat{b}a'} [K^{-1}]_{a'a} r_a(0) \quad (\text{C48})$$

under the frozen QNTK regime, where \tilde{K} denotes the QNTK for the whole dataset $\mathcal{A} \cup \mathcal{B}$. Notice that Eq. (C48) shares the same formulation with Eq. (C4). After some calculation, we could derive the generalization error,

$$\mathcal{R}_{\mathcal{B}|\mathcal{A}} := \mathcal{E}_{\mathcal{B}|\mathcal{A}} - \mathcal{L}_{\mathcal{B}}(0) \quad (\text{C49})$$

$$= \frac{1}{2|\mathcal{B}|} \sum_{\hat{b} \in \mathcal{B}, a_1, a_2 \in \mathcal{A}} g_{\hat{b}a_1} g_{\hat{b}a_2} r_{a_1}(0) r_{a_2}(0) - \frac{1}{|\mathcal{B}|} \sum_{\hat{b} \in \mathcal{B}, a \in \mathcal{A}} g_{\hat{b}a} r_{\hat{b}}(0) r_a(0), \quad (\text{C50})$$

where the metric

$$g_{\hat{b}a} = \sum_{a' \in \mathcal{A}} \tilde{K}_{\hat{b}a'} [K^{-1}]_{a'a}. \quad (\text{C51})$$

We remark that $g_{\hat{b}a} \in \mathbb{R}$ since all entries in the QNTK are real elements. Therefore, the first term in Eq. (C50) is a positive semidefinite quadratic form, which is greater than or equal to zero. Thus, it suffices to show the following result:

$$\mathbb{E}_{\mathcal{A}} \mathbb{E}_{\mathcal{B}} \mathbb{E}_U [g_{\hat{b}a} r_{\hat{b}}(0) r_a(0)] \leq \frac{1}{2^{2N} - 1} \mathbb{E}_{\mathcal{B}} \mathbb{E}_U \mathcal{L}_{\mathcal{B}}(0). \quad (\text{C52})$$

The rest part of the proof is to derive Eq. (C52). First, we calculate the expectation of the initial loss on the test set. The main idea is to conduct the average over the distribution of the target unitary U , and then deal with the sample \hat{b} . We have

$$\mathbb{E}_{\mathcal{B}} \mathbb{E}_U \mathcal{L}_{\mathcal{B}}(0) = \frac{1}{2|\mathcal{B}|} \sum_{\hat{b} \in \mathcal{B}} \mathbb{E}_{\hat{b}} \left[\mathbb{E}_U \left[(z_{\hat{b}}(0) - y_{\hat{b}})^2 \right] \right] \quad (\text{using } r = z(0) - y)$$

$$= \frac{1}{2|\mathcal{B}|} \sum_{\hat{b} \in \mathcal{B}} \mathbb{E}_{\hat{b}} \left[\mathbb{E}_U \left[\left(\text{Tr}[O W_{D:1} \rho_{\hat{b}} W_{D:1}^\dagger] - \text{Tr}[O U \rho_{\hat{b}} U^\dagger] \right)^2 \right] \right] \quad (\text{C53})$$

$$= \frac{1}{2|\mathcal{B}|} \sum_{\hat{b} \in \mathcal{B}} \mathbb{E}_{\hat{b}} \left[\left(\text{Tr}[O W_{D:1} \rho_{\hat{b}} W_{D:1}^\dagger] \right)^2 + \frac{1}{2^N (2^N + 1)} \text{Tr}[O^2] \right] \quad (\text{C54})$$

$$= \frac{1}{2^N (2^N + 1)} \text{Tr}[O^2]. \quad (\text{C55})$$

Eq. (C53) follows by using the detailed formulation of $z_{\hat{b}}(0)$ and $y_{\hat{b}}$ in terms of measurement results. The variational quantum circuit is denoted as $W_{D:1}$. Eq. (C54) is derived by taking the average over the distribution of U using Lemma S2 and the condition $\text{Tr}[O] = 0$. Eq. (C55) is derived similarly by taking the average over the distribution of $U_{\hat{b}}$ in $\rho_{\hat{b}} := U_{\hat{b}}|0\rangle\langle 0|U_{\hat{b}}^\dagger$ using Lemma S2 and the condition $\text{Tr}[O] = 0$.

Next, we calculate the expectation in the left part of Eq. (C52). The main idea is to first decompose $g_{\hat{b}a}$ into items with independent \hat{b} or a . Next, we conduct the average over the distribution of the target unitary U , and then deal with the sample \hat{b} . We finish the decomposition and the expectation of the U part as follows,

$$\begin{aligned}
\mathbb{E}_{\mathcal{A}} \mathbb{E}_{\mathcal{B}} \mathbb{E}_U [g_{\hat{b}a} r_{\hat{b}}(0) r_a(0)] &= \mathbb{E}_{\mathcal{A}} \mathbb{E}_{\hat{b}} \left[\sum_{a' \in \mathcal{A}} [K^{-1}]_{a'a} \tilde{K}_{\hat{b}a'} \mathbb{E}_U [r_{\hat{b}}(0) r_a(0)] \right] && \text{(using Eq. (C51))} \\
&= \frac{1}{D} \sum_{d=1}^D \mathbb{E}_{\mathcal{A}} \left[\sum_{a' \in \mathcal{A}} [K^{-1}]_{a'a} J_{da'} \mathbb{E}_{\hat{b}} \left[J_{d\hat{b}} \mathbb{E}_U [r_{\hat{b}}(0) r_a(0)] \right] \right] && \text{(using Eq. (C46))} \\
&= \frac{1}{D} \sum_{d=1}^D \mathbb{E}_{\mathcal{A}} \left[\sum_{a' \in \mathcal{A}} [K^{-1}]_{a'a} J_{da'} z_a(0) \mathbb{E}_{\hat{b}} [J_{d\hat{b}} z_{\hat{b}}(0)] \right] \\
&\quad + \frac{1}{(2^{2N} - 1)D} \text{Tr}[O^2] \sum_{d=1}^D \mathbb{E}_{\mathcal{A}} \left[\sum_{a' \in \mathcal{A}} [K^{-1}]_{a'a} J_{da'} \mathbb{E}_{\hat{b}} [J_{d\hat{b}} \text{Tr}[\rho_a \rho_{\hat{b}}]] \right] \\
&\quad - \frac{1}{2^N (2^{2N} - 1)D} \text{Tr}[O^2] \sum_{d=1}^D \mathbb{E}_{\mathcal{A}} \left[\sum_{a' \in \mathcal{A}} [K^{-1}]_{a'a} J_{da'} \mathbb{E}_{\hat{b}} [J_{d\hat{b}}] \right]. && \text{(C56)}
\end{aligned}$$

Eq. (C56) is obtained by taking the expectation of U as follows,

$$\begin{aligned}
\mathbb{E}_U [r_{\hat{b}}(0) r_a(0)] &= \mathbb{E}_U (z_{\hat{b}}(0) - y_{\hat{b}}) (z_a(0) - y_a) && \text{(using } r(0) = z(0) - y) \\
&= \mathbb{E}_U (z_{\hat{b}}(0) - \text{Tr}[OU \rho_{\hat{b}} U^\dagger]) (z_a(0) - \text{Tr}[OU \rho_a U^\dagger]) \\
&= z_{\hat{b}}(0) z_a(0) + \frac{1}{2^{2N} - 1} \text{Tr}[O^2] \text{Tr}[\rho_a \rho_{\hat{b}}] - \frac{1}{2^N (2^{2N} - 1)} \text{Tr}[O^2], && \text{(C57)}
\end{aligned}$$

where Eq. (C57) follows from Lemmas S1 and S2 and the condition $\text{Tr}[O] = 0$.

Next, we deal with the three $\mathbb{E}_{\hat{b}}$ -related terms in Eq. (C56) separately. The third $\mathbb{E}_{\hat{b}}$ -related term in Eq. (C56) is

$$\mathbb{E}_{\hat{b}} [J_{d\hat{b}}] = \frac{-i}{2} \mathbb{E}_{\hat{b}} \left[\text{Tr} \left[[W_{D:d+1}^\dagger O W_{D:d+1}, H_d] W_{d:1} \rho_{\hat{b}} W_{d:1}^\dagger \right] \right] \quad \text{(C58)}$$

$$= \frac{-i}{2 \times 2^N} \text{Tr} \left[W_{d:1}^\dagger [W_{D:d+1}^\dagger O W_{D:d+1}, H_d] W_{d:1} \right] \quad \text{(C59)}$$

$$= \frac{-i}{2 \times 2^N (2^N + 1)} \text{Tr} \left[[W_{D:d+1}^\dagger O W_{D:d+1}, H_d] \right] \quad \text{(C60)}$$

$$= 0. \quad \text{(C61)}$$

Eq. (C58) follows from the formulation of the partial derivative in Eq. (C45). Eq. (C59) follows by taking the average over the distribution of $U_{\hat{b}}$ in $\rho_{\hat{b}} := U_{\hat{b}}|0\rangle\langle 0|U_{\hat{b}}^\dagger$ using Lemma S1. Eq. (C60) is derived by using $\text{Tr}[ABC] = \text{Tr}[BCA]$. Eq. (C61) is derived by using $\text{Tr}[[A, B]] = \text{Tr}[AB - BA] = 0$.

The second $\mathbb{E}_{\hat{b}}$ -related term in Eq. (C56) is

$$\mathbb{E}_{\hat{b}} [J_{d\hat{b}} \text{Tr}[\rho_a \rho_{\hat{b}}]] = \frac{-i}{2} \mathbb{E}_{\hat{b}} \left[\text{Tr} \left[[W_{D:d+1}^\dagger O W_{D:d+1}, H_d] W_{d:1} \rho_{\hat{b}} W_{d:1}^\dagger \right] \text{Tr} [\rho_a \rho_{\hat{b}}] \right] \quad \text{(using Eq. (C45))}$$

$$\begin{aligned}
&= \frac{-i}{2 \times 2^N (2^N + 1)} \text{Tr} \left[W_{d:1}^\dagger [W_{D:d+1}^\dagger O W_{D:d+1}, H_d] W_{d:1} \right] \text{Tr} [\rho_a] \\
&\quad + \frac{-i}{2 \times 2^N (2^N + 1)} \text{Tr} \left[W_{d:1}^\dagger [W_{D:d+1}^\dagger O W_{D:d+1}, H_d] W_{d:1} \rho_a \right] && \text{(C62)}
\end{aligned}$$

$$= \frac{-i}{2 \times 2^N (2^N + 1)} \text{Tr} \left[W_{d:1}^\dagger [W_{D:d+1}^\dagger O W_{D:d+1}, H_d] W_{d:1} \rho_a \right]. \quad \text{(C63)}$$

Eq. (C62) follows by taking the average over the distribution of $U_{\hat{b}}$ in $\rho_{\hat{b}} := U_{\hat{b}}|0\rangle\langle 0|U_{\hat{b}}^\dagger$ using Lemma S2. Eq. (C63) follows by noticing that the first term in Eq. (C62) equals to zero by using the derivation in Eqs. (C59-C61).

The first $\mathbb{E}_{\hat{b}}$ -related term in Eq. (C56) is

$$\mathbb{E}_{\hat{b}} [J_{d\hat{b}} z_{\hat{b}}(0)] = \frac{-i}{2} \mathbb{E}_{\hat{b}} \left[\text{Tr} \left[[W_{D:d+1}^\dagger \overline{O} W_{D:d+1}, H_d] W_{d:1} \rho_{\hat{b}} W_{d:1}^\dagger \right] \text{Tr} \left[O W_{D:1} \rho_{\hat{b}} W_{D:1}^\dagger \right] \right] \quad (\text{using Eq. (C45)})$$

$$\begin{aligned} &= \frac{-i}{2 \times 2^N (2^N + 1)} \text{Tr} \left[W_{d:1}^\dagger [W_{D:d+1}^\dagger \overline{O} W_{D:d+1}, H_d] W_{d:1} \right] \text{Tr} \left[W_{D:1}^\dagger \overline{O} W_{D:1} \right] \\ &\quad + \frac{-i}{2 \times 2^N (2^N + 1)} \text{Tr} \left[W_{d:1}^\dagger [W_{D:d+1}^\dagger \overline{O} W_{D:d+1}, H_d] W_{d:1} W_{D:1}^\dagger \overline{O} W_{D:1} \right] \end{aligned} \quad (\text{C64})$$

$$= \frac{-i}{2 \times 2^N (2^N + 1)} \text{Tr} \left[[W_{D:d+1}^\dagger \overline{O} W_{D:d+1}, H_d] W_{D:d+1}^\dagger \overline{O} W_{D:d+1} \right] \quad (\text{C65})$$

$$= 0. \quad (\text{C66})$$

Eq. (C64) follows by taking the average over the distribution of $U_{\hat{b}}$ in $\rho_{\hat{b}} := U_{\hat{b}}|0\rangle\langle 0|U_{\hat{b}}^\dagger$ using Lemma S2. Eq. (C65) follows by noticing that the first term in Eq. (C64) equals to zero by using the derivation in Eqs. (C59-C61). Eq. (C66) follows by noticing that $\text{Tr}[[A, B]A] = \text{Tr}[ABA - BAA] = 0$.

By using Eq. (C61), (C63), and (C66) jointly in Eq. (C56), we obtain

$$\begin{aligned} &\mathbb{E}_{\mathcal{A}} \mathbb{E}_{\mathcal{B}} \mathbb{E}_{\mathcal{U}} [g_{ba} r_{\hat{b}}(0) r_a(0)] \\ &= \frac{-i}{2^{N+1} (2^N + 1) (2^{2N} - 1) D} \text{Tr}[O^2] \sum_{d=1}^D \mathbb{E}_{\mathcal{A}} \left[\sum_{a' \in \mathcal{A}} [K^{-1}]_{a'a} J_{da'} \text{Tr} \left[W_{d:1}^\dagger [W_{D:d+1}^\dagger \overline{O} W_{D:d+1}, H_d] W_{d:1} \rho_a \right] \right] \\ &= \frac{1}{2^N (2^N + 1) (2^{2N} - 1) D} \text{Tr}[O^2] \sum_{d=1}^D \mathbb{E}_{\mathcal{A}} \left[\sum_{a' \in \mathcal{A}} [K^{-1}]_{a'a} J_{da'} J_{da} \right] \quad (\text{using Eq. (C45)}) \\ &= \frac{1}{2^N (2^N + 1) (2^{2N} - 1)} \text{Tr}[O^2] \mathbb{E}_{\mathcal{A}} \left[\sum_{a' \in \mathcal{A}} [K^{-1}]_{a'a} K_{aa'} \right] \quad (\text{using Eq. (C46)}) \\ &= \frac{1}{2^N (2^N + 1) (2^{2N} - 1)} \text{Tr}[O^2]. \end{aligned} \quad (\text{C67})$$

Comparing Eqs. (C55) and (C67), we obtain Eq. (C52). Thus, we have proved Theorem S2. \square

Appendix D: Spectral analysis of the quantum neural tangent kernel

We begin with a warm-up example that shows the exponentially small spectrum of QNTK with 2-designs states as datasets.

Lemma S8. *Let $\mathcal{A}\{\rho_a, y_a\}$ be the training datasets with independent N -qubit 2-design states ρ_a . Denote by $z_a = \text{Tr}[OV(\boldsymbol{\theta})\rho_a V(\boldsymbol{\theta})^\dagger]$ the QNN with the observable O and the variational circuit $V(\boldsymbol{\theta}) = \prod_{d=D}^1 \exp[-iH_d \theta_d / 2] W_d$, where the hamiltonian H_d is Hermitian unitary and W_d is the fixed unitary. Then the QNTK has exponentially small spectrum, i.e. there exists a constant $C > 0$ such that*

$$\lambda_{\max} [K(\boldsymbol{\theta})] \leq \frac{\|O\|_F^2}{4^N} \left(1 + \frac{C|\mathcal{A}|}{2^N \delta} \sqrt{\ln |\mathcal{A}|} \right) \quad (\text{D1})$$

with probability at least $1 - \delta$.

Proof. We follow notations in Lemma S3. For convenience, we assume the value of each parameter θ_d is absorbed into the fixed unitary W_d , i.e., $\theta_d \equiv 0$. Denote by

$$O_d := -\frac{i}{2} W_{d:1}^\dagger [W_{D:d+1}^\dagger \overline{O} W_{D:d+1}, H_d] W_{d:1}. \quad (\text{D2})$$

We can write the partial derivative of z_a in the formulation with Pauli decomposition coefficients:

$$\begin{aligned}
\frac{\partial z_a}{\partial \theta_d} &= \text{Tr}[O_d \rho_a] && \text{(using Lemma S3)} \\
&= \frac{1}{2^N} [B^\otimes (\mathbf{c}_{O_d} \otimes \mathbf{c}_{\rho_a})]_{\mathbf{0}} && \text{(using notation in Lemma S5)} \\
&= \frac{1}{2^N} \mathbf{c}_{O_d}^T \mathbf{c}_{\rho_a}. && \text{(calculating } B^\otimes \text{ in Lemma S5)}
\end{aligned}$$

Therefore, the Jacobian matrix is

$$J = \frac{1}{2^N} C_O^T A, \quad (\text{D3})$$

where $C_O \in \mathbb{R}^{(4^N-1) \times D}$ stores the Pauli decomposition of matrices $\{O_d\}_{d=1}^D$ for $d \in \{1, 2, \dots, D\}$. We remark that the each matrix O_d only corresponds to $4^N - 1$ coefficients since the coefficient $c_{O_d, \mathbf{0}} = \frac{1}{2^N} \text{Tr}[O_d I] = 0$. Similarly the matrix $A \in \mathbb{R}^{(4^N-1) \times |\mathcal{A}|}$ stores the Pauli decomposition of states $\{\rho_a\}_{a \in \mathcal{A}}$, which is the same with the notation in Eq. (C14). By using Eq. (9), the QNTK is

$$\begin{aligned}
K(\boldsymbol{\theta}) &= \frac{1}{D} J^T J \\
&= \frac{1}{4^N D} A^T C_O C_O^T A.
\end{aligned}$$

Thus, the largest eigenvalue is upper bounded as

$$\lambda_{\max}[K(\boldsymbol{\theta})] \leq \frac{1}{4^N D} \lambda_{\max}[A^T A] \lambda_{\max}[C_O C_O^T]. \quad (\text{D4})$$

We remark that by using Eqs. (C18-C21), there exists a constant $C > 0$ such that

$$\lambda_{\max}[A^T A] \leq \frac{1}{2^N} + \frac{C|\mathcal{A}|}{4^N \delta} \sqrt{\ln |\mathcal{A}|} \quad (\text{D5})$$

with probability at least $1 - \delta$. Besides, we have

$$\begin{aligned}
& \lambda_{\max} [C_O C_O^T] \\
& \leq \|C_O\|_F^2 \\
& = \sum_{d=1}^D \sum_{\mathbf{i} \in \{0,1,2,3\}^N / \mathbf{0}} (c_{O_d, \mathbf{i}})^2 \\
& = \sum_{d=1}^D 2^N \text{Tr} [O_d^2] \tag{using Lemma S5} \\
& = -2^{N-2} \sum_{d=1}^D \text{Tr} \left[\left(W_{d:1}^\dagger [W_{D:d+1}^\dagger O W_{D:d+1}, H_d] W_{d:1} \right)^2 \right] \tag{using Eq. (D2)} \\
& = -2^{N-2} \sum_{d=1}^D \text{Tr} \left[[W_{D:d+1}^\dagger O W_{D:d+1}, H_d]^2 \right] \\
& = 2^{N-1} \sum_{d=1}^D \text{Tr} \left[O \left(O - W_{D:d+1} H_d W_{D:d+1}^\dagger O W_{D:d+1} H_d W_{D:d+1}^\dagger \right) \right] \\
& = 2^{N-1} \sum_{d=1}^D \|O\|_F \left\| O - W_{D:d+1} H_d W_{D:d+1}^\dagger O W_{D:d+1} H_d W_{D:d+1}^\dagger \right\|_F \\
& \leq 2^{N-1} \sum_{d=1}^D \|O\|_F \left(\|O\|_F + \left\| W_{D:d+1} H_d W_{D:d+1}^\dagger O W_{D:d+1} H_d W_{D:d+1}^\dagger \right\|_F \right) \\
& = 2^{N-1} \sum_{d=1}^D \|O\|_F \left(\|O\|_F + \sqrt{\text{Tr} \left[\left(W_{D:d+1} H_d W_{D:d+1}^\dagger O W_{D:d+1} H_d W_{D:d+1}^\dagger \right)^2 \right]} \right) \tag{Tr}[X^\dagger X] = \|X\|_F^2} \\
& = 2^{N-1} \sum_{d=1}^D \|O\|_F \left(\|O\|_F + \sqrt{\text{Tr} [O^2]} \right) \tag{Tr}[XY] = \text{Tr}[YX]} \\
& = 2^N D \|O\|_F^2. \tag{D6}
\end{aligned}$$

Collaborating Eqs. (D4), (D5), and (D6), we obtain Eq. (D1). \square

The remaining part of this section focuses on the spectrum of the asymptotic QNTK with non-uniformly distributed quantum states, i.e. the QNTK with infinite number of gates and parameters, which is denoted by

$$K_\infty(\boldsymbol{\theta}) = \lim_{D \rightarrow +\infty} K(\boldsymbol{\theta}) = \lim_{D \rightarrow +\infty} \frac{1}{D} J(\boldsymbol{\theta})^T J(\boldsymbol{\theta}). \tag{D7}$$

Specifically, we consider the N -qubit ansatz $V(\boldsymbol{\theta}) = \prod_{d=D}^1 G_d(\theta_d)$, where each gate $G_d(\theta_d) = \exp[-iH_d\theta_d/2]$ is implemented on qubits $\mathcal{S}_d \subseteq \{1, 2, \dots, N\}$ with $|\mathcal{S}_d| = S$. Each Hamiltonian is sampled from the set \mathcal{H} . We assume general assignments of the qubits set $\mathcal{Q} := \{\mathcal{S}_d\}$ if there has no additional instruction. One example of \mathcal{Q} is shown in Fig. 9, where each \mathcal{S}_d is deployed in the hardware-efficient manner [62] with N different choices.

1. Bounds of $K_\infty(\mathbf{0})$

Let $A \in \mathbb{R}^{4^N \times |\mathcal{A}|}$ be the matrix that stores the Pauli decomposition coefficients of input states $\{\rho_a\}_{a \in \mathcal{A}}$, i.e. $A_{\mathbf{p}a} = \text{Tr}[\sigma_{\mathbf{p}} \rho_a]$. As shown in Lemmas S9 and S10, $K_\infty(\mathbf{0})$ could be bounded by the linear sum of the gram of the sub-matrix of A , where we consider $\mathcal{H} = \{X, Y, Z\}^{\otimes S}$ and $\mathcal{H} = \{X, Y\}^{\otimes S}$, respectively.

Lemma S9. *Let the observable be $O = \sum_{k=1}^N o_k Z_k$, where each Z_k is the product of Pauli matrices that is Z on the k -th qubit and I on other qubits. Denote by H_d the Hamiltonian of the d -th quantum gate in the circuit $V(\boldsymbol{\theta}) = \prod_{d=D}^1 \exp[-iH_d\theta_d/2]$ that acts on qubits $\mathcal{S}_d \subseteq \{1, 2, \dots, N\}$. We assume that H_d is randomly sampled from*

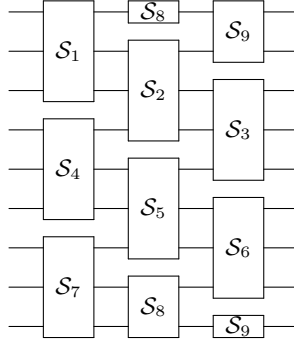


FIG. 9: An assignment of $\mathcal{Q} = \{\mathcal{S}_1, \dots, \mathcal{S}_N\}$ in the hardware-efficient manner for $(N, S) = (9, 3)$.

the set $\mathcal{H} := \{H, H \in \{X, Y, Z\}^{\otimes S}\}$. Let $\mathcal{Q} := \{\mathcal{S}_d\}$. Let $A \in \mathbb{R}^{4^N \times |A|}$ be the matrix with elements $A_{\mathbf{p}a} = \text{Tr}[\sigma_{\mathbf{p}} \rho_a]$. Then the asymptotic QNTK at $\boldsymbol{\theta} = \mathbf{0}$ could be bounded as

$$\frac{1}{3^S |\mathcal{Q}|} \sum_{w=0}^{S-1} \|O\|_2^2 A_{\mathcal{Q},w}^T A_{\mathcal{Q},w} \succcurlyeq K_\infty(\mathbf{0}) \succcurlyeq \frac{1}{3^S |\mathcal{Q}|} \sum_{w=0}^{S-1} \Delta_{S-w} A_{\mathcal{Q},w}^T A_{\mathcal{Q},w}, \quad (\text{D8})$$

where we denote by \succcurlyeq the semi-definite partial order and $\Delta_j := \min_{\mathbf{g} \in \{0, \pm 1\}^{\otimes N}, 1 \leq \|\mathbf{g}\|_1 \leq j} (\mathbf{g}^T \mathbf{o})^2$. The matrix $A_{\mathcal{Q},w}$ is formed by extracting rows from matrix A corresponding to indices \mathbf{p} , if there exists some $\mathcal{S}_d \in \mathcal{Q}$ that matches the non-zero elements in \mathbf{p} with w numbers of element 3.

Proof. Denote by σ_i the Hamiltonian H_d . Denote by $K_d \in \mathbb{R}^{|A| \times |A|}$ the QNTK corresponding to the gate G_d at $\boldsymbol{\theta} = \mathbf{0}$. By using Lemma S3, we have

$$[K_d]_{aa'} = \frac{\partial z_a}{\partial \theta_d}(\mathbf{0}) \frac{\partial z_{a'}}{\partial \theta_d}(\mathbf{0}) = -\frac{1}{4} \text{Tr} \left[[O, \sigma_i] \rho_a \right] \text{Tr} \left[[O, \sigma_i] \rho_{a'} \right]. \quad (\text{D9})$$

We remark that σ_i and each Z_i in the linear sum of the observable are products of Pauli matrices, so $[Z_i, \sigma_i]$ could be 0 or $2Z_i \sigma_i$. For convenience, we proceed to analyze the term $\text{Tr} \left[[O, \sigma_i] \rho_a \right]$ first:

$$\text{Tr} \left[[O, \sigma_i] \rho_a \right] = \sum_{k=1}^N o_k \text{Tr} \left[[Z_k, \sigma_i] \rho_a \right] \quad (\text{using } O = \sum_{k=1}^N o_k Z_k)$$

$$= \sum_{k=1}^N o_k \text{Tr} \left[\frac{1}{2^N} \sum_{\mathbf{p} \in \{0,1,2,3\}^{\otimes N}} c_{[Z_k, \sigma_i], \mathbf{p}} \sigma_{\mathbf{p}} \frac{1}{2^N} \sum_{\mathbf{p}' \in \{0,1,2,3\}^{\otimes N}} c_{\rho_a, \mathbf{p}'} \sigma_{\mathbf{p}'} \right] \quad (\text{D10})$$

$$= \sum_{k=1}^N o_k \frac{1}{2^N} \sum_{\mathbf{p} \in \{0,1,2,3\}^{\otimes N}} c_{[Z_k, \sigma_i], \mathbf{p}} A_{\mathbf{p}a} \quad (\text{D11})$$

$$= \sum_{k=1}^N o_k \frac{1}{4^N} \sum_{\mathbf{p} \in \{0,1,2,3\}^{\otimes N}} [B^{\otimes} (\mathbf{c}_{Z_k} \otimes \mathbf{c}_{\sigma_i}) - B^{\otimes} (\mathbf{c}_{\sigma_i} \otimes \mathbf{c}_{Z_k})]_{\mathbf{p}} A_{\mathbf{p}a} \quad (\text{D12})$$

$$= \sum_{k=1}^N o_k \sum_{\mathbf{p} \in \{0,1,2,3\}^{\otimes N}} [2i B_k \mathbf{e}_{i'}]_{\mathbf{p}} A_{\mathbf{p}a} \quad (\text{D13})$$

$$= \sum_{k=1}^N 2o_k i [A^T B_k]_{a i'}. \quad (\text{D14})$$

Eq. (D10) is derived by using the Pauli decomposition with coefficients: $X = \frac{1}{2^N} \sum_{\mathbf{p}} c_{X, \mathbf{p}} \sigma_{\mathbf{p}}$. Eq. (D11) is derived by tracing out the index \mathbf{p}' and using the notation $A_{\mathbf{p}a}$. Eq. (D12) follows from Lemma S5, where B^{\otimes} follows the notation in Lemma S5. Eq. (D13) is derived by using the formulation of B^{\otimes} , where the notation i' is defined by zero-padding the vector $i \in \{1, 2, 3\}^{\otimes S}$ in the space $\{0, 1, 2, 3\}^{\otimes N}$. We denote $\mathbf{e}_{i'} := \otimes_{q=1}^N e_{i'_q}$, which is a 4^N -dimensional vector,

and

$$B_k = I_4^{\otimes(k-1)} \otimes \begin{bmatrix} & & & 0 \\ & & -1 & \\ & 1 & & \\ 0 & & & \end{bmatrix} \otimes I_4^{\otimes(N-k)}. \quad (\text{D15})$$

Thus, the average of K_d w.r.t. the Hamiltonian set $\mathcal{H} = \{X, Y, Z\}^{\otimes S}$ is

$$\mathbb{E}_{H_d \in \mathcal{H}} [K_d]_{aa'} = \frac{1}{3^S} \sum_{H_d \in \{X, Y, Z\}^{\otimes S}} -\frac{1}{4} \text{Tr} [O, H_d] \rho_a \text{Tr} [O, H_d] \rho_{a'} \quad (\text{D16})$$

$$= \frac{1}{3^S} \sum_{\mathbf{i} \in \{1, 2, 3\}^{\otimes S}} \sum_{k, k'=1}^N o_k o_{k'} [A^T B_k]_{a\mathbf{i}'} [A^T B_{k'}]_{a'\mathbf{i}}. \quad (\text{D17})$$

Eqs. (D16) and (D17) are derived by using Eqs. (D9) and (D14), respectively.

Next, we proceed with the matrix formulation K_d . We have

$$\mathbb{E}_{H_d \in \mathcal{H}} K_d = \frac{1}{3^S} \sum_{w=0}^{S-1} \sum_{\substack{\mathbf{z}=(z_1, \dots, z_w) \\ \{z_1, \dots, z_w\} \subset \mathcal{S}_d}} \sum_{\mathbf{i}/i_{\mathbf{z}} \in \{1, 2\}^{\otimes(S-w)}} \sum_{k, k'=1}^N o_k o_{k'} \{ [A^T B_k]_{a\mathbf{i}'} [A^T B_{k'}]_{a'\mathbf{i}} \}_{aa'} \quad (\text{D18})$$

$$= \frac{1}{3^S} \sum_{k, k' \in \mathcal{S}_d} o_k o_{k'} A_d^T C_k C_{k'}^T A_d + \frac{1}{3^S} \sum_{w=1}^{S-1} \sum_{\substack{\mathbf{z}=(z_1, \dots, z_w) \\ \{z_1, \dots, z_w\} \subset \mathcal{S}_d}} \sum_{k, k' \in \mathcal{S}_d / \{z_1, \dots, z_w\}} o_k o_{k'} A_{d, \mathbf{z}}^T C_{k, \mathbf{z}} C_{k', \mathbf{z}}^T A_{d, \mathbf{z}}. \quad (\text{D19})$$

We obtain Eq. (D18) by rearranging the summation with kernels corresponding to Hamiltonians with $w \in \{0, 1, \dots, S\}$ number of Z components, where the case $w = S$ induces a zero term by noticing $[Z^{\otimes S}, O] = 0$. Eq. (D19) follows from using notations A_d , $A_{d, \mathbf{z}}$, C_k , and $C_{k, \mathbf{z}}$. The matrix $A_d \in \mathbb{R}^{2^S \times |A|}$ is derived by extracting rows from matrix A corresponding to indices from the set $\{\mathbf{i} | i_x \in \{1, 2\} \forall x \in \mathcal{S}_d, i_x = 0 \forall x \notin \mathcal{S}_d\}$. The matrix $A_{d, \mathbf{z}} \in \mathbb{R}^{2^{S-w} \times |A|}$ is derived by extracting rows from matrix A corresponding to indices from the set

$$\left\{ \mathbf{i} = (i_1, \dots, i_N) | i_x \in \{1, 2\} \forall x \in \mathcal{S}_d / \{z_1, \dots, z_w\}, i_x = 3 \forall x \in \{z_1, \dots, z_w\}, i_x = 0 \forall x \notin \mathcal{S}_d \right\}. \quad (\text{D20})$$

The matrix $C_k \in \mathbb{R}^{2^S \times 2^S}$ is derived by extracting columns and rows from B_k corresponding to indices from the set mentioned above, i.e.,

$$C_k = I_2^{\otimes(k_d-1)} \otimes \begin{bmatrix} & -1 \\ 1 & \end{bmatrix} \otimes I_2^{\otimes(S-k_d)}, \quad (\text{D21})$$

where k_d is the index of k in the set \mathcal{S}_d . The matrix $C_{k, \mathbf{z}} \in \mathbb{R}^{2^{S-w} \times 2^{S-w}}$ is obtained from matrix C_k by dropping tensor product components corresponding to indices in \mathbf{z} .

We remark that both C_k and $C_{k, \mathbf{z}}$ are of full rank with singular values ± 1 . Therefore the eigenvalue of the positive semi-definite matrix $\sum_{k, k' \in \mathcal{S}_d} o_k o_{k'} C_k C_{k'}^T$ can be bounded as follows

$$\|O\|_2^2 = \left(\sum_{k=1}^N |o_k| \right)^2 \geq \sum_{k, k' \in \mathcal{S}_d} |o_k| |o_{k'}| \geq \lambda \left[\sum_{k, k' \in \mathcal{S}_d} o_k o_{k'} C_k C_{k'}^T \right] \geq \min_{\mathbf{g} \in \{-1, 1\}^{\otimes S}} (\mathbf{g}^T \mathbf{o}_d)^2 \geq \Delta_S, \quad (\text{D22})$$

where we denote by $\mathbf{o}_d \in \mathbb{R}^S$ the vector formed by extracting elements in \mathbf{o} corresponding to indices in \mathcal{S}_d . Similarly, we have

$$\|O\|_2^2 \geq \lambda \left(\sum_{k, k' \in \mathcal{S}_d / \{z_1, \dots, z_w\}} o_k o_{k'} C_{k, \mathbf{z}} C_{k', \mathbf{z}}^T \right) \geq \min_{\mathbf{g} \in \{-1, 1\}^{\otimes(S-w)}} (\mathbf{g}^T \mathbf{o}_{d, \mathbf{z}})^2 \geq \Delta_{S-w}, \quad (\text{D23})$$

where we denote by $\mathbf{o}_{d, \mathbf{z}} \in \mathbb{R}^{S-w}$ the vector formed by extracting elements in \mathbf{o} corresponding to indices in $\mathcal{S}_d / \{z_1, \dots, z_w\}$.

Next, we proceed to take the average w.r.t. the qubit group \mathcal{Q} . Denote by \succcurlyeq the semi-definite partial order, i.e., $X \succcurlyeq Y \iff \mathbf{a}^T(X - Y)\mathbf{a} \geq 0$, we have

$$K_\infty(\mathbf{0}) = \mathbb{E}_{\mathcal{S}_d \in \mathcal{Q}} \mathbb{E}_{H_d \in \mathcal{H}} K_d \succcurlyeq \frac{1}{3^S |\mathcal{Q}|} \sum_{\mathcal{S}_d \in \mathcal{Q}} \sum_{w=0}^{S-1} \sum_{\substack{\mathbf{z}=(z_1, \dots, z_w) \\ \{z_1, \dots, z_w\} \subset \mathcal{S}_d}} \Delta_{S-w} A_{d,\mathbf{z}}^T A_{d,\mathbf{z}}, \quad (\text{D24})$$

$$= \frac{1}{3^S |\mathcal{Q}|} \sum_{w=0}^{S-1} \Delta_{S-w} A_{\mathcal{Q},w}^T A_{\mathcal{Q},w}. \quad (\text{D25})$$

Eq. (D24) is obtained from Eqs. (D19) and (D23) by noticing that XYX^T is positive semi-definite if Y is positive semi-definite. Eq. (D25) is obtained by using the notation $A_{\mathcal{Q},w}$, which is the matrix with dimension $(2^{S-w} \binom{S}{w} |\mathcal{Q}|, |\mathcal{A}|)$ formed by vertically concatenating matrices $A_{d,\mathbf{z}}$ for all $\mathcal{S}_d \in \mathcal{Q}$ and $\dim(\mathbf{z}) = w$. Similarly we have

$$K_\infty(\mathbf{0}) = \mathbb{E}_{\mathcal{S}_d \in \mathcal{Q}} \mathbb{E}_{H_d \in \mathcal{H}} K_d \preccurlyeq \frac{1}{3^S |\mathcal{Q}|} \sum_{\mathcal{S}_d \in \mathcal{Q}} \sum_{w=0}^{S-1} \sum_{\substack{\mathbf{z}=(z_1, \dots, z_w) \\ \{z_1, \dots, z_w\} \subset \mathcal{S}_d}} \|O\|_2^2 A_{d,\mathbf{z}}^T A_{d,\mathbf{z}}, \\ = \frac{1}{3^S |\mathcal{Q}|} \sum_{w=0}^{S-1} \|O\|_2^2 A_{\mathcal{Q},w}^T A_{\mathcal{Q},w}.$$

Thus, we obtain Eq. (D8). □

Lemma S10. *Let the observable be $O = \sum_{k=1}^N o_k Z_k$, where each Z_k is the product of Pauli matrices that is Z on the k -th qubit and I on other qubits. Denote by H_d the Hamiltonian of the d -th quantum gate in the circuit $V(\boldsymbol{\theta}) = \prod_{d=D}^1 \exp[-iH_d \theta_d / 2]$ that acts on qubits $\mathcal{S}_d \subseteq \{1, 2, \dots, N\}$. We assume that H_d is randomly sampled from the set $\mathcal{H} := \{X, Y\}^{\otimes S}$. Let $\mathcal{Q} := \{\mathcal{S}_d\}$. Let $A \in \mathbb{R}^{4^N \times |\mathcal{A}|}$ be the matrix with elements $A_{\mathbf{p}\mathbf{a}} = \text{Tr}[\sigma_{\mathbf{p}} \rho_{\mathbf{a}}]$. Then the asymptotic QNTK at $\boldsymbol{\theta} = \mathbf{0}$ could be bounded as*

$$\frac{1}{2^S |\mathcal{Q}|} \|O\|_2^2 A_{\mathcal{Q}}^T A_{\mathcal{Q}} \succcurlyeq K_\infty(\mathbf{0}) \succcurlyeq \frac{1}{2^S |\mathcal{Q}|} \Delta_S A_{\mathcal{Q}}^T A_{\mathcal{Q}}, \quad (\text{D26})$$

where we denote by \succcurlyeq the semi-definite partial order and $\Delta_j := \min_{\mathbf{g} \in \{0, \pm 1\}^{\otimes N}, 1 \leq \|\mathbf{g}\|_1 \leq j} (\mathbf{g}^T \mathbf{o})^2$. The matrix $A_{\mathcal{Q}}$ is formed by extracting rows from matrix A corresponding to indices \mathbf{p} , if there exists some $\mathcal{S}_d \in \mathcal{Q}$ that matches the non-zero elements in \mathbf{p} with elements in $\{1, 2\}$.

Proof. We follow notations and derivations in Eqs. (D9-D15) in Lemma S9. Thus, the average of K_d w.r.t. the Hamiltonian set $\mathcal{H} = \{X, Y\}^{\otimes S}$ is

$$\mathbb{E}_{H_d \in \mathcal{H}} [K_d]_{aa'} = \frac{1}{2^S} \sum_{H_d \in \{X, Y\}^{\otimes S}} -\frac{1}{4} \text{Tr}[[O, H_d] \rho_a] \text{Tr}[[O, H_d] \rho_{a'}] \quad (\text{D27})$$

$$= \frac{1}{2^S} \sum_{\mathbf{i} \in \{1, 2\}^{\otimes S}} \sum_{k, k'=1}^N o_k o_{k'} [A^T B_k]_{a\mathbf{i}'} [A^T B_{k'}]_{a'\mathbf{i}'}. \quad (\text{D28})$$

Eqs. (D27) and (D28) are derived by using Eqs. (D9) and (D14), respectively. The notation \mathbf{i}' is defined by zero-padding the vector $\mathbf{i} \in \{1, 2\}^{\otimes S}$ in the space $\{0, 1, 2, 3\}^{\otimes N}$.

Next, we proceed with the matrix formulation K_d . We have

$$\mathbb{E}_{H_d \in \mathcal{H}} K_d = \frac{1}{2^S} \sum_{\mathbf{i} \in \{1, 2\}^{\otimes S}} \sum_{k, k'=1}^N o_k o_{k'} [[A^T B_k]_{a\mathbf{i}'} [A^T B_{k'}]_{a'\mathbf{i}'}]_{aa'} \quad (\text{D29})$$

$$= \frac{1}{2^S} \sum_{k, k' \in \mathcal{S}_d} o_k o_{k'} A_d^T C_k C_{k'}^T A_d. \quad (\text{D30})$$

The derivation of Eq. (D29) is similar to that of Eq. (D18) with $w = 0$, since the notation \mathbf{i}' in this Lemma has no z terms. Eq. (D30) follows from using notations A_d and C_k . The matrix $A_d \in \mathbb{R}^{2^{S \times |\mathcal{A}|}}$ is derived by extracting rows

from matrix A corresponding to indices from the set $\{i|i_x \in \{1, 2\} \forall x \in \mathcal{S}_d, i_x = 0 \forall x \notin \mathcal{S}_d\}$. The matrix $C_k \in \mathbb{R}^{2^S \times 2^S}$ is derived by extracting columns and rows from B_k corresponding to indices from the set mentioned above, i.e.,

$$C_k = I_2^{\otimes(k_d-1)} \otimes \begin{bmatrix} & -1 \\ 1 & \end{bmatrix} \otimes I_2^{\otimes(S-k_d)}, \quad (\text{D31})$$

where k_d is the index of k in the set \mathcal{S}_d .

We remark that C_k is of full rank with singular values ± 1 . The eigenvalue of the positive semi-definite matrix $\sum_{k, k' \in \mathcal{S}_d} c_k c_{k'} C_k C_{k'}^T$ can be bounded as follows

$$\|O\|_2^2 = \left(\sum_{k=1}^N |o_k| \right)^2 \geq \lambda \left[\sum_{k, k' \in \mathcal{S}_d} o_k o_{k'} C_k C_{k'}^T \right] \geq \min_{\mathbf{g} \in \{-1, 1\}^{\otimes S}} (\mathbf{g}^T \mathbf{o}_d)^2 \geq \Delta_S, \quad (\text{D32})$$

where we denote by $\mathbf{o}_d \in \mathbb{R}^S$ the vector formed by extracting elements in \mathbf{c} corresponding to indices in \mathcal{S}_d .

Next, we proceed to take the average w.r.t. the qubit group \mathcal{Q} . Denote by \succcurlyeq the semi-definite partial order, i.e., $X \succcurlyeq Y \iff \mathbf{a}^T (X - Y) \mathbf{a} \geq 0$, we have

$$K_\infty(\mathbf{0}) = \mathbb{E}_{\mathcal{S}_d \in \mathcal{Q}} \mathbb{E}_{H_d \in \mathcal{H}} K_d \succcurlyeq \frac{1}{2^S |\mathcal{Q}|} \sum_{\mathcal{S}_d \in \mathcal{Q}} \Delta_S A_d^T A_d, \quad (\text{D33})$$

$$= \frac{1}{2^S |\mathcal{Q}|} \Delta_S A_{\mathcal{Q}}^T A_{\mathcal{Q}}. \quad (\text{D34})$$

Eq. (D33) is obtained from Eq. (D30) by noticing that XYX^T is positive semi-definite if Y is positive semi-definite. Eq. (D34) is obtained by using the notation $A_{\mathcal{Q}}$, which is the matrix with dimension $(2^S |\mathcal{Q}|, |\mathcal{A}|)$ formed by vertically concatenating matrices A_d for all $\mathcal{S}_d \in \mathcal{Q}$. Similarly we have

$$\begin{aligned} K_\infty(\mathbf{0}) &= \mathbb{E}_{\mathcal{S}_d \in \mathcal{Q}} \mathbb{E}_{H_d \in \mathcal{H}} K_d \preccurlyeq \frac{1}{2^S |\mathcal{Q}|} \sum_{\mathcal{S}_d \in \mathcal{Q}} \|O\|_2^2 A_d^T A_d, \\ &= \frac{1}{2^S |\mathcal{Q}|} \|O\|_2^2 A_{\mathcal{Q}}^T A_{\mathcal{Q}}. \end{aligned}$$

Thus, we obtain Eq. (D26). □

2. Bounds of $\lambda_{\min}[K_\infty(\mathbf{0})]$ and $\lambda_{\max}[K_\infty(\mathbf{0})]$

Different randomness within $\{\rho_a\}_{a \in \mathcal{A}}$ or elements of A and different choice of \mathcal{H} can lead to separate lower bound guarantees on the asymptotic QNTK. Here we provide two examples. The former is the random state distribution described in the main text with a bias on local terms, where the Hamiltonian set is $\mathcal{H} = \{X, Y, Z\}^S$. The latter is a state distribution based on the qubit embedding model and the Hamiltonian set is $\mathcal{H} = \{X, Y\}^S$. Roughly speaking, we found that for both cases, the least eigenvalue of the asymptotic QNTK deviates from zero with high probability when $S \geq \mathcal{O}(\log |\mathcal{A}|)$. Detailed results are presented in Lemmas S11 and S12, respectively. Both results are derived based on the random matrix theory.

Lemma S11. *We follow conditions and notations in Lemma S9. Let $\rho_a = \sum_{\mathbf{p} \in \{0, 1, 2, 3\}^{\otimes N}} \frac{1}{2^N} A_{\mathbf{p}a} \sigma_{\mathbf{p}}$ be the Pauli decomposition of state ρ_a , where A follows Proposition 1. Denote by $A_{\mathcal{Q}}$ the matrix with dimension $((3^S - 1)|\mathcal{Q}|, |\mathcal{A}|)$ formed by vertically concatenating matrices $A_{\mathcal{Q}, w}$ for $w \in \{0, 1, \dots, S-1\}$. Denote by $\alpha_{\min} := \min_i \alpha_i$, $\alpha_{\max} := \max_i \alpha_i$, and $\text{Var}_{\mathcal{Q}} := \text{diag}(\alpha_i)$, where i corresponds to the index of rows of $A_{\mathcal{Q}}$. Denote by $A'_{\mathcal{Q}} := \text{Var}_{\mathcal{Q}}^{-1/2} A_{\mathcal{Q}}$, $A'_{\mathcal{Q}, \min} := \frac{1}{\sqrt{(3^S - 1)|\mathcal{Q}|}} \min_{a \in \mathcal{A}} \|[A'_{\mathcal{Q}}]_{\cdot, a}\|_2$, and $A'_{\mathcal{Q}, \max} := \frac{1}{\sqrt{(3^S - 1)|\mathcal{Q}|}} \max_{a \in \mathcal{A}} \|[A'_{\mathcal{Q}}]_{\cdot, a}\|_2$. Then there exists two constants $C > 0$ and $k < 1$ such that for $S \geq \log_3 \left[1 + \frac{C^2 |A|^2 \ln |A|}{k^2 A_{\mathcal{Q}, \min}^2 |\mathcal{Q}| \delta^2} \right]$, we have*

$$(1 - k) \frac{3^S - 1}{3^S} \Delta_S \alpha_{\min} A_{\mathcal{Q}, \min}^2 \leq \lambda_{\min}[K_\infty(\mathbf{0})] \leq \lambda_{\max}[K_\infty(\mathbf{0})] \leq (1 + k) \frac{3^S - 1}{3^S} \|O\|_2^2 \alpha_{\max} A_{\mathcal{Q}, \max}^2 \quad (\text{D35})$$

with probability at least $1 - \delta$.

Proof. Denote by $D_{\mathcal{Q}}$ a $|\mathcal{A}| \times |\mathcal{A}|$ diagonal matrix with elements $[D_{\mathcal{Q}}]_{aa} := \|[A'_{\mathcal{Q}}]_{\cdot,a}\|_2$, i.e., $D_{\mathcal{Q}}$ stores the norm of columns of $A'_{\mathcal{Q}}$. Let

$$R := \sqrt{(3^S - 1)|\mathcal{Q}|} \text{Var}_{\mathcal{Q}}^{-1/2} A_{\mathcal{Q}} D_{\mathcal{Q}}^{-1}. \quad (\text{D36})$$

We denote that R matches the random matrix condition in Lemma S7. Specifically, columns of R are independent isotropic random vectors:

$$\mathbb{E}_{\mathbf{p}, \mathbf{q}, a, b} R_{\mathbf{p}a} R_{\mathbf{q}b} = (3^S - 1)|\mathcal{Q}| \mathbb{E}_{\mathbf{p}, \mathbf{q}, a, b} \frac{[A'_{\mathcal{Q}}]_{\mathbf{p},a} [A'_{\mathcal{Q}}]_{\mathbf{q},b}}{\|[A'_{\mathcal{Q}}]_{\cdot,a}\|_2 \|[A'_{\mathcal{Q}}]_{\cdot,b}\|_2} = \delta_{\mathbf{p}\mathbf{q}} \delta_{ab}.$$

All columns of R have the same norm:

$$\|R_{\cdot,a}\|_2 = \sqrt{(3^S - 1)|\mathcal{Q}|} \frac{\|[A'_{\mathcal{Q}}]_{\cdot,a}\|_2}{\|[A'_{\mathcal{Q}}]_{\cdot,a}\|_2} = \sqrt{(3^S - 1)|\mathcal{Q}|}. \quad (\text{D37})$$

We have

$$\begin{aligned} h_{\mathcal{Q},\mathcal{A}} &:= \frac{1}{(3^S - 1)|\mathcal{Q}|} \mathbb{E} \max_{a \in \mathcal{A}} \sum_{b \in \mathcal{A}, b \neq a} (R_{\cdot,a}^T R_{\cdot,b})^2 \\ &= (3^S - 1)|\mathcal{Q}| \mathbb{E} \max_{a \in \mathcal{A}} \sum_{b \in \mathcal{A}, b \neq a} \left(\frac{[A'_{\mathcal{Q}}]_{\cdot,a}^T [A'_{\mathcal{Q}}]_{\cdot,b}}{\|[A'_{\mathcal{Q}}]_{\cdot,a}\|_2 \|[A'_{\mathcal{Q}}]_{\cdot,b}\|_2} \right)^2 && \text{(using Eq. (D36))} \\ &\leq \frac{1}{(3^S - 1)|\mathcal{Q}|} \mathbb{E} \sum_{a, b \in \mathcal{A}, b \neq a} \frac{1}{A_{\mathcal{Q},\min}^4} \left(\sum_{\mathbf{p}} [A'_{\mathcal{Q}}]_{\mathbf{p},a} [A'_{\mathcal{Q}}]_{\mathbf{p},b} \right)^2 && \text{(using the notation of } D_{\mathcal{Q},\min}) \\ &= \frac{|\mathcal{A}|(|\mathcal{A}| - 1)}{A_{\mathcal{Q},\min}^4}, && (\text{D38}) \end{aligned}$$

where Eq. (D38) is obtained by using the distribution condition of A in Proposition 1. Then by using Lemma S7, there exists a constant C such that

$$\mathbb{E} \left| \frac{1}{(3^S - 1)|\mathcal{Q}|} (s[R])^2 - 1 \right| \leq C \sqrt{\frac{h_{\mathcal{Q},\mathcal{A}} \ln |\mathcal{A}|}{(3^S - 1)|\mathcal{Q}|}}, \quad (\text{D39})$$

where $s[X]$ denotes the singular value of a matrix X . Thus, with probability at least $1 - \delta$, we have

$$\begin{aligned} \lambda_{\min} [A_{\mathcal{Q}}^T A_{\mathcal{Q}}] &= (s_{\min} [A_{\mathcal{Q}}])^2 \\ &= \frac{1}{(3^S - 1)|\mathcal{Q}|} \left(s_{\min} [\text{Var}_{\mathcal{Q}}^{1/2} R D_{\mathcal{Q}}] \right)^2 && \text{(using Eq. (D36))} \\ &\geq \alpha_{\min} A_{\mathcal{Q},\min}^2 (s_{\min} [R])^2 \\ &\geq (3^S - 1)|\mathcal{Q}| \alpha_{\min} A_{\mathcal{Q},\min}^2 \left(1 - \frac{C}{\delta} \sqrt{\frac{h_{\mathcal{Q},\mathcal{A}} \ln |\mathcal{A}|}{(3^S - 1)|\mathcal{Q}|}} \right) && \text{(using Eq. (D39))} \\ &\geq (3^S - 1)|\mathcal{Q}| \alpha_{\min} A_{\mathcal{Q},\min}^2 \left(1 - \frac{C|\mathcal{A}|}{\delta A_{\mathcal{Q},\min}^2} \sqrt{\frac{\ln |\mathcal{A}|}{(3^S - 1)|\mathcal{Q}|}} \right) && \text{(using Eq. (D38))} \\ &\geq (1 - k)(3^S - 1)|\mathcal{Q}| \alpha_{\min} A_{\mathcal{Q},\min}^2 && (\text{D40}) \end{aligned}$$

and

$$\begin{aligned}
\lambda_{\max} [A_{\mathcal{Q}}^T A_{\mathcal{Q}}] &= (s_{\max} [A_{\mathcal{Q}}])^2 \\
&= \frac{1}{(3^S - 1)|\mathcal{Q}|} \left(s_{\max} \left[\text{Var}_{\mathcal{Q}}^{1/2} R D_{\mathcal{Q}} \right] \right)^2 && \text{(using Eq. (D36))} \\
&\leq \alpha_{\max} A_{\mathcal{Q}, \max}^{\prime 2} (s_{\max} [R])^2 \\
&\leq (3^S - 1)|\mathcal{Q}| \alpha_{\max} A_{\mathcal{Q}, \max}^{\prime 2} \left(1 + \frac{C}{\delta} \sqrt{\frac{h_{\mathcal{Q}, \mathcal{A}} \ln |\mathcal{A}|}{(3^S - 1)|\mathcal{Q}|}} \right) && \text{(using Eq. (D39))} \\
&\leq (3^S - 1)|\mathcal{Q}| \alpha_{\max} A_{\mathcal{Q}, \max}^{\prime 2} \left(1 + \frac{C|\mathcal{A}|}{\delta A_{\mathcal{Q}, \min}^{\prime 2}} \sqrt{\frac{\ln |\mathcal{A}|}{(3^S - 1)|\mathcal{Q}|}} \right) && \text{(using Eq. (D38))} \\
&\leq (1+k)(3^S - 1)|\mathcal{Q}| \alpha_{\max} A_{\mathcal{Q}, \max}^{\prime 2}. && \text{(D41)}
\end{aligned}$$

Eqs. (D40) and (D41) follows from the condition on S :

$$S \geq \log_3 \left[1 + \frac{C^2 |\mathcal{A}|^2 \ln |\mathcal{A}|}{k^2 A_{\mathcal{Q}, \min}^{\prime 4} |\mathcal{Q}| \delta^2} \right].$$

By using Lemma S9, we could finally provide the lower bound and the upper bound on the least and the largest eigenvalue of the asymptotic QNTK, respectively. With probability at least $1 - \delta$, we have

$$\begin{aligned}
\lambda_{\min} [K_{\infty}(\mathbf{0})] &\geq \frac{1}{3^S |\mathcal{Q}|} \Delta_S \lambda_{\min} [A_{\mathcal{Q}}^T A_{\mathcal{Q}}] \geq (1-k) \frac{3^S - 1}{3^S} \Delta_S \alpha_{\min} A_{\mathcal{Q}, \min}^{\prime 2}, \\
\lambda_{\max} [K_{\infty}(\mathbf{0})] &\leq \frac{1}{3^S |\mathcal{Q}|} \|O\|_2^2 \lambda_{\max} [A_{\mathcal{Q}}^T A_{\mathcal{Q}}] \leq (1+k) \frac{3^S - 1}{3^S} \|O\|_2^2 \alpha_{\max} A_{\mathcal{Q}, \max}^{\prime 2}.
\end{aligned}$$

□

Lemma S12. *We follow conditions and notations in Lemma S10. Let ρ_a be the density matrix of the qubit embedding of the vector \mathbf{x}_a via Eq. (18), where each entry of \mathbf{x}_a is an independent random variable distributed uniformly in $[-1, 1]$. Then there exists two constants $C > 0$ and $k < 1$ such that for $S \geq 2 + \log_2 \frac{C^2 |\mathcal{A}|^2 \ln |\mathcal{A}|}{k^2 |\mathcal{Q}| \delta^2}$,*

$$(1-k) \frac{\Delta_S}{2^S} \leq \lambda_{\min} [K_{\infty}(\mathbf{0})] \leq \lambda_{\max} [K_{\infty}(\mathbf{0})] \leq (1+k) \frac{\|O\|_2^2}{2^S} \quad \text{(D42)}$$

with probability at least $1 - \delta$.

Proof. By using Lemma S10, we have

$$\frac{\Delta_S}{2^{2S} |\mathcal{Q}|} \left(s_{\min} \left[2^{S/2} A_{\mathcal{Q}} \right] \right)^2 \leq \lambda_{\min} [K_{\infty}(\mathbf{0})] \leq \lambda_{\max} [K_{\infty}(\mathbf{0})] \leq \frac{\|O\|_2^2}{2^{2S} |\mathcal{Q}|} \left(s_{\max} \left[2^{S/2} A_{\mathcal{Q}} \right] \right)^2,$$

so it suffices to prove

$$s_{\min} \left[2^{S/2} A_{\mathcal{Q}} \right] \geq \sqrt{2^S |\mathcal{Q}|} - \frac{C}{\delta} \sqrt{|\mathcal{A}| (|\mathcal{A}| - 1) \ln |\mathcal{A}|} \geq \sqrt{(1-k) 2^S |\mathcal{Q}|}, \quad \text{(D43)}$$

$$s_{\max} \left[2^{S/2} A_{\mathcal{Q}} \right] \leq \sqrt{2^S |\mathcal{Q}|} + \frac{C}{\delta} \sqrt{|\mathcal{A}| (|\mathcal{A}| - 1) \ln |\mathcal{A}|} \leq \sqrt{(1+k) 2^S |\mathcal{Q}|}, \quad \text{(D44)}$$

with probability at least $1 - \delta$, where the final inequality is derived from the condition of S . Our main idea is to employ Lemma S7 to obtain bounds of singular values of the matrix $2^{S/2} A_{\mathcal{Q}}$ with $d_1 = 2^S |\mathcal{Q}|$ and $d_2 = |\mathcal{A}|$.

By using the qubit embedding with R_Z rotations on the initial state $\otimes_{n=1}^N \frac{|0\rangle + |1\rangle}{\sqrt{2}}$, we have

$$\begin{aligned}
\rho_a &= \bigotimes_{n=1}^N \exp[-iZ\pi x_{a,n}/2] \frac{(|0\rangle + |1\rangle)(\langle 0| + \langle 1|)}{2} \exp[iZ\pi x_{a,n}/2] \\
&= \bigotimes_{n=1}^N \exp[-iZ\pi x_{a,n}/2] \frac{I + X}{2} \exp[iZ\pi x_{a,n}/2] \\
&= \bigotimes_{n=1}^N \frac{I + X \cos(\pi x_{a,n}) + Y \sin(\pi x_{a,n})}{2}.
\end{aligned} \quad \text{(D45)}$$

Denote by $[A_{\mathcal{Q}}]_{\cdot,a}$ the a -th column of $A_{\mathcal{Q}}$. By using the definition of $A_{\mathcal{Q}}$ and Eq. (D45), we have

$$[A_{\mathcal{Q}}]_{\cdot,a} = \bigoplus_{\mathcal{S}_d \in \mathcal{Q}} \bigotimes_{n \in \mathcal{S}_d} \begin{bmatrix} \cos(\pi x_{a,n}) \\ \sin(\pi x_{a,n}) \end{bmatrix} \quad (\text{D46})$$

$$:= \bigoplus_{\mathcal{S}_d \in \mathcal{Q}} \mathbf{v}_{d,a}, \quad (\text{D47})$$

where we split $[A_{\mathcal{Q}}]_{\cdot,a}$ into $|\mathcal{Q}|$ vectors $\mathbf{v}_{1,a}, \dots, \mathbf{v}_{|\mathcal{Q}|,a}$ in Eq. (D47). The vector $\mathbf{v}_{d,a}$ corresponds to the qubit group \mathcal{S}_d . Thus, we have

$$\begin{aligned} \left\| 2^{S/2} [A_{\mathcal{Q}}]_{\cdot,a} \right\|_2^2 &= 2^S \sum_{d=1}^{|\mathcal{Q}|} \|\mathbf{v}_{d,a}\|_2^2 \\ &= 2^S \sum_{d=1}^{|\mathcal{Q}|} \prod_{n \in \mathcal{S}_d} (\cos^2(\pi x_{a,n}) + \sin^2(\pi x_{a,n})) \\ &= 2^S |\mathcal{Q}|. \end{aligned} \quad (\text{D48})$$

Next, we prove that $2^{S/2} [A_{\mathcal{Q}}]_{\cdot,a}$ are independent isotropic random vectors, i.e.,

$$\mathbb{E}_{\mathbf{x}_a} 2^S [A_{\mathcal{Q}}]_{\cdot,a} [A_{\mathcal{Q}}]_{\cdot,a}^T = I_{2^S |\mathcal{Q}|}. \quad (\text{D49})$$

We consider the diagonal term first. By noticing Eq. (D47), we remark that the vector $[A_{\mathcal{Q}}]_{\cdot,a}$ could be written as the direct sum of $|\mathcal{Q}|$ vectors $\mathbf{v}_{d,a}$, where the element of each $\mathbf{v}_{d,a}$ is assigned with an index $\mathbf{p}_d \in \{1, 2\}^{\otimes S}$. Thus, we could denote by $v_{\mathbf{p}_d,a}$ the element of $[A_{\mathcal{Q}}]_{\cdot,a}$. Suppose $\mathcal{S}_d = \{q_1, \dots, q_S\}$. For any \mathbf{p}_d , we have

$$\mathbb{E}_{\mathbf{x}_a} 2^S v_{\mathbf{p}_d,a}^2 = 2^S \mathbb{E}_{\mathbf{x}_a} \prod_{n=1}^S (\delta_{p_n 1} \cos^2(\pi x_{a,q_n}) + \delta_{p_n 2} \sin^2(\pi x_{a,q_n})) \quad (\text{D50})$$

$$= 2^S \prod_{n=1}^S \mathbb{E}_{x_{a,n}} (\delta_{p_n 1} \cos^2(\pi x_{a,q_n}) + \delta_{p_n 2} \sin^2(\pi x_{a,q_n})) \quad (\text{D51})$$

$$= 2^S \prod_{n=1}^S \frac{\delta_{p_n 1} + \delta_{p_n 2}}{2} \quad (\text{using } \mathbb{E}_x \cos^2(\pi x) = \mathbb{E}_x \sin^2(\pi x) = \frac{1}{2})$$

$$= 1. \quad (\text{D52})$$

Eq. (D50) follows from Eq. (D46). Eq. (D51) is obtained by noticing that $\{x_n^m\}_{n=1}^N$ are independent random variables. Eq. (D52) is obtained by noticing that $p_n \in \{1, 2\}$. Next, we consider the off-diagonal term in $[A_{\mathcal{Q}}]_{\cdot,a} [A_{\mathcal{Q}}]_{\cdot,a}^T$. Similar to the diagonal case, we assign two entries $v_{\mathbf{p}_d,a}$ and $v_{\mathbf{p}'_d,a}$ with two indices \mathbf{p}_d and \mathbf{p}'_d , respectively. For the case $d \neq d'$, i.e. $\mathcal{S}_d \neq \mathcal{S}_{d'}$, there exists a qubit $q \in \mathcal{S}_d$ and $q \notin \mathcal{S}_{d'}$. Then the expectation $\mathbb{E}_{\mathbf{x}_a} v_{\mathbf{p}_d,a} v_{\mathbf{p}'_d,a}$ contains a factor $\mathbb{E} \cos(\pi x_{a,q}) = 0$ or $\mathbb{E} \sin(\pi x_{a,q}) = 0$, where both induce the zero result. For the case $d = d'$, we remark that $\mathbf{p}_d \neq \mathbf{p}'_d$ due to the off-diagonal condition. Thus, there exists at least one index $i \in \{1, \dots, S\}$ such that $p_i \neq p'_i$ and the qubit $q_i \in \mathcal{S}_d$. Therefore the expectation $\mathbb{E}_{\mathbf{x}_a} v_{\mathbf{p}_d,a} v_{\mathbf{p}'_d,a}$ contains a factor $\mathbb{E} \cos(\pi x_{a,q_i}) \sin(\pi x_{a,q_i}) = 0$, which induces the zero result. Thus, we have proved Eq. (D49).

Next, we proceed to calculate the term d_3 in Lemma S7. We have

$$[A_{\mathcal{Q}}]_{\cdot,a}^T [A_{\mathcal{Q}}]_{\cdot,b} = \sum_{\mathcal{S}_d \in \mathcal{Q}} \prod_{n \in \mathcal{S}_d} (\cos \pi x_{a,n} \cos \pi x_{b,n} + \sin \pi x_{a,n} \sin \pi x_{b,n}) \quad (\text{D53})$$

$$= \sum_{\mathcal{S}_d \in \mathcal{Q}} \prod_{n \in \mathcal{S}_d} \cos(\pi x_{a,n} - \pi x_{b,n}), \quad (\text{D54})$$

where Eq. (D53) follows from Eq. (D46). Thus

$$\begin{aligned} d_3 &= \frac{1}{2^S |\mathcal{Q}|} \mathbb{E} \max_{a \in \mathcal{A}} \sum_{b \in \mathcal{A}, b \neq a} (2^S [A_{\mathcal{Q}}]_{:,a}^T [A_{\mathcal{Q}}]_{:,b})^2 \\ &\leq \frac{2^S}{|\mathcal{Q}|} \mathbb{E} \sum_{a,b \in \mathcal{A}, b \neq a} \left(\sum_{S_d \in \mathcal{Q}} \prod_{n \in S_d} \cos(\pi x_{a,n} - \pi x_{b,n}) \right)^2 \end{aligned} \quad (\text{D55})$$

$$\begin{aligned} &= \frac{2^S}{|\mathcal{Q}|} \mathbb{E} \sum_{a,b \in \mathcal{A}, b \neq a} \sum_{S_d \in \mathcal{Q}} \prod_{n \in S_d} \cos^2(\pi x_{a,n} - \pi x_{b,n}) \\ &= \frac{2^S}{|\mathcal{Q}|} \sum_{a,b \in \mathcal{A}, b \neq a} \sum_{S_d \in \mathcal{Q}} \prod_{n \in S_d} \frac{1}{2} \\ &= |\mathcal{A}|(|\mathcal{A}| - 1). \end{aligned} \quad (\text{D56})$$

Eq. (D55) follows from Eq. (D54). Eq. (D56) is derived by noticing that for $S_d \neq S_{d'}$, the expectation of the cos term is zero.

Thus, by using Lemma S7, there exists a constant C such that

$$\mathbb{E} \max_j \left| s_j (2^{S/2} A_{\mathcal{Q}}) - \sqrt{2^S |\mathcal{Q}|} \right| \leq C \sqrt{|\mathcal{A}|(|\mathcal{A}| - 1) \ln |\mathcal{A}|}. \quad (\text{D57})$$

Eqs. (D43) and (D44) follow from Eq. (D57) by using the Markov's inequality. Thus, we have proved Lemma S12. \square

3. Proof of Lemma 1

The main idea is to analyze the stability of the QNTK when the depth is large but finite. Specifically, we are interested in the distance between the asymptotic QNTK $K_{\infty}(\mathbf{0})$ with the finite QNTK $K(\mathbf{0})$ with D gates. We follow notations in Lemmas S9 and S11. We remark that

$$K(\boldsymbol{\theta}) = \frac{1}{D} J(\boldsymbol{\theta})^T J(\boldsymbol{\theta})$$

by Eq. (9), where the row $J_d(\boldsymbol{\theta}) = \{\frac{\partial z_a}{\partial \theta_d}(\boldsymbol{\theta})\}_{a \in \mathcal{A}}$. Thus, $K(\mathbf{0})$ and $K_{\infty}(\mathbf{0})$ are the empirical and the explicit covariance matrix of independent random vectors $\{J_d(\mathbf{0})\}$, respectively. Since each Hamiltonian H_d involves S qubits, we have

$$\mathbb{E} J_{da}(\mathbf{0})^2 = \mathbb{E} \frac{1}{4} (\text{Tr}[i[O, H_d] \rho_a])^2 \leq \|O\|_2^2 \alpha_{\max},$$

where $\alpha_{\max} := \max_{\|i\|_1=S} \alpha_i$. We remark that each element in the vector $J_d(\mathbf{0})$ is independent from each other due to the independent sample $a \in \mathcal{A}$. By using the central limit theorem, there exists an absolute constant $c_1 > 0$, such that

$$P \left(\|J_d(\mathbf{0})\|_2^2 \geq c_1 |\mathcal{A}| \|O\|_2^2 \alpha_{\max} \ln \frac{D}{\delta} \right) \leq 1 - \frac{\delta}{3D}.$$

Thus, with probability at least $1 - \delta/3$ we have that for all $d = 1, 2, \dots, D$,

$$\|J_d(\mathbf{0})\|_2^2 \leq c_1 |\mathcal{A}| \|O\|_2^2 \alpha_{\max} \ln \frac{D}{\delta}. \quad (\text{D58})$$

By using Lemma S6 and Eq. (D58), we have that with probability at least $1 - 2\delta/3$,

$$\begin{aligned} &\|K(\mathbf{0}) - K_{\infty}(\mathbf{0})\|_2 \\ &= \left\| \frac{1}{D} \sum_{d=1}^D J_d(\mathbf{0}) J_d(\mathbf{0})^T - K_{\infty}(\mathbf{0}) \right\|_2 \\ &\leq \epsilon \cdot \max \left(\sqrt{\|K_{\infty}(\mathbf{0})\|_2}, \epsilon \right), \end{aligned} \quad (\text{D59})$$

where

$$\epsilon = \sqrt{\frac{c_1 |\mathcal{A}| \|O\|_2^2 \alpha_{\max}}{D} \ln \frac{D}{\delta}} \cdot \sqrt{\frac{1}{c_2} \ln \frac{|\mathcal{A}|}{\delta}} \quad (\text{D60})$$

and $c_2 > 0$ is an absolute constant. Let $C_2 := 9 \max(c_1/c_2, 1)$ in the condition $D_0 = C_2 \frac{\|O\|_2^4 \alpha_{\max}^2 A'_{\mathcal{Q},\max}{}^2}{k^2 \Delta_S^2 \alpha_{\min}^2 A'_{\mathcal{Q},\min}{}^4} |\mathcal{A}| \ln \frac{|\mathcal{A}|}{\delta}$ such that $D \geq D_0 \ln \frac{D_0}{\delta}$, we have

$$\begin{aligned} \frac{\frac{D}{\delta}}{\ln \frac{D}{\delta}} &\geq \frac{\frac{D_0}{\delta} \ln \frac{D_0}{\delta}}{\ln \frac{D_0}{\delta} + \ln \ln \frac{D_0}{\delta}} && \text{(function } f(x) = x/\ln x \text{ is increasing for } x \geq e) \\ &\geq \frac{\frac{D_0}{\delta} \ln \frac{D_0}{\delta}}{\ln \frac{D_0}{\delta} + \frac{1}{2} \ln \frac{D_0}{\delta}} && (\ln x \leq \frac{x}{2} \text{ for } x > 0) \\ &= \frac{2}{3} \frac{D_0}{\delta} = \frac{6}{k^2} \max(c_1/c_2, 1) \frac{|\mathcal{A}| \|O\|_2^4 \alpha_{\max}^2 A'_{\mathcal{Q},\max}{}^2}{\Delta_S^2 \alpha_{\min}^2 A'_{\mathcal{Q},\min}{}^4} \frac{1}{\delta} \ln \frac{|\mathcal{A}|}{\delta}. \end{aligned} \quad (\text{D61})$$

Using Eq. (D61) in Eq. (D60), we obtain

$$\epsilon = \sqrt{\frac{c_1 |\mathcal{A}| \|O\|_2^2 \alpha_{\max}}{c_2} \frac{1}{\delta} \ln \frac{|\mathcal{A}|}{\delta}} \cdot \sqrt{\frac{\ln \frac{D}{\delta}}{\frac{D}{\delta}}} \leq \frac{k}{\sqrt{6}} \cdot \frac{\Delta_S \alpha_{\min} A'_{\mathcal{Q},\min}{}^2}{\sqrt{\|O\|_2^2 \alpha_{\max} A'_{\mathcal{Q},\max}{}^2}}. \quad (\text{D62})$$

Besides, by using Lemma S11, we have

$$\left(1 - \frac{k}{2}\right) \Delta_S \alpha_{\min} A'_{\mathcal{Q},\min}{}^2 \leq \lambda_{\min} [K_{\infty}(\mathbf{0})] \leq \lambda_{\max} [K_{\infty}(\mathbf{0})] \leq \left(1 + \frac{k}{2}\right) \|O\|_2^2 \alpha_{\max} A'_{\mathcal{Q},\max}{}^2 \quad (\text{D63})$$

with probability at least $1 - \delta/3$ for $S \geq \log_3 \left[1 + \frac{C_1^2 |\mathcal{A}|^2 \ln |\mathcal{A}|}{k^2 A'_{\mathcal{Q},\min}{}^4 |\mathcal{Q}| \delta^2}\right]$, where $C_1 = 6C$ and the constant C follows the notation in Lemma S11. Using Eqs. (D62) and (D63) in Eq. (D59) could yield the result. With probability at least $1 - \delta$ we have

$$\begin{aligned} \lambda_{\min} [K(\mathbf{0})] &\geq \lambda_{\min} [K_{\infty}(\mathbf{0})] - \|K(\mathbf{0}) - K_{\infty}(\mathbf{0})\|_2 \\ &\geq \left(1 - \frac{k}{2}\right) \Delta_S \alpha_{\min} A'_{\mathcal{Q},\min}{}^2 - \frac{k}{\sqrt{6}} \cdot \frac{\Delta_S \alpha_{\min} A'_{\mathcal{Q},\min}{}^2}{\sqrt{\|O\|_2^2 \alpha_{\max} A'_{\mathcal{Q},\max}{}^2}} \cdot \sqrt{1 + \frac{k}{2}} \cdot \sqrt{\|O\|_2^2 \alpha_{\max} A'_{\mathcal{Q},\max}{}^2} \\ &\geq (1 - k) \Delta_S \alpha_{\min} A'_{\mathcal{Q},\min}{}^2 \end{aligned}$$

and

$$\begin{aligned} \lambda_{\max} [K(\mathbf{0})] &\leq \lambda_{\max} [K_{\infty}(\mathbf{0})] + \|K(\mathbf{0}) - K_{\infty}(\mathbf{0})\|_2 \\ &\leq \left(1 + \frac{k}{2}\right) \|O\|_2^2 \alpha_{\max} A'_{\mathcal{Q},\max}{}^2 + \frac{k}{\sqrt{6}} \cdot \frac{\Delta_S \alpha_{\min} A'_{\mathcal{Q},\min}{}^2}{\sqrt{\|O\|_2^2 \alpha_{\max} A'_{\mathcal{Q},\max}{}^2}} \cdot \sqrt{1 + \frac{k}{2}} \cdot \sqrt{\|O\|_2^2 \alpha_{\max} A'_{\mathcal{Q},\max}{}^2} \\ &\leq \left(1 + \frac{k}{2}\right) \|O\|_2^2 \alpha_{\max} A'_{\mathcal{Q},\max}{}^2 + \frac{k}{2} \Delta_S \alpha_{\min} A'_{\mathcal{Q},\min}{}^2 \\ &\leq (1 + k) \|O\|_2^2 \alpha_{\max} A'_{\mathcal{Q},\max}{}^2. \end{aligned}$$

4. Proof of Lemma 2

The main idea is similar to Section D3. We follow notations in Lemmas S10 and S12. We remark that

$$K(\boldsymbol{\theta}) = \frac{1}{D} J(\boldsymbol{\theta})^T J(\boldsymbol{\theta})$$

by Eq. (9), where the row $J_d(\boldsymbol{\theta}) = \{\frac{\partial z_a}{\partial \theta_d}(\boldsymbol{\theta})\}_{a \in \mathcal{A}}$. Thus, $K(\mathbf{0})$ and $K_\infty(\mathbf{0})$ are the empirical and the explicit covariance matrix of independent random vectors $\{J_d(\mathbf{0})\}$, respectively. Since each Hamiltonian H_d involves S qubits, we have

$$\mathbb{E}_a J_{da}(\mathbf{0})^2 = \mathbb{E}_a \frac{1}{4} (\text{Tr}[i[O, H_d]\rho_a])^2 \leq \frac{\|O\|_2^2}{2^S}$$

by using Eq. (D49). We remark that each element in the vector $J_d(\mathbf{0})$ is independent from each other due to the independent sample $a \in \mathcal{A}$. By using the central limit theorem, there exists an absolute constant $c_1 > 0$, such that

$$P\left(\|J_d(\mathbf{0})\|_2^2 \geq c_1 |\mathcal{A}| \frac{\|O\|_2^2}{2^S} \ln \frac{D}{\delta}\right) \leq 1 - \frac{\delta}{3D}.$$

Thus, with probability at least $1 - \delta/3$ we have that for all $d = 1, 2, \dots, D$,

$$\|J_d(\mathbf{0})\|_2^2 \leq c_1 |\mathcal{A}| \frac{\|O\|_2^2}{2^S} \ln \frac{D}{\delta}. \quad (\text{D64})$$

By using Lemma S6 and Eq. (D64), we have that with probability at least $1 - 2\delta/3$,

$$\begin{aligned} & \|K(\mathbf{0}) - K_\infty(\mathbf{0})\|_2 \\ &= \left\| \frac{1}{D} \sum_{d=1}^D J_d(\mathbf{0}) J_d(\mathbf{0})^T - K_\infty(\mathbf{0}) \right\|_2 \\ &\leq \epsilon \cdot \max\left(\sqrt{\|K_\infty(\mathbf{0})\|_2}, \epsilon\right), \end{aligned} \quad (\text{D65})$$

where

$$\epsilon = \sqrt{\frac{c_1 |\mathcal{A}| \|O\|_2^2}{2^S D} \ln \frac{D}{\delta}} \cdot \sqrt{\frac{1}{c_2} \ln \frac{|\mathcal{A}|}{\delta}} \quad (\text{D66})$$

and $c_2 > 0$ is an absolute constant. Let $C_2 := 9 \max(c_1/c_2, 1)$ in the condition $D_0 = C_2 \frac{|\mathcal{A}| \|O\|_2^4}{k^2 \Delta_S^2} \ln \frac{|\mathcal{A}|}{\delta}$ such that $D \geq D_0 \ln \frac{D_0}{\delta}$, we have

$$\begin{aligned} \frac{D}{\delta} \ln \frac{D}{\delta} &\geq \frac{\frac{D_0}{\delta} \ln \frac{D_0}{\delta}}{\ln \frac{D_0}{\delta} + \ln \ln \frac{D_0}{\delta}} && \text{(function } f(x) = x/\ln x \text{ is increasing for } x \geq e) \\ &\geq \frac{\frac{D_0}{\delta} \ln \frac{D_0}{\delta}}{\ln \frac{D_0}{\delta} + \frac{1}{2} \ln \frac{D_0}{\delta}} && (\ln x \leq \frac{x}{2} \text{ for } x > 0) \\ &= \frac{2}{3} \frac{D_0}{\delta} = 6 \max(c_1/c_2, 1) \frac{\|O\|_2^4}{k^2 \Delta_S^2} \frac{|\mathcal{A}|}{\delta} \ln \frac{|\mathcal{A}|}{\delta}. \end{aligned} \quad (\text{D67})$$

Using Eq. (D67) in Eq. (D66), we obtain

$$\epsilon = \sqrt{\frac{c_1 |\mathcal{A}| \|O\|_2^2}{2^S c_2} \ln \frac{|\mathcal{A}|}{\delta}} \cdot \sqrt{\frac{\ln \frac{D}{\delta}}{D}} \leq \frac{k \Delta_S}{\sqrt{6} \|O\|_2 \sqrt{2^S}}. \quad (\text{D68})$$

Besides, by using Lemma S12, we have

$$\left(1 - \frac{k}{2}\right) \frac{\Delta_S}{2^S} \leq \lambda_{\min}[K_\infty(\mathbf{0})] \leq \lambda_{\max}[K_\infty(\mathbf{0})] \leq \left(1 - \frac{k}{2}\right) \frac{\|O\|_2^2}{2^S} \quad (\text{D69})$$

with probability at least $1 - \delta/3$ for $S \geq 2 + \log_2 \frac{C_1^2 |\mathcal{A}|^2 \ln |\mathcal{A}|}{k^2 |\mathcal{Q}| \delta^2}$, where $C_1 = 6C$ and the constant C follows the notation in Lemma S12. Using Eqs. (D68) and (D69) in Eq. (D65) could yield the result. With probability at least $1 - \delta$ we have

$$\begin{aligned} \lambda_{\min}[K(\mathbf{0})] &\geq \lambda_{\min}[K_\infty(\mathbf{0})] - \|K(\mathbf{0}) - K_\infty(\mathbf{0})\|_2 \\ &\geq \left(1 - \frac{k}{2}\right) \frac{\Delta_S}{2^S} - \frac{k \Delta_S}{\sqrt{6} \|O\|_2 \sqrt{2^S}} \cdot \sqrt{1 + \frac{k}{2} \frac{\|O\|_2}{\sqrt{2^S}}} \\ &\geq (1 - k) \frac{\Delta_S}{2^S} \end{aligned}$$

and

$$\begin{aligned}
\lambda_{\max} [K(\mathbf{0})] &\leq \lambda_{\max} [K_{\infty}(\mathbf{0})] + \|K(\mathbf{0}) - K_{\infty}(\mathbf{0})\|_2 \\
&\leq \left(1 + \frac{k}{2}\right) \frac{\|O\|_2^2}{2^S} + \frac{k\Delta_S}{\sqrt{6}\|O\|_2\sqrt{2^S}} \cdot \sqrt{1 + \frac{k}{2}} \frac{\|O\|_2}{\sqrt{2^S}} \\
&\leq \left(1 + \frac{k}{2}\right) \frac{\|O\|_2^2}{2^S} + \frac{k}{2} \frac{\Delta_S}{2^S} \\
&\leq (1+k) \frac{\|O\|_2^2}{2^S}.
\end{aligned}$$

Appendix E: Linear convergence of QNN training

We first present a linear convergence theory for quantum neural networks under general settings in Section E.1. Next, we provide the proof of the linear convergence result, i.e., Theorems 4 and 5 in the main text, in Sections E.2 and E.3, respectively.

1. QNN training in the locally smooth region

We begin by analyzing the general QNN case. In this section, we prove the convergence rate of training general QNNs and demonstrate the lazy training regime in Theorem S3. Analogous to Theorem G.1 in the work [63], our analysis requires the local Lipschitz continuity of the Jacobian matrix $J(\boldsymbol{\theta})$ with constants of the order $\mathcal{O}(D^{\frac{1}{2}})$ as shown in Assumption 1. In the locally smooth region defined in Assumption 1, the loss function decays linearly during the gradient descent training with high probability. The decay rate is independent of the number of parameter D for any $D \geq D_0 := \text{poly}(|\mathcal{A}|, \lambda_{\max}, \lambda_{\min}^{-1})$, where $\lambda_{\min}, \lambda_{\max}$ denotes the least and the largest eigenvalue of the initial QNTK, respectively. We remark that the linear convergence threshold in this work is milder than that in previous research with $D \geq \text{poly}(2^N)$ when $\lambda_{\min}^{-1} \lesssim \text{poly}(N)$.

Theorem S3. *Let $\boldsymbol{\theta}(t) \in \mathbb{R}^D$ be the parameter of a QNN $\{V(\boldsymbol{\theta}), O\}$ at the t -th step of the gradient descent training on the dataset $A = \{(\rho_a, y_a)\}$. Let $\mathcal{L}_{\mathcal{A}}(t)$ and $K(t)$ be the loss function and the QNTK at the t -th step, respectively. Denote by λ_{\max} and λ_{\min} the largest and the least eigenvalue of $K(0)$, respectively. Let $\eta = \frac{|\mathcal{A}|}{D}\eta_0$ be the learning rate, where $\eta_0 \leq \lambda_{\min}^{-1}$. Then for any $k \in (0, 1/2]$, there exists two constants $C_0, C_3 > 0$, such that if Assumption 1 holds for the parameter $\boldsymbol{\theta}(0)$ with the constant C_0 and $R_0 := \frac{5}{2}\lambda_{\min}^{-1}\sqrt{2|\mathcal{A}|\lambda_{\max}\mathcal{L}_{\mathcal{A}}(0)}$ for every $D \geq D_0 := C_3k^{-2}\lambda_{\max}^2\lambda_{\min}^{-4}|\mathcal{A}|\mathcal{L}_{\mathcal{A}}(0)$, we have,*

$$\mathcal{L}_{\mathcal{A}}(T) \leq (1 - (1-k)\eta_0\lambda_{\min})^{2T} \mathcal{L}_{\mathcal{A}}(0), \quad (\text{E1})$$

$$\|\boldsymbol{\theta}(T) - \boldsymbol{\theta}(0)\|_2 \leq \frac{R_0}{\sqrt{D}}. \quad (\text{E2})$$

Proof. For convenience, we will denote by $\mathbf{r}(t) := \mathbf{r}(\boldsymbol{\theta}(t))$ and $J(t) := J(\boldsymbol{\theta}(t))$ the residual vector and the Jacobian matrix at the parameter $\boldsymbol{\theta}(t)$, respectively. Notations such as $\mathbf{r}(\boldsymbol{\theta})$ will also be employed without ambiguity. Denote by

$$k_1 = \frac{2\lambda_{\min}}{5\lambda_{\max}}k. \quad (\text{E3})$$

Choose the proper constant C_3 such that

$$\begin{aligned}
D_0 &\geq \left(\frac{2}{k} + \frac{4}{5}\right)^2 \frac{25\lambda_{\max}^2}{4\lambda_{\min}^4} C_0 2|\mathcal{A}|\mathcal{L}_{\mathcal{A}}(0) \\
&\geq \frac{1}{k^2} \left(\frac{1 + \frac{2}{5}k}{1-k}\right)^2 \frac{25\lambda_{\max}^2}{4\lambda_{\min}^4} C_0 2|\mathcal{A}|\mathcal{L}_{\mathcal{A}}(0) \\
&\geq \frac{1}{k_1^2} \left(\frac{1+k_1}{1-k}\right)^2 \frac{1}{\lambda_{\min}^2} C_0 \|\mathbf{r}(0)\|_2^2.
\end{aligned} \quad (\text{E4})$$

Our main idea is to prove the following two equations jointly by induction:

$$\|\mathbf{r}(t)\|_2 \leq [1 - (1 - k)\eta_0\lambda_{\min}]^t \|\mathbf{r}(0)\|_2, \quad (\text{E5})$$

$$\|\boldsymbol{\theta}(t+1) - \boldsymbol{\theta}(t)\|_2 \leq (1 + k_1)\eta_0\sqrt{\frac{\lambda_{\max}}{D}} [1 - (1 - k)\eta_0\lambda_{\min}]^t \|\mathbf{r}(0)\|_2. \quad (\text{E6})$$

Then Eqs. (E1) and (E2) could be obtained subsequently.

Next we prove Eqs. (E6) and (E5) by induction. For the $t = 0$ case, Eq. (E5) holds trivially, and Eq. (E6) holds by considering the gradient updation rule:

$$\|\boldsymbol{\theta}(1) - \boldsymbol{\theta}(0)\|_2 = \eta \|\nabla \mathcal{L}_{\mathcal{A}}(0)\|_2 = \frac{\eta}{|\mathcal{A}|} \|J(0)\mathbf{r}(0)\|_2 \leq \frac{\eta_0}{D} \|J(0)\|_2 \|\mathbf{r}(0)\|_2 = \frac{\eta_0}{D} \sqrt{D\lambda_{\max}} \|\mathbf{r}(0)\|_2.$$

Next we assume that Eqs. (E6) and (E5) holds for $t = 0, 1, \dots, j$ and proceed to the $t = j + 1$ case. By using $t \in \{0, 1, \dots, j\}$ cases of Eq. (E6), we have the following bound for any $\boldsymbol{\theta} \in \{\boldsymbol{\theta} \mid \|\boldsymbol{\theta} - \boldsymbol{\theta}(j)\|_2 \leq \|\boldsymbol{\theta}(j+1) - \boldsymbol{\theta}(j)\|_2\}$,

$$\begin{aligned} \|J(\boldsymbol{\theta}) - J(\boldsymbol{\theta}(0))\|_2 &\leq \sqrt{C_0 D} \|\boldsymbol{\theta} - \boldsymbol{\theta}(0)\|_2 \\ &\leq \sqrt{C_0 D} \left(\|\boldsymbol{\theta} - \boldsymbol{\theta}(j)\|_2 + \sum_{t=0}^{j-1} \|\boldsymbol{\theta}(t+1) - \boldsymbol{\theta}(t)\|_2 \right) \\ &\leq \sqrt{C_0 D} \sum_{t=0}^j \|\boldsymbol{\theta}(t+1) - \boldsymbol{\theta}(t)\|_2 \\ &\leq \sqrt{C_0 D} (1 + k_1)\eta_0 \sqrt{\frac{\lambda_{\max}}{D}} \frac{1 - [1 - (1 - k)\eta_0\lambda_{\min}]^{j+1}}{1 - [1 - (1 - k)\eta_0\lambda_{\min}]} \|\mathbf{r}(0)\|_2 \\ &\leq \frac{1 + k_1}{1 - k} \sqrt{C_0 \lambda_{\max}} \frac{1}{\lambda_{\min}} \|\mathbf{r}(0)\|_2 \\ &\leq k_1 \sqrt{D\lambda_{\max}}. \end{aligned} \quad (\text{E7})$$

The last term follows from $D \geq D_0$ and Eq. (E4). Then the $t = j + 1$ case of Eq. (E5) could be derived as follows:

$$\begin{aligned} \|\mathbf{r}(j+1)\|_2 &= \|\mathbf{r}(j+1) - \mathbf{r}(j) + \mathbf{r}(j)\|_2 \\ &= \|J(\boldsymbol{\theta}')^T [\boldsymbol{\theta}(j+1) - \boldsymbol{\theta}(j)] + \mathbf{r}(j)\|_2 \\ &= \left\| -\frac{\eta}{|\mathcal{A}|} J(\boldsymbol{\theta}')^T J(j)\mathbf{r}(j) + \mathbf{r}(j) \right\|_2 \end{aligned} \quad (\text{E8})$$

$$\begin{aligned} &\leq \left\| 1 - \frac{\eta_0}{D} J(\boldsymbol{\theta}')^T J(j) \right\|_2 \|\mathbf{r}(j)\|_2 \\ &\leq [1 - (1 - k)\eta_0\lambda_{\min}] \|\mathbf{r}(j)\|_2, \end{aligned} \quad (\text{E9})$$

where $\boldsymbol{\theta}'$ is a point derived from the Taylor expansion, which satisfies $\|\boldsymbol{\theta}' - \boldsymbol{\theta}(j)\|_2 \leq \|\boldsymbol{\theta}(j+1) - \boldsymbol{\theta}(j)\|_2$. Eq. (E8) comes from the gradient descent rule. Eq. (E9) is derived as follows:

$$\begin{aligned} &\left\| 1 - \frac{\eta_0}{D} J(\boldsymbol{\theta}')^T J(j) \right\|_2 \\ &\leq \left\| 1 - \frac{\eta_0}{D} J(0)^T J(0) \right\|_2 + \frac{\eta_0}{D} \|J(0)^T J(0) - J(0)^T J(j)\|_2 + \frac{\eta_0}{D} \|J(0)^T J(j) - J(\boldsymbol{\theta}')^T J(j)\|_2 \\ &\leq 1 - \eta_0\lambda_{\min} + \frac{\eta_0}{D} (\|J(0)\|_2 \|J(0) - J(j)\|_2 + \|J(j) - J(0) + J(0)\|_2 \|J(0) - J(\boldsymbol{\theta}')\|_2) \\ &\leq 1 - \eta_0\lambda_{\min} + \frac{\eta_0}{D} \sqrt{D\lambda_{\max}} \cdot k_1 \sqrt{D\lambda_{\max}} + \frac{\eta_0}{D} \left(k_1 \sqrt{D\lambda_{\max}} + \sqrt{D\lambda_{\max}} \right) k_1 \sqrt{D\lambda_{\max}} \quad (\text{using Eq. (E7)}) \\ &= 1 - \eta_0\lambda_{\min} + k_1(2 + k_1)\eta_0\lambda_{\max} \\ &\leq 1 - \eta_0\lambda_{\min} + \frac{2}{5}k(2 + k_1)\eta_0\lambda_{\min} \\ &\leq 1 - (1 - k)\eta_0\lambda_{\min}, \end{aligned}$$

where the last term is derived by using $k_1 \leq 2/5$. The $t = j + 1$ case of Eq. (E6) could be obtained accordingly:

$$\begin{aligned} \|\boldsymbol{\theta}(j+2) - \boldsymbol{\theta}(j+1)\|_2 &= \eta \|\nabla \mathcal{L}_{\mathcal{A}}(j+1)\|_2 \\ &\leq \frac{|\mathcal{A}|}{D} \eta_0 \frac{1}{|\mathcal{A}|} \|J(j+1)\|_2 \|\mathbf{r}(j+1)\|_2 \end{aligned} \quad (\text{E10})$$

$$\begin{aligned} &= \frac{\eta_0}{D} \|J(j+1) - J(0) + J(0)\|_2 \|\mathbf{r}(j+1)\|_2 \\ &\leq (1+k_1) \frac{\eta_0}{D} \sqrt{D\lambda_{\max}} \|\mathbf{r}(j+1)\|_2 \end{aligned} \quad (\text{E11})$$

$$\leq (1+k_1) \eta_0 \sqrt{\frac{\lambda_{\max}}{D}} [1 - (1-k)\eta_0\lambda_{\min}]^{j+1} \|\mathbf{r}(0)\|_2. \quad (\text{E12})$$

Eq. (E10) follows from $\eta = \frac{|\mathcal{A}|}{D} \eta_0$ and $\mathcal{L}_{\mathcal{A}} = \frac{1}{2|\mathcal{A}|} \|\mathbf{r}\|_2^2$. Eq. (E11) is derived by using the local smoothness bound of J in Eq. (E7). Eq. (E12) is derived by using the $t = j + 1$ case of Eq. (E5). Thus, we have proved Eqs. (E6) and (E5) for $t = 0, 1, \dots, +\infty$.

Finally, we proceed to derive the main result in the theorem. The linear convergence result in Eq. (E1) could be obtained from Eq. (E5) and $\mathcal{L}_{\mathcal{A}}(t) = \frac{1}{2|\mathcal{A}|} \|\mathbf{r}(t)\|_2^2$. The frozen parameter regime in Eq. (E2) could be obtained from Eq. (E6) as follows:

$$\begin{aligned} \|\boldsymbol{\theta}(T) - \boldsymbol{\theta}(0)\|_2 &\leq \sum_{t=0}^{T-1} \|\boldsymbol{\theta}(t+1) - \boldsymbol{\theta}(t)\|_2 \\ &\leq \sum_{t=0}^{T-1} (1+k_1) \eta_0 \sqrt{\frac{\lambda_{\max}}{D}} [1 - (1-k)\eta_0\lambda_{\min}]^t \|\mathbf{r}(0)\|_2 \\ &\leq (1+k_1) \eta_0 \sqrt{\frac{\lambda_{\max}}{D}} \frac{1}{1 - [1 - (1-k)\eta_0\lambda_{\min}]} \|\mathbf{r}(0)\|_2 \\ &= \frac{1+k_1}{1-k} \frac{\sqrt{\lambda_{\max}}}{\lambda_{\min}} \sqrt{2|\mathcal{A}|\mathcal{L}_{\mathcal{A}}(0)} \frac{1}{\sqrt{D}} \\ &\leq \frac{1+\frac{2}{5}k}{1-\frac{1}{2}} \frac{1}{\lambda_{\min}} \sqrt{2|\mathcal{A}|\lambda_{\max}\mathcal{L}_{\mathcal{A}}(0)} \frac{1}{\sqrt{D}} \\ &\leq \frac{R_0}{\sqrt{D}}. \end{aligned} \quad (\text{E13})$$

□

2. Proof of Theorem 4

We choose constants $c_1 = \frac{9}{4}C_2$, $c_2 = 4C_3$, and $c_3 = 9C_1^2$, where constants C_1 and C_2 follow from Lemma 1 and the constant C_3 follows from Theorem S3. Then by using Lemma 1, for $D \geq D_1 \ln \frac{D_1}{\delta}$ with $D_1 = \left(\frac{\lambda'_{\max}}{\lambda'_{\min} A'_{\mathcal{Q},\max}}\right)^2 c_1 |\mathcal{A}| \ln \frac{|\mathcal{A}|}{\delta}$ and $S \geq \log_3 \left[1 + c_3 \frac{|\mathcal{A}|^2 \ln |\mathcal{A}|}{A'_{\mathcal{Q},\min} |\mathcal{Q}| \delta^2}\right]$, the following holds with probability at least $1 - \delta$:

$$\lambda'_{\min} = \frac{2}{3} \Delta_S \alpha_{\min} A'^2_{\mathcal{Q},\min} \leq \lambda[K(\boldsymbol{\theta}(0))] \leq \frac{4}{3} \|O\|_2^2 \alpha_{\max} A'^2_{\mathcal{Q},\max} = \lambda'_{\max}, \quad (\text{E14})$$

Our main idea is to derive the convergence result based on Theorem S3, which holds with probability at least $1 - \delta$ with eigenvalues in terms of λ'_{\min} and λ'_{\max} . Let $k = 1/2$, the threshold D_2 satisfies

$$\begin{aligned} D_2 &= c_2 \lambda'^2_{\max} \lambda'^{-4}_{\min} |\mathcal{A}| \mathcal{L}_{\mathcal{A}}(0) \\ &= C_3 k^{-2} \lambda'^2_{\max} \lambda'^{-4}_{\min} |\mathcal{A}| \mathcal{L}_{\mathcal{A}}(0). \end{aligned} \quad (\text{E15})$$

By employing the formulation of D_2 in Eq. (E15) in Theorem S3, we have the following result that holds with

probability $1 - \delta$,

$$\begin{aligned}\mathcal{L}_{\mathcal{A}}(T) &\leq \left(1 - \frac{1}{2}\eta_0\lambda'_{\min}\right)^{2T} \mathcal{L}_{\mathcal{A}}(0), \\ \|\boldsymbol{\theta}(T) - \boldsymbol{\theta}(0)\|_2 &\leq \frac{R_0}{\sqrt{D}}.\end{aligned}$$

Thus, we have proved Theorem 4.

3. Proof of Theorem 5

We choose constants $c_1 = 9C_2$, $c_2 = 36C_3$, and $c_3 = 9C_1^2$, where constants C_1 and C_2 follow from Lemma 2 and the constant C_3 follows from Theorem S3. Then by using Lemma 2, for $D \geq D_1 \ln \frac{D_1}{\delta}$ with $D_1 = 9C_2 \frac{|\mathcal{A}|\|O\|_2^4}{\Delta_S^2} \ln \frac{|\mathcal{A}|}{\delta}$ and $S \geq 2 + \log_2 \frac{9C_1^2|\mathcal{A}|^2 \ln |\mathcal{A}|}{|\mathcal{Q}|\delta^2}$, the following holds with probability at least $1 - \delta$:

$$\lambda'_{\min} := \frac{2}{3} \frac{\Delta_S}{2^S} \leq \lambda[K(\boldsymbol{\theta}(0))] \leq \frac{4}{3} \frac{\|O\|_2^2}{2^S} := \lambda'_{\max}. \quad (\text{E16})$$

Our main idea is to derive the convergence result based on Theorem S3, which holds with probability at least $1 - \delta$ with eigenvalues in terms of λ'_{\min} and λ'_{\max} . Specifically, the term R_0 in the locally smooth condition in Assumption 1 satisfies

$$\begin{aligned}R_0 &= \frac{5}{2} \frac{\|O\|_2}{\Delta_S} \sqrt{6 \times 2^S |\mathcal{A}| \mathcal{L}_{\mathcal{A}}(0)} \\ &= \frac{5}{2} \frac{1}{\frac{2}{3} \Delta_S 2^{-S}} \sqrt{\frac{4}{3} \|O\|_2^2 2^{-S} \cdot 2 |\mathcal{A}| \mathcal{L}_{\mathcal{A}}(0)} \\ &= \frac{5}{2} \lambda'_{\min}^{-1} \sqrt{2 |\mathcal{A}| \lambda'_{\max} \mathcal{L}_{\mathcal{A}}(0)}.\end{aligned} \quad (\text{E17})$$

Let $k = 1/2$, the threshold D_2 satisfies

$$\begin{aligned}D_2 &= 36C_3 \frac{\|O\|_2^4 2^{2S}}{\Delta_S^4} |\mathcal{A}| \mathcal{L}_{\mathcal{A}}(0) \\ &= C_3 k^{-2} \frac{\frac{16}{9} \|O\|_2^4 2^{-2S}}{\frac{16}{81} \Delta_S^4 2^{-4S}} |\mathcal{A}| \mathcal{L}_{\mathcal{A}}(0) \\ &= C_3 k^{-2} \lambda'_{\max}{}^2 \lambda'_{\min}{}^{-4} |\mathcal{A}| \mathcal{L}_{\mathcal{A}}(0).\end{aligned} \quad (\text{E18})$$

By employing the formulation of R_0 and D_2 in Eqs. (E17) and (E18) in Theorem S3, we have the following result that holds with probability $1 - \delta$,

$$\begin{aligned}\mathcal{L}_{\mathcal{A}}(T) &\leq \left(1 - \frac{1}{2}\eta_0\lambda'_{\min}\right)^{2T} \mathcal{L}_{\mathcal{A}}(0), \\ \|\boldsymbol{\theta}(T) - \boldsymbol{\theta}(0)\|_2 &\leq \frac{R_0}{\sqrt{D}}.\end{aligned}$$

Theorem 5 could be easily derived by using eigenvalue bounds in Eq. (E16).